Development of Therapies for Spinal Muscular Atrophy Using Gene Therapy and Nanotechnology

Daniel Little

Submitted for the degree of Doctor of Philosophy (PhD)

Academic Unit of Neurology
Sheffield Institute for Translational Neuroscience
University of Sheffield

May 2013

ABSTRACT

Spinal muscular atrophy (SMA) is a genetic disease which is characterized by muscle weakness and atrophy. The disease arises from mutations in the survival motor neuron 1 (SMN1) gene causing degeneration of spinal cord motor neurons. No effective treatment is currently available for SMA however it may be possible to treat the disease using gene therapy. The aim of this project is to develop potential therapies for SMA by investigating different viral and non-viral gene therapy vectors and assessing the effect of potential disease modifying genes. The data collected are described under four chapters as follows:

1: The aim here was to develop a novel approach based on polymer nanoparticles (polymersomes) for gene delivery. Encapsulation of DNA by polymersomes was optimised and polymersomes were used to restore SMN levels into a fibroblast cell line isolated from a child with severe SMA. 2: The ability of adeno-associated virus serotype 5 (AAV5) vectors expressing GFP to transduce the central nervous system (CNS) following intravenous injection was tested in neonatal wild-type mice. Overall transduction efficiency of AAV5-GFP in the brain was low and very few lumbar spinal cord neurons were found to be transduced, suggesting that AAV5 is not an appropriate vector to treat diseases such as SMA. 3: AAV6 was used to overexpress hnRNP R in an *in vivo* model of SMA. hnRNP R is a candidate disease modifying gene for SMA due to its interaction with SMN and β-actin. However this strategy had only a very marginal effect on the phenotype and life-span of this SMA mouse model. 4: Finally AAV9 was used to silence phosphatase and tensin homolog (PTEN) in an *in vivo* model of SMA. PTEN is a negative regulator of growth which acts on the PI3K/Akt pathway. AAV9-mediated PTEN silencing resulted in a significant increase in the lifespan of a SMA mouse model coupled with an improved phenotype.

In conclusion this work highlights two major findings: i) polymersomes can be used to deliver SMN plasmid DNA to restore SMN mRNA and protein levels in an *in vitro* model of SMA; ii) AAV9-mediated silencing of PTEN can improve the phenotype and increase lifespan of a SMA mouse model.

ACKNOWLEDGEMENTS

I must thank my supervisors Prof. Mimoun Azzouz, Prof. Giuseppe Battaglia and Dr. Ke Ning for their continued support and guidance throughout this project. I am also very grateful to the Engineering and Physical Sciences Research Council (EPSRC) for funding this project.

I must thank all of my colleagues in the University of Sheffield and in particular at the Sheffield Institute for Translational Research including Prof. Pamela Shaw and everyone in Professor Mimoun Azzouz's lab. In particular I am very grateful to Dr. Chiara Valori for introducing me to this project and to lab work in general, and always being willing to help with any questions I have. Furthermore I would like to thank Dr. Aikaterini Nanou for helping with many laboratory techniques and *in vivo* work. I also must thank Dr. Ellen Bennett and Ian Coldicott for helping out with *in vivo* work when necessary and I would like to thank Matt Wyles and Dr. Adrian Higginbottom for helping with various technical difficulties.

I am also very grateful to everyone in Professor Giuseppe Battaglia's lab for their continued assistance and support. In particular I am indebted to Dr. Nicholas Warren and Dr. Jeppe Madsen for supplying polymer, without which parts of this project would have been impossible. I also must thank Dr. Irene Canton and Dr. Linge Wang for teaching me various techniques and Russell Pearson for answering many questions I had about polymersomes. Finally I appreciate all the work that has been carried out within the University of Sheffield and elsewhere that precedes this project.

I must also thank all my friends in Sheffield and throughout the UK for providing emotional support and giving me opportunities to take my mind off work when necessary. Most importantly I must thank my family and in particular my parents for their constant support.

Table of Contents

1. INTRODUCTION 14

1.1 Spinal Muscular Atrophy 15

1.1.1 Clinical Features 15

1.1.2 Motor Neuron Dysfunction in SMA 16

1.1.3 Non-neuronal Pathology 18

1.1.4 Genetics of SMA 19

1.1.5 Role of SMN 21

1.1.5.1 Neuron Specific Role of SMN 22

1.1.6 Other Molecules Involved in SMA 22

1.1.7 Models of SMA 24

1.1.7.1 *In Vitro* Models of SMA 24

1.1.7.2 Animal Models of SMA 24

1.1.8 Treatment Strategies for SMA 28

1.1.8.1 Drug Treatment Approaches 29

1.1.8.2 Gene Therapy Approaches 31

1.1.8.3 Gene Repair 32

1.2 Gene Therapy 33

1.2.1 Viral Vectors for Gene Therapy 34

1.2.1.1 Retroviral and Lentiviral Vectors 34

1.2.1.2 Adenoviral Vectors 35

1.2.1.3 Adeno-associated Viral Vectors 36

1.2.1.3.1 Adeno-associated Virus Serotype 5 39

1.2.1.3.2 Adeno-associated Virus Serotype 6 39

1.2.1.3.3 Adeno-associated Virus Serotype 9 40

1.3 Non-viral Mediated Gene Therapy 41

1.3.1 Polymersomes 43

1.3.1.1 Formation of Polymersomes 43

1.3.1.2 Polymersome Characteristics 44

1.3.1.3 Biological Applications 46

1.3.1.4 Polmersomes for Gene Therapy 46

1.4 Aims of the Project 48

2. MATERIALS & METHODS 49
2.1. Materials 50
2.1.1. Polymer Synthesis 50
2.1.2. DNA Preparation 50
2.1.4. Viral Vectors 50
vp - virus particles, gc – genome copies 51
2.1.5. Protein Extraction and Analysis 51
2.1.6. Antibodies 52
2.1.7. Spectrophotometry 52
2.2. *In Vitro* Experimental Methods 52
2.2.1. Cell Lines and Cell Culture 52
2.2.2. Polymersome Production 53
2.2.3. Polymersome Characterisation 54
2.2.4. Encapsulation Assessment 54
2.2.5. Toxicity Assay 55
2.2.6. Luciferase Assay 55
2.2.7. Real-time Quantitative-PCR 55
2.2.8. Western Blot 56
2.2.9. Immunofluorescence 57
2.3. *In Vivo* Experimental Methods 59
2.3.1. Breeding and Genotyping of Transgenic Mice 59
2.3.2. Recruiting Experimental Mice 60
2.3.3. Viral Vector Delivery 61
2.3.4. Behavioural and Clinical Assessment 61
2.3.5. Tissue Collection 62
2.3.6. Histological Analysis 62
2.3.6.1. Immunohistochemistry 62
2.3.6.2. Immunofluorescence 63

RESULTS 65
3. Polymersomes as Gene Therapy Vectors 66
3.1 Introduction 67
3.2 Results 70

3.2.1 Polymersome Characterisation 70
3.2.1.1 Cell Viability Following Incubation with Polymersomes 70
3.2.1.2 Uptake of Rhodamine-labelled Polymersomes by HEK293T Cells 71
3.2.1.3 Encapsulation of Plasmid DNA in Polymersomes 73
..... 74
3.2.1.4 Using Centrifugation to Sort Polymersomes by Size 74
3.2.1.5 Size Dependent Encapsulation of DNA 76
3.2.2 Polymersomes as DNA Delivery System 77
3.2.2.1 Luciferase Transfection with Polymersomes Sorted by Centrifugation 77
3.2.2.2 Using Polymersomes to Overexpress SMN 78
3.2.2.3 Overexpression of SMN in an *In Vitro* Model of SMA 80
3.3 Discussion 83
4. AAV5-mediated Transduction in the CNS 88
4.1 Introduction 89
4.2 Results 91
4.2.1 AAV5-mediated GFP Transduction in the Brain 91
4.2.1.1 Transduction of Neurons and Astrocytes in the Brain 91
4.2.1.2 Quantification of Transduced Astrocytes and Neurons in the Brain 92
4.2.1.3 Transduction of the Cerebellum 95
4.2.1.4 Transduction within the Ventricles 95
4.2.2 AAV5-mediated Transduction in the Spinal Cord 97
4.2.2.1 Transduction of Spinal Cord Neurons 98
4.2.2.2 Transduction of Astrocytes in the Spinal Cord 100
4.2.2.3 Transduction of Dorsal Root and White Matter 103
4.3 Discussion 105
5. AAV6-mediated Expression of hnRNP R 110
5.1 Introduction 111
5.2 Results 114
5.2.1 *In Vivo* Assessment 114
5.2.1.1 Body Weight 114
5.2.1.2 Righting-reflex 115
5.2.2 Histological assessment 117
5.2.2.1 Motor Neuron Survival 117
5.2.2.2 Transduction Efficiency of AAV6 118

5.3 Discussion 120
6. Effect of PTEN Silencing on SMA 124
6.1 Introduction 125
6.2 Results 129
6.2.1 Body Weight 129
6.2.2 Righting Reflex 130
6.2.3 Survival 131
6.2.4 Transduction and PTEN Depletion in Spinal Cord Motor Neurons 134
6.2.5 Motor Neuron Survival 135
6.3 Discussion 137
7. DISCUSSION 142
7.1 Project Outcomes 143
7.2 Further Considerations 146
7.2.1 Polymersomes as Gene Therapy Vectors 146
7.2.2 AAV5 Transduction in the CNS 147
7.2.3 AAV9-mediated silencing of PTEN 149
7.2.4 AAV6-mediated expression of hnRNP R 150
7.3 Conclusions 151
7.4 Future Perspectives 154

List of Figures

Figure 1.1 Variable splicing of SMN1 and SMN2. 20
Figure 1.2 The Role of the SMN complex. 21

Figure 3.1 HEK293T cell viability after treatment with Rhd-PMPC-PDPA. 71
Figure 3.2 Uptake of rhodamine-labelled polymersomes in HEK293T cells. 72
Figure 3.3 Encapsulation of plasmid DNA in polymersomes 74
Figure 3.4 Size sorting of polymersomes by centrifugation. 75
Figure 3.5 Encapsulation of DNA in different polymersome fractions. 76
Figure 3.6 Luciferase transfection with different polymersome fractions. 77
Figure 3.7 Polymersome-mediated SMN transduction in HEK293T cells 79
Figure 3.8 Increased levels of SMN mRNA following transfection by polymersomes. 79
Figure 3.9 Polymersome-mediated SMN gene replacement in type I SMA fibroblasts. 80
Figure 3.10 Polymersome-mediated SMN replacement in type I SMA patient fibroblasts. 82

Figure 4.1 AAV5-mediated GFP expression in the brain. 93
Figure 4.2 Quantification of astrocytes and neurons transduced in the brain. 94
Figure 4.3 Transduction in the cerebellum. 95
Figure 4.5 Transduction of the pineal gland and surrounding area. 97
Figure 4.4 Transduction within the 3rd ventricle. 97
Figure 4.6 Neuronal transduction in the lumbar spinal cord. 99
Figure 4.7 AAV5-mediated transduction of astrocytes in the spinal cord. 100
Figure 4.8 Quantification of neurons and astrocytes transduced in the spinal cord. 102
Figure 4.9 AAV5-mediated transduction in spinal cord white matter. 104

Figure 5.1 Body weight assessment. 114
Figure 5.2 Righting reflex assessment 115
Figure 5.3 Survival analysis of SMNΔ7 mice. 116
Figure 5.4 Quantification of lumbar spinal cord motor neurons. 117
Figure 5.5 AAV6-mediated GFP transduction of lumbar spinal cord in SMNΔ7 mice. 119
Figure 5.6 AAV6-hnRNP R transduction of gastrocnemius muscle in SMNΔ7 mice. 119

Figure 6.1 PTEN function in the PI3K / Akt pathway 126
Figure 6.2 scAAV9-siPTEN improves growth in SMNΔ7 mice. 130

Figure 6.3 Motor function assessment in rescued SMNΔ7 mice..... 131
Figure 6.4 Kaplan-Meier survival curve..... 133
Figure 6.5 scAAV9-siPTEN causes transduction of motor neurons and a reduction in PTEN expression..... 133
Figure 6.6 Effect of PTEN depletion on motor neuron survival in the spinal cord of SMNΔ7 mice..... 136

List of Tables

Table 1.1 Classification of spinal muscular atrophy..... 16
Table 1.2 Animal models of SMA..... 27
Table 2.1 List of viral vectors used..... 50
Table 2.2 List of antibodies used..... 52
Table 2.3 Centrifugations to separate polymersomes by size..... 54
Table 2.4 Primers used for QPCR..... 56
Table 2.5 Primers used for genotyping..... 59
Table 2.6 Viral vector dose administered..... 61

List of Abbreviations

AAV	Adeno-associated virus
Akt	*Also known as* protein kinase B
APS	Ammonium persulfate
BBB	Blood brain barrier
BSA	Bovine serum albumin
cDNA	Copy deoxyribonucleic acid
CGRP	Calcitonin-gene related peptide
CMV	Cytomegalovirus
CNS	Central nervous system
CPG-15	Candidate plasticity-related gene 15
CSF	Cerebrospinal fluid
DAB	Diaminobenzidine
DAPI	Diamidino-2-phenylindole
DLS	Dynamic light scattering
DMEM	Dulbecco's minimum essential medium
DNA	Deoxyribonucleic acid
DPX	Di-N-Butyle Phthalate in Xylene
DRG	Dorsal root ganglion
ECG	Electrocardiogram
EDTA	Ethylenediaminetetraacetic acid
ERK	Extracellular signal-regulated kinases
FITC	Fluorescein isothiocyanate 1
GAPDH	Glyceraldehyde 3-phosphate dehydrogenase
GFP	Green fluorescent protein
GFAP	Glial fibrillary acidic protein
HA	Human influenza hemagglutinin
HDAC	Histone deacetylase inhibitors

HEK	Human embryonic kidney
hnRNP	Heterogeneous ribonucleoproteins
hrGFP	Humanised recombinant GFP
IGF-1	Insulin-like growth factor 1
Igfals	IGF-binding protein, acid labile subunit
ITR	Inverted terminal repeat
IP	Intraperitoneal
IV	Intravenous
LV	Lentivirus
MAPK	Mitogen-activated protein kinases
MEME	Minimum Essential Medium Eagle
mRNA	Messenger RNA
mTOR	Mammalian target of rapamycin
MTT	3-(4,5-dimethylthiazol-2-yl)-2,5-diphenyl tetrasodium bromide
NeuN	Neuronal nuclei
NGS	Normal goat serum
NMJ	Neuromuscular junction
OCT	Optimum cutting temperature medium
PAGE	Polyacrylamide gel electrophoresis
PBS	Phosphate buffered saline
PCR	Polymerase chain reaction
PDPA	Poly(2-(diisopropylamino)ethyl methacrylate)
PEG	Poly(ethylene glycol) *also known as PEO*
PEO	Poly(ethylene oxide) *also known as PEG*
PFA	Paraformaldehyde
PI3K	Phorphoinositide 3-kinase
PIP3	Phosphatidylinositol 3,4,5-triphosphate
PMPC	Poly(2-(methacryloyloxy)ethyl phosphorylcholine)
POEGMA	Poly(oligo(ethylene glycol) methacrylate)
PTEN	Phosphatase and tensin homolog
PVDF	Polyvinylidene difluoride

QPCR	Quantitative PCR
RNA	Ribonucleic acid
rcf	Relative centrifugal force
RT-PCR	Real time PCR
scAAV	Self-complementary AAV
SDS	Sodium dodecyl sulphate
SEM	Standard error of the mean
shRNA	Short hairpin RNA
siRNA	Small interfering RNA
SMA	Spinal muscular atrophy
SMN	Survival of motor neuron
snRNPs	Small nucleotide ribonuclear proteins
ssDNA/RNA	Single stranded DNA/RNA
TEMED	Tetramethylethylenediamine
TRITC	Tetramethyl rhodamine isothiocyanate
Triton X-100	Polyethylene glycol tert-octylphenyl ether
Tween 20	Polyoxyethylene-sorbitan monolaurate
UTR	Untranslated region
VEGF	Vascular endothelial growth factor

Chapter 1

INTRODUCTION

1.1 Spinal Muscular Atrophy

1.1.1 Clinical Features

Spinal muscular atrophy (SMA) was estimated to have an incidence of 1 in 24,100 live births and a prevalence of 1.2 per 10,000 live births in a study conducted in the north-east of England in 1978 (Pearn, 1978). More recent studies estimate the incidence of SMA to be as high as 1 in 6,000 with a carrier frequency of 1:38 (Wilson & Ogino, 2008). There appears to be some discrepancy between the carrier frequency and the incidence of disease seen, with a lower incidence than the carrier frequency suggests. This may be due to severe prenatal forms of the disease that are not counted in incidence data (Prior *et al.*, 2010). Classically this disease is characterised by weakness and atrophy in the proximal voluntary muscles which is known to be caused by loss of motor neurons in the anterior horn of the spinal cord. As the disease progresses more distal muscles become affected until muscles of the torso are also affected. SMA is a genetic disorder caused by mutation or deletion of the Survival motor neuron (SMN1) gene therefore diagnosis can be confirmed by genetic testing. The genetic cause of SMA will be discussed in more detail below. Diagnosis can be further assessed by electromyography and muscle biopsy. Electromyography measures the electrical activity of nerves in the muscle and can differentiate between SMA which is caused by nerve degeneration and muscle pathologies such as muscular dystrophy. Muscle biopsy is rarely used now due to the invasive nature of the procedure and the effectiveness of genetic testing.

The rate of disease progression and severity of disease differs between patients therefore SMA is divided into three main types; type I, II and III. Type I is the most severe and was the first to be described. Patients are usually asymptomatic at birth but start to display symptoms from around 2 months. These children present with weak, thin, hypertonic muscles and display poor breathing and feeding abilities (Wang *et al.*, 2007; Lunn & Wang, 2008; Markowitz *et al.*, 2012). SMA patients are usually divided into type I, II or III based on what major motor milestone they

achieve (Wang *et al.*, 2007) (table 1.1). For example type I patients are never able to sit, whereas intermediate type II patients are able to sit but cannot walk. Patients with the less severe type III SMA are able to walk however as they age and the disease worsens this ability is lost. There are also two further categories of SMA, type 0 and type IV. Type 0 denotes those patients that are symptomatic at birth whereas type IV is a rare form with onset in adulthood and a normal life expectancy. Type I SMA is the most common form of the disease and patients have a life expectancy of 2 years, with the cause of death usually being respiratory failure. Type II SMA has an onset of between 6 and 18 months, with a life expectancy of up to teenage years. Type III SMA has an onset from 18 months and these patients usually live to adulthood. However these classifications are not exact with variations seen in the age of onset and motor ability which reflects a spectrum of disease severity.

Table 1.1 Classification of spinal muscular atrophy

Disease Type	Onset	Major Function Achieved	Life expectancy
0	Prenatal	Need respirator from birth	< 6 months
I	< 6 months	Never sit	< 2 years
II	6 – 18 months	Sits with assistance	> 2 years
III	> 18 months	Stand and walk	Adulthood
IV	10 – 30 years	Walks normally	Normal

(Wang et al., 2007; Markowitz et al., 2012)

1.1.2 Motor Neuron Dysfunction in SMA

The classical presentation of muscle weakness and atrophy in SMA is caused by degeneration of spinal cord motor neurons. Electrophysiological testing has been used to estimate the number of motor units innervating a muscle group in SMA patients. This revealed a decrease in muscle innervation over time in type I, II and III SMA (Swoboda *et al.*, 2005). Animal models of SMA show axon degeneration and neuromuscular junction (NMJ) defects caused by decreased SMN protein in zebrafish, drosophila and mice (Chan *et al.*, 2003; McWhorter *et al.*, 2003; Rossoll *et*

al., 2003; Jablonka *et al.*, 2004; Winkler *et al.*, 2005; Boon *et al.*, 2009; Kong *et al.*, 2009). Motor neurons in spinal cords of SMA patients display abnormal migration towards the ventral root and a lack of differentiation (Simic *et al.*, 2008). Furthermore lack of differentiation and poor synapse formation causes abnormal migration of motor neurons towards the ventral roots of spinal cords before later succumbing to necrosis. Impaired growth of axons is caused by a lack of SMN protein in the growth cone of motor neurons. This leads to abnormalities at the synapse and neuromuscular junction. Defects in axonal growth are caused by impaired trafficking of molecules such as β-actin which causes neurons to become chromatolytic and eventually die (Rossoll *et al.*, 2003). Neuromuscular junctions also display defects in the structure of pre- and post-synaptic apparatus including changes in receptor clustering and accumulation of vesicles (Martinez-Hernandez *et al.*, 2013). A mild model of SMA displays altered NMJ morphologies and decreased neurotransmitter release (Ruiz & Tabares, 2013).

Defects in NMJ and muscles appear to only affect some muscles; NMJ defects have been reported in the diaphragm but not the soleus muscle (Voigt *et al.*, 2010; Lee *et al.*, 2011b). Selective denervation of muscles has been reported throughout the body with various muscle fibre types being affected (Ling *et al.*, 2012). Loss of innervation of muscles is thought to be due to defects in synaptic maintenance or maturation. Interestingly selective expression of SMN protein in neurons can restore motor neuron synapses and NMJ defects however this can only increase survival by up to three weeks, suggesting that SMN replacement is required in other tissues to be an effective treatment (Martinez *et al.*, 2012). Furthermore zebrafish with low levels of SMN have shorter axons with fewer branches and significant motor defects (Hao *et al.*, 2013). Defects in axonal transport of synapse proteins have been reported in a mouse model of SMA which suggests a reason for defects in synapses and NMJs of motor neurons (Dale *et al.*, 2011). Defects in the NMJ have been linked with muscle dysfunction which may also be independent from the motor neuron pathology of SMA. This reveals the possibility of other tissues also being affected by SMN deficiency.

Interestingly there is evidence that sensory nerves are also affected in SMA. Drosophila with mutations in the SMN gene have defects in proprioceptive nerves and interneurons (Imlach *et al.*, 2012). Meanwhile SMN-deficient mice display a reduction in the strength of connections between primary afferent neurons and motor neurons (Mentis *et al.*, 2011). Patients with type I SMA have also been shown to have abnormalities in peripheral nerves (Yonekawa *et al.*, 2013).

1.1.3 Non-neuronal Pathology

SMN is a ubiquitously expressed protein (Lefebvre *et al.*, 1995) therefore the reduced levels of SMN protein seen in SMA is likely to affect other cell types as well as motor neurons. It has recently become apparent that many other tissues are also affected in SMA (Hamilton & Gillingwater, 2013). This is partially due to prolonging the lifespan of SMA patients revealing symptoms that do not usually become apparent such as digital necrosis. Digital necrosis has been reported in type I SMA patients (Heier *et al.*, 2010; Rudnik-Schoneborn *et al.*, 2010) which is thought to be due to defects in the vasculature. This is supported by the presence of cardiac defects which have been reported in SMA patients and in animal models (Rudnik-Schoneborn *et al.*, 2008; Heier *et al.*, 2010; Shababi *et al.*, 2010). In the most severe cases of SMA patients various congenital cardiac problems such as atrial and ventricular septal defects have been reported (Rudnik-Schoneborn *et al.*, 2008). Assessment of the cardiac function of SMA mice revealed that these mice suffer from severe bradyarrhythmia from as early as 2 days of age which worsened as the disease developed (Heier *et al.*, 2010). The hearts of these mice appeared smaller and lacked a defined shape however the ratio of heart weight to body weight was comparable to that of unaffected litter-mates. Histological analysis has shown that hearts of SMA mice have thinner inter-ventricular septums (Shababi *et al.*, 2010). Interestingly muscle capillaries are also defective in a mouse model of SMA, with defects becoming apparent as mice age (Somers *et al.*, 2012). Interestingly ECG studies on milder type II and III patients reveal that these patients do not have any cardiac dysfunction (Palladino *et al.*, 2011).

Other organs such as the lung, liver, pancreas and intestine also display abnormalities in SMA patients or animal models. In a mouse model of severe SMA analysis of pancreatic cells revealed increased glucagon-producing α cells and fewer insulin-producing β cells (Bowerman *et al.*, 2012). This causes these mice to display fasting hyperglycaemia, hyperglucagonemia and glucose resistance. Children with type I SMA also have abnormalities in pancreatic islets with some patients displaying glucose intolerance (Bowerman *et al.*, 2012). The liver also appears to be affected in SMA; a decrease in hepatic IGF-binding protein acid labile subunit (Igfals) and resulting reduced levels of circulating IGF1 has been reported in SMA mice (Hua *et al.*, 2007). This corroborates with the finding that the liver specific deletion of murine SMN exon 7 causes severe impairment of liver development (Vitte *et al.*, 2004). Bone abnormalities have been reported in vertebrae of a severe mouse model of SMA (Shanmugarajan *et al.*, 2007; Shanmugarajan *et al.*, 2009).

1.1.4 Genetics of SMA

The genetic cause of SMA was determined in 1995 as the mutation of a gene on chromosome 5q13 which was termed the survival motor neuron (SMN) gene (Lefebvre *et al.*, 1995). The area of the chromosome where this gene is located is unstable and contains duplications. There are two copies of the SMN gene, a telomeric copy (SMN1) and a centromeric copy (SMN2), these two genes differ by 5 single nucleotide changes however it is the difference in exon 7 which is most important. This single nucleotide change in exon 7 of SMN2 affects how it is spliced. The C-T transition at codon 280 does not alter the sequence of amino acids but does result in the loss of an exon splice enhancer, and the creation of a novel splicing silencer. This causes exclusion of exon 7 and the production of a truncated protein which is unstable and quickly degraded (Lorson *et al.*, 1999; Cartegni & Krainer, 2002). However exon 7 of SMN 2 is not always skipped, resulting in around 10% of full length protein being produced by SMN2. Since SMN1 is either deleted or mutated in patients only have the small amount of SMN protein produced from SMN2. The number of copies of the SMN2 gene varies throughout

the population. Increased SMN2 copy number reduces the severity of SMA by providing greater amounts of full-length SMN. Type II SMA patients usually have 3 or more copies of SMN2 which produce around 14% of the normal amount of SMN protein whereas patients with the milder type III form can have up to 8 copies of the SMN2 gene (Simic, 2008). The correlation between SMN2 copy number and disease severity is not perfect however; patients with three copies of SMN2 have been seen to have all three main disease types. This suggests that there may be disease modifying genes acting in some SMA patients. Interestingly a mutation in SMN2 has been reported which increases the inclusion of exon 7 resulting in a less severe phenotype. There appears to be an inverse correlation between SMN1 and SMN2 levels in the general population (Ogino *et al.*, 2003). People with more copies of SMN1 have fewer copies of SMN2. De novo mutations in SMN1 have been reported in patients with SMA resulting in conversion to SMN2 (Prior *et al.*, 2010) and SMN2 can also be converted into SMN1 through mutations.

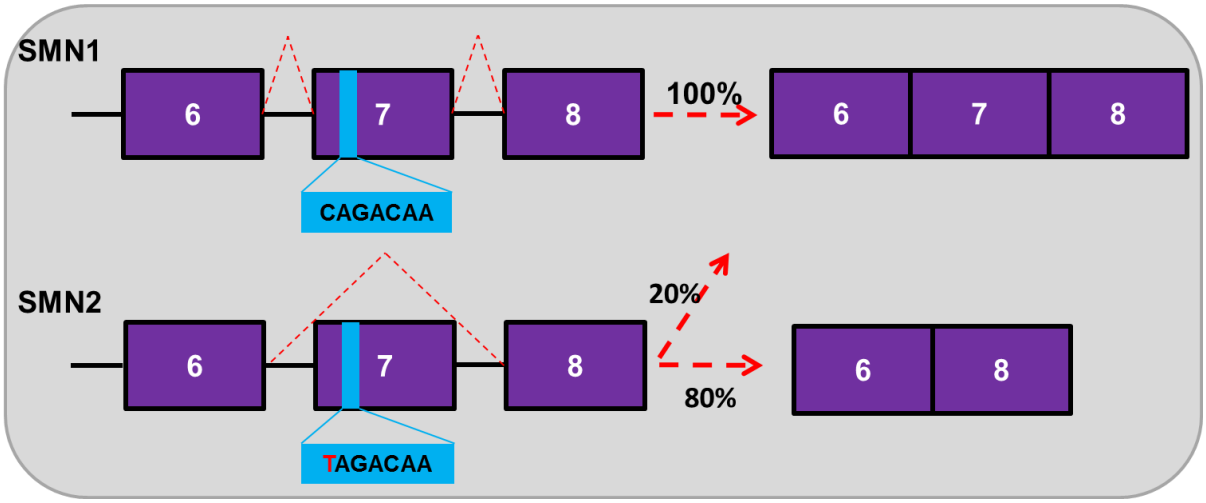

Figure 1.1 Variable splicing of SMN1 and SMN2. A single nucleotide mutation in exon 7 of the SMN2 gene causes exon 7 to be skipped resulting in the production of a truncated protein. However a small amount of full length protein is still produced by the SMN2 gene. (Lorson *et al.*, 1999; Cartegni & Krainer, 2002)

1.1.5 Role of SMN

The SMN protein is present in both the cytoplasm and the nucleus of all cells. In the nucleus it forms a complex with many other molecules and associates in structures known as gems (Liu & Dreyfuss, 1996). The core of the complex consists of SMN, Gemin7 and Gemin8, with other Gemins and Unrip binding to these three proteins (Otter *et al.*, 2007). The SMN complex is involved in initiating pre-mRNA splicing by causing Sm core proteins to bind small nuclear RNAs and assemble specific uridine rich small nucleotide ribonuclear proteins (snRNPs). These snRNPs are then translocated to the nucleus to perform pre-mRNA splicing as components of the spliceosome complex. The SMN protein is therefore indirectly involved in mRNA processing through the assembly of snRNPs and can also bind various other proteins involved in RNA processing such as RNA-helicase A, fibrillin and ribonucleoproteins. Furthermore SMN can also directly bind mRNA to act as a translational regulator (Sanchez *et al.*, 2013).

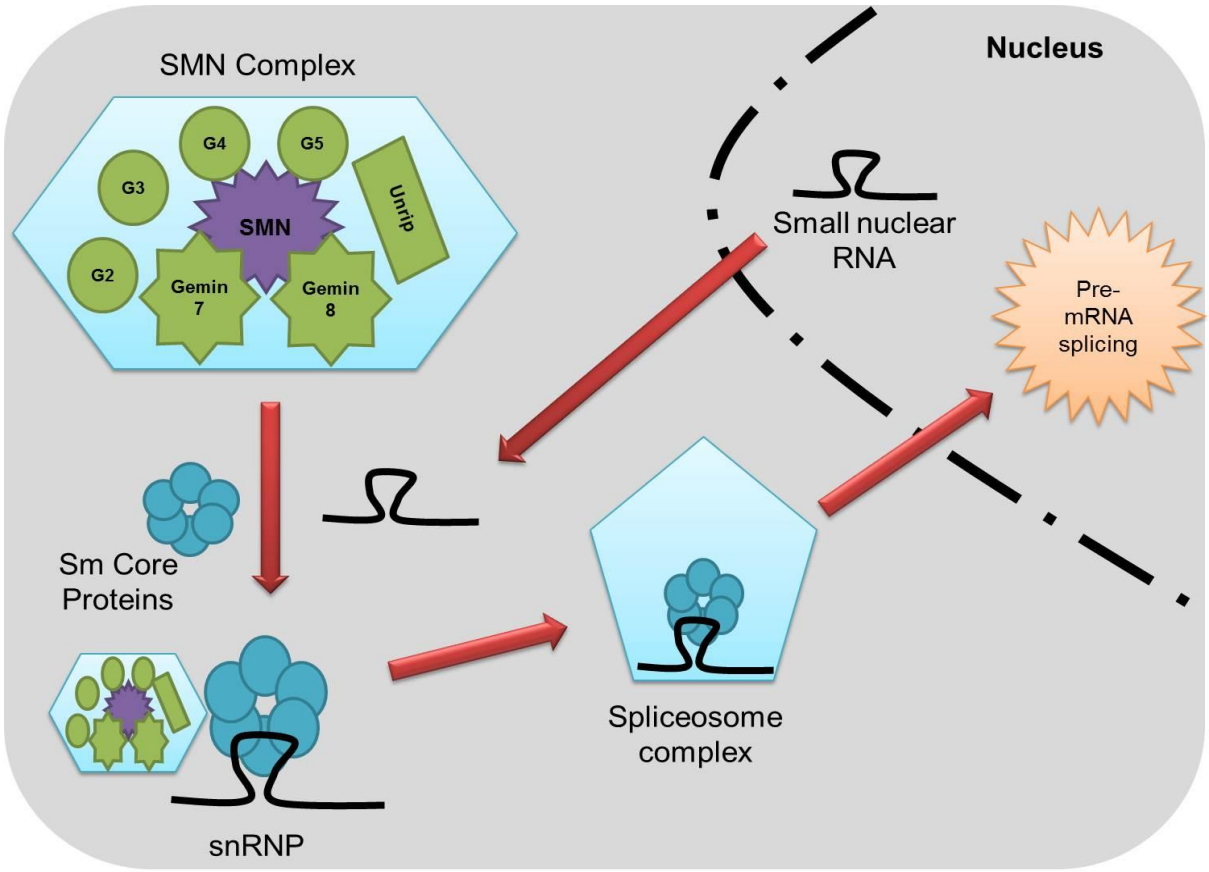

Figure 1.2 The Role of the SMN complex. The SMN complex initiates binding of Sm core proteins and small nuclear RNA to assemble snRNPs which are then incorporated in the spliceosome complex to perform pre-mRNA splicing in the nucleus.

1.1.5.1 Neuron Specific Role of SMN

Since motor neurons are most affected by SMN disruption in SMA it stands to reason that the SMN protein may play a specific role in motor neurons. SMN is widely expressed in the central nervous system (CNS), particularly in lower motor neurons of the spinal cord (Battaglia *et al.*, 1997). A differentially spliced form of SMN was identified which was termed axonal-SMN and was found to be selectively expressed in motor neurons and was mainly localized in axons (Setola *et al.*, 2007). The SMN protein appears to play a variety of roles within the motor neuron including neurite outgrowth as it is found in the growth cone and axon branching points. The SMN protein is trafficked along axons of motor neurons in granules along with Gemin 2 and Gemin 3. SMN reduction is associated with a decrease in β-actin protein and mRNA levels in motor neuron axons. SMN regulates β-actin levels through interaction with hnRNP R which associates with β-actin mRNA and with profillin II. Profillin II inhibits β-actin polymerisation however upon binding with SMN actin polymerisation occurs. Neurite growth is reduced in differentiated PC12 cells following SMN knockdown (Rossoll *et al.*, 2003). Similarly reduced SMN levels in zebrafish cause axon growth defects, increased branching and defective path-finding (McWhorter *et al.*, 2003). Furthermore motor neurons cultured from a severe SMA mouse model display truncated axons (Rossoll *et al.*, 2003). The effect of SMN on β-actin suggests a mechanism for the axon outgrowth defects seen in SMA models. However SMN deficiency also causes defects in motor neuron synapses and neuromuscular junctions. Disruption of presynaptic organisation and synaptic maturation has been reported in motor neuron terminals of SMA mice (Torres-Benito *et al.*, 2011).

1.1.6 Other Molecules Involved in SMA

As mentioned above SMN interacts with many other proteins both in the nucleus and in motor neuron axons and growth cones. Furthermore a variety of proteins have been shown to modify SMA pathology. Actin appears to play an important role

in the motor neuron pathology of SMA highlighted by the reduction of actin protein and mRNA levels in growth cones of SMN-deficient motor neurons (Rossoll *et al.*, 2003; Ning *et al.*, 2010). Profilin II and hnRNP R have been shown to interact with both SMN and β-actin. Plastin and profilin have also been implicated in actin dysregulation in SMA, profilin II is increased in SMA mice whilst plastin 3 is down-regulated however restoration of both these proteins to the correct level does not rescue the SMA phenotype (Bowerman *et al.*, 2009). Profilins are known to control β-actin dynamics and SMN strongly binds to profilin II which is predominantly expressed in motor neurons (Giesemann *et al.*, 1999). Furthermore SMN deficiency affects laminin mediated local translation of β-actin in the growth cone of motor neurons (Rathod *et al.*, 2012). As well as binding to other proteins SMN also associates with mRNA such as β-actin mRNA (Todd *et al.*, 2010).

The RNA binding protein hnRNP R co-localizes with SMN in purified motor neurons and also associates with β-actin mRNA (Rossoll *et al.*, 2003). Interestingly hnRNP R knockdown causes axon defects similar to SMN deficiency and hnRNP R overexpression can increase axon length. SMN has also been shown to associate with various other molecules in motor neurons involved in RNA binding including HuD and hnRNP Q (Chen *et al.*, 2008; Akten *et al.*, 2011; Fallini *et al.*, 2011; Hubers *et al.*, 2011). SMN is required for the recruitment of HuD and mRNA targets in neuronal RNA granules (Akten *et al.*, 2011; Hubers *et al.*, 2011). Furthermore SMN-deficient motor neurons display reduced levels of HuD protein and mRNA in axons (Fallini *et al.*, 2011). SMN and HuD interact with candidate plasticity-related gene 15 (cpg15) mRNA which is also reduced in SMN-deficient neurons (Akten *et al.*, 2011). Interestingly overexpression of cpg15 in SMN deficient zebrafish can partially rescue their phenotype. Furthermore silencing of PTEN which acts on the PI3K/Akt pathway to regulate cell growth can rescue the shortened axons of SMN-deficient cultured motor neurons (Ning *et al.*, 2010). Intramuscular injection of AAV6 expressing siRNA against PTEN leads to increased survival of spinal cord motor neurons. This suggests the possibility of modulating SMA pathology through modification of the expression of other molecules.

1.1.7 Models of SMA

1.1.7.1 *In Vitro* Models of SMA

The availability of SMA models has been important in elucidating the complex functions of the SMN protein and the pathology of SMA. *In vitro* models are especially useful for understanding molecular pathways involved in SMA and early testing of potential therapies. *In vivo* models are useful for understanding the full phenotype of SMA as well as in depth testing of potential therapeutics (table 1.2). RNAi can be used to create *in vitro* models by silencing SMN by delivering siRNA against SMN to cells (Trulzsch *et al.*, 2004; Trulzsch *et al.*, 2007). An SMA cell line has also been created from a type I SMA patient which can reduce the variability within the model. Fibroblasts from SMA patients display low SMN expression and almost complete absence of SMN gems (Coovert *et al.*, 1997). Differentiated P19 cells have also been used to model the effect of SMN depletion in motor neurons, as have primary motor neuron cultures (Trulzsch *et al.*, 2007).

1.1.7.2 Animal Models of SMA

SMA has been modelled in various animal species however modelling is complicated by the fact that only humans and chimpanzees carry multiple copies of the SMN gene. Complete knockout of SMN in mice is embryonically lethal therefore various strategies have been developed to produce a partial expression of SMN (Schrank *et al.*, 1997). Cre-loxP can be used to drive tissue specific SMN knockdown and has been used to knockdown SMN in either muscle or in neurons (Frugier *et al.*, 2000; Cifuentes-Diaz *et al.*, 2001). Interestingly targeted deletion in either muscle or neurons both cause motor defects. Specific knockdown of SMN in motor neurons caused tremors and severely reduced life expectancy (Frugier *et al.*, 2000). These mice also display denervation of skeletal muscle and motor neuron defects in the spinal cord. Meanwhile muscle specific silencing of SMN leads to severe muscle

defects by 4 weeks causing paralysis and necrosis of muscle cells (Cifuentes-Diaz *et al.*, 2001). Interestingly these mice have morphologically normal motor neurons. This suggests that SMN may also play an important role in skeletal muscle.

Another way of overcoming the lethality of SMN knockout in mice is to introduce a human SMN gene. A mouse model was created with a complete knockout of the mouse Smn gene but with the introduction of the human SMN2 gene in order to replicate the situation found in humans with SMA. These mice have a severe SMA phenotype with reduced numbers of motor neurons and survival of around 5 days. Interestingly the SMN2 copy number can determine the severity of this mouse model, as it does in humans (Hsieh-Li *et al.*, 2000; Monani *et al.*, 2000). Neuron-specific expression of SMN is also able to reduce the severity of the SMA phenotype in this mouse model. Furthermore mice have also been generated that carry the human SMN gene without exon 7 (SMNΔ7). These mice were bred with mice that carried the human SMN2 gene and mouse Smn knockout. This resulted in mice with both the SMN2 and SMNΔ7 genes but lacking any mouse Smn gene (Le *et al.*, 2005). These mice display a slightly less severe SMA-like phenotype and live for around 14 days.

Zebrafish have also been used to model SMA by reducing SMN levels using antisense morpholinos (McWhorter *et al.*, 2003). SMN-deficient zebrafish embryos died during development however developmental defects could still be investigated in the transparent embryos. Motor neuron axons from the spinal cord were truncated and displayed increased branching possibly due to a defect in axon growth. Use of siRNA mediated knockdown of SMN in zebrafish and xenopus which caused severe developmental defects (Winkler *et al.*, 2005). Zebrafish carrying homozygous mutations in the SMN gene died during development and displayed abnormal neuromuscular junctions with reduced synaptic vesicle protein SV2. Drosophila mutants have been discovered with point mutations in Smn causing defects in motor neurons and locomotive ability (Rajendra *et al.*, 2007). These flies had axon defects in motor neurons innervating flight muscles and also displayed actin disorganization. Another drosophila Smn mutant displayed abnormal motor

behaviour due to reduced synaptic transmission and disrupted glutamate receptor clustering (Chan *et al.*, 2003).

Table 1.2 Animal models of SMA

Animal	Genotype	Phenotype	Lifespan	Reference
Mouse	$Smn^{-/-}$;$SMN2^{+/+}$	Severe spinal cord and skeletal muscle defects	4-5 days	(Hsieh-Li *et al.*, 2000; Monani *et al.*, 2000)
Mouse	$Smn^{-/-}$; $SMN2^{+/+}$; $SMN\Delta7^{+/+}$	Less severe than $Smn^{-/-}$; SMN2	13 days	(Le *et al.*, 2005)
Mouse	$Smn^{-/-}$; $SMN2^{+/+}$; $SMN(A111G)^{+/+}$	Moderate	Over 1 year	(Workman *et al.*, 2009)
Mouse	Neuron specific SMN exon 7 deletion	Tremors and muscle denervation	25 days	(Frugier *et al.*, 2000)
Mouse	Muscle specific SMN exon 7 deletion	Severe muscle defects and paralysis	33 days	(Cifuentes-Diaz *et al.*, 2001)
Zebrafish	Smn knock-down	Truncated axons	Larval lethal	(McWhorter *et al.*, 2003)
Zebrafish	siRNA-mediated SMN silencing	Severe developmental complications	Embryonic lethal	(Winkler *et al.*, 2005)
Zebrafish	Mutations smnY262, smnL265, smnG264	Neuromuscular junction abnormalities	Embryonic lethal	(Boon *et al.*, 2009)
Xenopus	siRNA-mediated SMN silencing	Severe developmental complications	Embryonic lethal	(Winkler *et al.*, 2005)
Drosophila	Hypomorphic Smn mutations	Flightlessness, axon defects	Depends on Smn expression levels	(Rajendra *et al.*, 2007)
Drosophila	Smn73Ao zygotic mutant	Progressive loss of mobility	Adult, due to maternal smn	(Chan *et al.*, 2003)

1.1.8 Treatment Strategies for SMA

There is currently no cure for SMA therefore treatment is centred around increasing the quality of life of patients through palliative care and relieving secondary symptoms. Many complications can arise due to the range of muscles that are affected and the various other organs affected by SMN deficiency. The main cause of mortality in type I and II SMA is pulmonary complications that arise from weakness of respiratory muscles (Oskoui & Kaufmann, 2008). Muscle weakness prevents efficient clearance of the lungs which leads to reduced gas exchange and alveolar collapse. Furthermore inefficient lung clearance can cause recurrent infection, however immunisation can prevent the risk of this. Chest physiotherapy used alongside postural drainage procedures and mechanically assisted cough devices can help improve lung clearance. Non-invasive ventilation systems can also be used to improve breathing and reduce the risk of asphyxiation, which is especially dangerous when patients are sleeping (Bach *et al.*, 2000). Non-invasive ventilators are becoming smaller and more user friendly, with soft masks designed to fit young babies (Iannaccone, 2007). As well as reducing the risk of asphyxiation non-invasive ventilation can improve the growth of the lungs and prevent pectus excavatum and avoids the need for tracheostomy (Bach & Bianchi, 2003).

Complications involving the gastrointestinal tract are common in SMA patients including constipation, delayed gastric emptying and gastroesophageal reflux. A combination of drugs can be used to control these symptoms including drugs to neutralize stomach acid, inhibit acid secretions and promote motility. Avoiding patients becoming malnourished is also an important consideration for the care of SMA patients. Type I patients have a higher energy expenditure due to breathing difficulties however fatigue and swallowing dysfunction may discourage feeding (Iannaccone, 2007).

Weakness and immobility caused by SMA leads to problems with posture and spinal defects. Contractures and scoliosis develops gradually and incidence of kyphoscoliosis increases with age and loss of walking ability in type III patients (Oskoui & Kaufmann, 2008). Patients are encouraged to practice weight bearing,

standing and range of motion exercises and undergo physiotherapy to improve posture and reduce or delay onset of spinal defects. However the progression of kyphoscoliosis cannot be stopped and surgery is often required to maintain function and respiratory ability (Oskoui & Kaufmann, 2008). To aid development and increase independence young children can now use motorized wheelchairs to move around. This improves social interaction and enables children to better explore their environment (Jones *et al.*, 2003).

1.1.8.1 Drug Treatment Approaches

Various compounds have been investigated for their ability to increase SMN2 expression in clinical trials. One class of drug being investigated is histone deacetylase (HDAC) inhibitors. Histone acetylation plays an important role in gene expression and HDAC proteins associate with an SMN promoter, therefore it is thought that HDAC inhibitors could increase SMN2 expression levels. Phenylbutyrate, hydroxyurea and valproate are all drugs that have been approved for use in the treatment of other diseases and have been tested in patients and cell lines. Salbutamol and phenylbutyrate have been shown to increase SMN2 levels in patient fibroblasts. Treatment of type II and type III patients with salbutamol resulted in increased body mass, improved forced vital capacity and improved strength (Kinali *et al.*, 2002). Daily treatment with salbutamol has also been tested in a pilot trial of 23 children with type II SMA. Patients displayed significantly increased motor function over 12 months with no severe side effects (Pane *et al.*, 2008). Salbutamol has been shown to cause an increase in SMN2 full length transcript levels in SMA type II and III patients following treatment for 6 months (Tiziano *et al.*, 2010). Interestingly the increase in full length SMN2 was directly proportional to SMN2 copy number. Phenylbutyrate has been shown to increase SMN2 levels in leukocytes of four patients with type II SMA as well as two patients with type III SMA (Brahe *et al.*, 2005). However in a randomized double-blind trial of over 100 children there was no apparent effect on motor function or forced vital capacity (Mercuri *et al.*, 2007).

Treatment with Valproate generated an increase in SMN2 levels in the blood of patients (Brichta *et al.*, 2006) as well as an increase in muscle strength in type III patients (Weihl *et al.*, 2006). Furthermore analysis of the effects of Valproate treatment in different age groups revealed the drug caused the greatest increase in muscle strength in children, with a reduced effect seen in adolescents and no increase in the two adults tested (Tsai *et al.*, 2007). Mice treated with Valproate displayed increased motor function, increased motor neuron survival and increased SMN protein levels. Following 12 months of valproic acid treatments type II and III SMA patients did not gain muscle strength however type II children did show improved activities of daily living and motor function (Darbar *et al.*, 2011). A phase II study of valproic acid treatment in patients with type I, II and III SMA also showed some positive effects. Motor function improved in some type II patients however these were almost all below 5 years of age (Swoboda *et al.*, 2009). Combinational treatment of valproic acid and L-carnitine has been tested in a phase II clinical trial of type II and III SMA patients. Type II patients showed no change in motor function after 6 months of treatments and many suffered from excessive weight gain. However children aged between 2 and 3 years showed improvement of motor function in the first 6 months when adjusted for weight (Swoboda *et al.*, 2010). Type III patients also incurred excessive weight gain with no significant change in motor function (Kissel *et al.*, 2011).

Rizuole, a drug used to treat motor neuron disease, has also been trialled as a treatment for SMA (Russman *et al.*, 2003). Survival in SMA mice was increased following Rizuole treatment however SMA patients that received Rizuole displayed no improvement in motor function. Thyrotropin-releasing hormone therapy has been shown to increase muscle strength and myometry in treated SMA children (Tzeng *et al.*, 2000). Furthermore a single adolescent type III patient treated with Thyrotropin-releasing hormone therapy displayed increased muscle strength and motor abilities with no adverse effects (Kato *et al.*, 2009). Hydroxyurea was trialled in type II and III SMA patients but showed no improvement compared to placebo treated controls (Chen *et al.*, 2010a).

Therefore there has been some success in finding compounds that can increase SMN2 levels and improve motor abilities in SMA patients however these molecules have mainly been tested on type II and III patients and have led to no significant improvement of lifespan or motor function. Whether these therapies can also successfully treat more severe type I patients is still to be elucidated.

1.1.8.2 Gene Therapy Approaches

Gene therapy has been used to successfully increase SMN expression in animal models of SMA. Self-complimentary adeno-associated viral vectors (scAAV) have been used to overexpress SMN resulting in an increase in lifespan and amelioration of the SMA phenotype. Three independent groups have used scAAV9 administered intravenously at postnatal day 1 to rescue the SMA phenotype and improve motor function in mice as well as increasing survival to over 340 days (Foust *et al.*, 2010; Valori *et al.*, 2010; Dominguez *et al.*, 2011). Interestingly administration of scAAV8 into cerebrospinal fluid (CSF) has also been shown to cause increased SMN expression in the spinal cord and increase median survival to 157 days (Passini *et al.*, 2010). Furthermore intramuscular injection of scAAV9 to neonatal SMA mice can also cause widespread transduction of the spinal cord and also peripheral tissues. Astonishingly a single injection of AAV9 expressing SMN to the gastrocnemius muscle was able to increase the median lifespan of SMA mice to 163 days (Benkhelifa-Ziyyat *et al.*, 2013). These recent studies demonstrate the potential of viral mediated gene therapy to rescue the SMA phenotype and point towards a promising method of treating SMA. AAV9 administration at postnatal day one can rescue the SMA phenotype in mice however administration at day 5 only partially ameliorated the phenotype and administration at day 10 had little effect (Foust *et al.*, 2010). This demonstrates the narrow window available for therapeutic intervention in more severe forms of this disease.

1.1.8.3 Gene Repair

One potential strategy for gene therapy to treat SMA is to target the SMN2 gene to drive the production of more full length protein. Antisense oligonucleotides can be used to block splicing in order to promote the inclusion of exon 7 in SMN2. Bi-functional oligonucleotides have been designed to bind to exon 7 with a non-complementary section known as the tail being used to mimic an exonic splice enhancer (Skordis *et al.*, 2003). This leads to SMN exon 7 inclusion in SMA patient fibroblasts. Oligonucleotides which are complementary to regions containing exon splice suppressors have also been used to promote exon seven inclusion and increased full-length SMN mRNA and protein levels in human fibroblasts (Hua *et al.*, 2007). Antisense oligonucleotides administered intravenously in a mouse model expressing the human SMN2 gene caused an increase in SMN2 levels in the liver but not in the spinal cord (Hua *et al.*, 2008). However delivery of oligonucleotides by intracerebroventricular injection was able to rescue tail and ear necrosis in a type III SMA mouse model (Hua *et al.*, 2010). Furthermore delivery of oligonucleotides directly to the CSF increased the level of full length SMN2 in the brains of SMA mice by blocking intronic splice suppressors (Williams *et al.*, 2009). Treated mice displayed improved self-righting abilities although they were still weaker than wild-type littermates.

Oligonucleotides have also been used to modify SMN2 in order to make it more like SMN1, causing an increase in SMN1-like DNA in SMA fibroblasts (DiMatteo *et al.*, 2008). Bi-functional RNA has been used which can block an exonic splice repressor on SMN2 and can also recruit proteins that promote splicing (Baughan *et al.*, 2006; Baughan *et al.*, 2009). Intraventricular injection of this bi-functional RNA increased the lifespan of severe SMA mice. Small nuclear RNA has been developed which also corrects splicing of SMN2 following incorporation into the small nuclear ribonucleoprotein. This increases SMN levels in SMA mice however not to wild-type levels. RNA that drives transplicing has also been used to repair SMN2 by causing the endogenous RNA to be spliced with the therapeutic RNA to create the correct

RNA sequence. This led to increased SMN levels in both patient fibroblasts and SMA mice (Coady *et al.*, 2007; Coady *et al.*, 2008).

1.2 Gene Therapy

The principal of gene therapy is the introduction of nucleic acid to a cell or organism to treat or prevent a disease. This can be achieved by either the introduction of DNA or RNA in order to express a gene, or the introduction of interfering RNA to reduce the expression of a certain gene. Various different gene therapy systems have been developed to aid the delivery of nucleic acids into cells since negatively charged nucleic acid cannot easily pass into cells and is quickly degraded by nucleases *in vivo*. The main hurdles to efficient gene therapy are enabling nucleic acids to reach the target tissue and ensuring it is expressed once it gets there. Different vectors have been developed with this aim in mind and each has varied advantages and disadvantages.

Different characteristics are needed for the treatment of different diseases due to different target tissues and different expression profiles needed. For example for neurodegenerative disorders gene therapy vectors must be able to reach the CNS and also must be able to transfect or transduce non-dividing cells. Furthermore it may be necessary for expression of the target gene to be long lasting in some diseases whilst still maintaining an appropriate safety profile. One major concern with some gene therapy vectors is safety following administration in humans, and this must be considered alongside the other characteristics of gene therapy vectors.

Gene therapy vectors can be divided into two main types, viral and non-viral with many different subtypes in each group. The features of some of these vectors will be discussed in more detail below with particular focus on adeno-associated viral vectors and polymer nanoparticles.

1.2.1 Viral Vectors for Gene Therapy

Various different viral vectors have been developed by harnessing the ability of naturally occurring viruses to enter cells and drive expression of the genes they are carrying. Viruses can be based on either RNA or DNA and can have different routes of internalisation and different methods of gene expression.

1.2.1.1 Retroviral and Lentiviral Vectors

Retroviruses use single stranded RNA that integrates into the host genome upon transduction. They can be characterised as simple or complex depending on the proteins they encode. Lentivirus is a type of complex retrovirus as it has additional genes within a double stranded RNA genome.. These viruses express the gag gene encoding structural proteins, pol gene encoding enzymes such as those for reverse transcription and the env gene encoding viral envelope proteins (Escors & Breckpot, 2010). The viral genome also contains two long terminal repeats (LTR) required for reverse transcription and integration into the host genome. Simple retroviruses are unable to transduce non-dividing cells such as post-mitotic mature neurons, and are therefore unsuitable for treating neurological diseases (Lewis & Emerman, 1994). Retroviruses initiate transduction through host genome integration to cause persistent gene expression. This causes a risk of insertional mutagenesis but can be useful for tissue culture models and *ex vivo* applications.

Lentiviral vectors can transduce both dividing and non-dividing cells and have therefore been used to transduce neuronal cells (Blomer *et al.*, 1997; Bensadoun *et al.*, 2000; Koerber *et al.*, 2008). Lentiviral vectors have been derived from animals infected with viruses such as the human immunodeficiency virus, simian immunodeficiency virus, equine immunodeficiency virus, feline immunodeficiency virus and bovine immunodeficiency virus. To make these viral vectors safer the majority of the viral genome has been deleted which makes them less immunogenic and stops their ability to replicate (Dull *et al.*, 1998; Zufferey *et al.*, 1998). Other advantages of these viral vectors are their large packaging capacity for target

genes, and expression of up to 44 months due to stable integration into the host genome (Naldini *et al.*, 1996; Blomer *et al.*, 1997; Kordower *et al.*, 2000; Deglon & Aebischer, 2002).

Lentiviral vectors have been previously used to express the human SMN1 gene in SMA fibroblasts and in motor neurons of SMA mice. The LV vector used was pseudotyped with a rabies glycoprotein to enable retrograde transport of these vectors following intramuscular injection (Mazarakis *et al.*, 2001; Azzouz *et al.*, 2004). This demonstrates that LV vectors can successfully transduce motor neurons *in vivo* and the addition of different envelope proteins via pseudotyping can alter mechanisms of uptake. Lentiviral vectors are very useful for *in vitro* studies due to their high efficiency of transduction and long-term expression. These vectors also show promise in the clinic and 67 clinical trials are either completed or on-going using lentiviral vectors (Gene Therapy Clinical Trials Worldwide database, J. Gene Med (Edelstein, 2013)) including two trials aimed at developing therapies for Parkinson's disease.

1.2.1.2 Adenoviral Vectors

Adenoviruses are small non-enveloped viruses with a linear double-stranded DNA genome. Following transduction this genome does not integrate into the host genome but is maintained as a linear episome, leading to transient expression (Hillgenberg *et al.*, 2001). This transient expression is not ideal for treatment of long term neurological disorders without repeat administration. Adenoviral vectors were developed lacking non-essential viral genes following concerns over the immunogenicity of the vector however there was still an immune response to capsid proteins (Kochanek *et al.*, 2001; Liu & Muruve, 2003; Sakhuja *et al.*, 2003; McKelvey *et al.*, 2004). These viral vectors have been shown to transduce cells of the CNS such as neurons and astroglia however toxicity leads to clearance of transduced cells (Thomas *et al.*, 2001; Thomas *et al.*, 2002; Candolfi *et al.*, 2007). This has been utilised for the treatment of cancer but these vectors are not particularly

suitable for treatment of neurodegenerative disorders (Germano *et al.*, 2003; Immonen *et al.*, 2004).

1.2.1.3 Adeno-associated Viral Vectors

Adeno-associated viruses (AAV) are single-stranded DNA viruses which have been found in many animal species including humans and can cause stable expression without any known pathogenicity. Various different AAV have been isolated from human subjects (Blacklow *et al.*, 1967) and presence of AAV DNA appears to be fairly common throughout human populations (Gao *et al.*, 2004). The different types of AAV have been classified into serotypes based on lack of cross-reactivity to neutralizing antibodies. The difference between serotypes can be narrowed down to unique capsid proteins which confer differential receptor binding and tissue tropism. Interestingly by changing the expression of capsid proteins through DNA shuffling novel vectors can be produced with unique cellular uptake profiles (Koerber *et al.*, 2008). Chimeric or mosaic vectors can also be created by combining capsids of various serotypes. Furthermore pseudotyped vectors have been developed which consist of the genome for one serotype enclosed in the capsid from another serotype (Burger *et al.*, 2004; Zincarelli *et al.*, 2008). These vectors are particularly useful for studying the effect of different serotype capsids on transduction efficiency of various tissues.

Different AAV serotypes display tropism for different tissue types, however there is some cross-over of the tissues targeted by various serotypes with all serotypes being able to transduce many cell types. Furthermore the route of delivery can also affect which tissues are transduced due to biological barriers, making it difficult to classify the transduction profile of AAV serotypes. Some studies have analysed the transduction profile of various AAV serotypes following intravenous injection in adult and neonatal mice (Zincarelli *et al.*, 2008; Zhang *et al.*, 2011). In summary many AAV serotypes transduce different tissues following adult IV administration with differing level of efficiency and stability of expression. Overall expression of

luciferase in adults revealed that AAV2, 3, 4 and 5 provided low expression, AAV1, 6 and 8 produce moderate expression and AAV7 and 9 give high expression (Zincarelli *et al.*, 2008). However bioluminescent in vivo imaging does not provide a clear understanding of which serotypes preferentially target different tissues. The three serotypes relevant to this thesis will be discussed in more detail below.

Interestingly following transduction by AAV vectors the viral DNA is often not integrated into the host genome but is maintained episomally (Penaud-Budloo *et al.*, 2008). This has the benefit of avoiding the risks associated with insertional mutagenesis whilst still providing stable, long-term gene expression (Kaplitt *et al.*, 1994; Koeberl *et al.*, 1997). Occasionally vector integration does occur which is often associated with small chromosomal rearrangements and integration into coding regions of the genome (Miller *et al.*, 2002; Nakai *et al.*, 2003; Donsante *et al.*, 2007). However risk of insertional mutagenesis from AAV is thought to be low (Li *et al.*, 2011).

As previously mentioned AAV infection has been found in many human subjects which raises the issue of pre-existing immunity. If a patient already has neutralizing antibodies to a certain AAV serotype transduction efficiency may be low and treatment could cause an unwanted immune response. There appears to be variation between pre-existing immunity for different serotypes, with AAV2 and AAV5 being associated with a high incidence of neutralizing antibodies. AAV7 and AAV8 are considered to have low pre-existing immunity due to low human exposure to these serotypes which were isolated from non-human primates. It may be possible to avoid pre-existing immunity by changing the capsid proteins of AAV vectors.

As with all gene therapy vectors the main hurdle to overcome is achieving a sufficient level of transduction in the target tissue for a therapy to be clinically relevant. Self-complementary vectors have been developed to increase the expression of AAV vectors. These have a duplication of the gene of interest within the vector which can re-anneal once inside the cell which removed the requirement of DNA synthesis by the host cell (McCarty *et al.*, 2001). Self-complimentary vectors therefore can produce quicker and more efficient transduction.

1.2.1.3.1 Adeno-associated Virus Serotype 5

AAV5 was isolated from a human penial wart and sequencing data revealed a relatively low consensus with other AAV serotypes (Bantel-Schaal *et al.*, 1999; Chiorini *et al.*, 1999). The reduced homology is particularly apparent in the capsid proteins suggesting that AAV5 may have a unique mechanism of cell entry. The structure of AAV5 was determined by cryo-electron microscopy and revealed a similar surface topology to AAV2 (Walters *et al.*, 2004). Interestingly however these two serotypes do not bind to the same receptors for endocytosis; AAV2 binds heparin whereas AAV5 binds scalic acid to enter cells by endocytosis of clathrin-coated pits (Kaludov *et al.*, 2001; Bantel-Schaal *et al.*, 2002).

AAV5 can transduce various cell types with high efficiency and generally has a slower onset of expression than other serotypes (Zabner *et al.*, 2000; Chen *et al.*, 2005a; Ogura *et al.*, 2006). Interestingly AAV5 can transduce neurons and astrocytes efficiently following direct injection to the brain or dorsal root ganglia (DRG) (Davidson *et al.*, 2000; Mason *et al.*, 2010; Lin *et al.*, 2011). Furthermore when directly injected into the brain AAV5 is able to spread through the CNS to transduce a greater area than other serotypes (Davidson *et al.*, 2000; Lin *et al.*, 2011). The effect of serotype on the ability of viral vectors to transduce the brain was investigated by comparing three different pseudotyped vectors injected directly into regions of the rat brain (Burger *et al.*, 2004). This study showed that the capsids of serotypes 1 and 5 enabled vectors to transduce larger areas of the rat brain than the capsid from serotype 2. This suggests that capsid proteins influence how well viral vectors can pass through tissue and can determine the distribution of transduction.

1.2.1.3.2 Adeno-associated Virus Serotype 6

AAV6 was isolated as a contaminant of laboratory stock of AAV5, its sequence is very similar to AAV1 apart from the left ITR and p5 promoter which is almost identical to AAV2. This suggests that AAV6 arose from a recombination between

AAV1 and AAV2. Despite some homology to AAV2, AAV6 has distinct characteristics and can transduce cells in the presence of serum from AAV2 transduced animals (Halbert *et al.*, 2000). However AAV6 has an almost identical serology to AAV1 suggesting that they are not technically separate serotypes but do have distinct biological properties.

Like AAV2, AAV6 can bind to heparin sulphate polyglycans on the cell surface to initiate cell binding and internalisation. However AAV6 does not possess the same capsid residues that AAV2 uses to bind heparin. Sialic acid binding is also utilised by AAV6 and AAV1 for the transduction of some cells types. The heparin binding capabilities of AAV6 can be exploited for the purification of AAV6 during manufacture through the use of heparin columns.

AAV6 has been shown to transduce skeletal muscle and the liver with high efficiency and a relatively quick onset of transgene expression peaking at around 4 weeks. When injected intravenously to a mouse model of familial amyotrophic lateral sclerosis (ALS) AAV6 mediated widespread transduction of heart, liver and skeletal muscle, as well as transducing 3-5% of lower motor neurons (Towne *et al.*, 2008). Furthermore AAV6 can also transduce motor neurons by retrograde transport following intramuscular injection, with efficient gene transfer to motor neurons being demonstrated following injection of AAV6 to the gastrocnemius muscle of primates (Towne *et al.*, 2010). Interestingly intramuscular injection of AAV6 to a mouse model of ALS generated efficient transduction to individually targeted motor neuron pools however this was not sufficient to affect disease progression (Towne *et al.*, 2011). This suggests that intramuscular injection of AAV6 may not be sufficient to rescue motor function in SMA.

1.2.1.3.3 Adeno-associated Virus Serotype 9

As mentioned earlier, AAV9 has been used to transduce spinal cord motor neurons following intravenous administration. AAV9-mediated expression of SMN in motor neurons ameliorates the SMA phenotype and extends lifespan in a mouse model.

AAV9 can successfully transduce neurons in the CNS following intravenous administration but can also strongly transduce cardiac tissue and skeletal muscle. Furthermore as mentioned above intramuscular injection of AAV9 has been shown to result in widespread transduction in the spinal cord and also peripheral tissues (Benkhelifa-Ziyyat *et al.*, 2013). The reason for the unique transduction characteristics of AAV9 is likely to be due to variation in capsid surface regions. Specifically, the VR-I and VR-IV amino acids which form surface loops on AAV capsids are arranged into a unique conformation in AAV9, conferring a unique transduction phenotype to this serotype (DiMattia *et al.*, 2012). AAV9 can enter many cell types through binding of unique capsid proteins to galactose (Bell *et al.*, 2012). Interestingly scAAV9 can also mediate transduction of motor neurons in neonatal macaques, which indicates that AAV9 may be successfully used in human patients (Foust *et al.*, 2010). Furthermore fetal administration of AAV9 to macaques can also generate transgene expression in neurons in the central nervous system and also in the peripheral nervous system (Mattar *et al.*, 2013). This raises the possibility of providing prenatal treatment for SMA which may be advantageous for the most severe cases.

1.3 Non-viral Mediated Gene Therapy

Various non-viral methods of delivering gene therapy have been developed with different ways of shielding DNA and gaining entry to the cell. One way of delivering DNA to cells is by forming a complex between DNA and a cationic polymer or a cationic lipid (Merdan *et al.*, 2002). Another way of delivering DNA is by encapsulating the nucleic acid within a vesicle. These can be made with either lipids and are known as liposomes, or with polymers and are known as polymersomes.

As with all gene therapy the limiting factor is transfection efficiency, to achieve a high efficiency vectors must overcome various biological barriers (Roth & Sundaram, 2004). Many non-viral approaches have been developed *in vitro* however transfer to an *in vivo* setting is difficult. For example *in vivo* vectors must be able to arrive at the target tissue with the nucleic acid cargo intact, they must be able to enter cells and facilitate endosomal escape. Finally for delivery of plasmid DNA the DNA must

then travel through the cytoplasm and enter the nucleus before transfection can occur. Polymersomes show much promise for *in vitro* and *in vivo* gene therapy due to their favourable characteristics such as low toxicity, efficient cellular uptake, relatively high circulation time *in vivo* (Bach & Bianchi, 2003; Lomas *et al.*, 2008; Massignani *et al.*, 2009; Lee *et al.*, 2011a; Rodriguez *et al.*, 2013). However since polymersomes are still a relatively new technology there is still much characterisation and optimisation to be done before they can be used successfully to deliver gene therapy for SMA.

1.3.1 Polymersomes

1.3.1.1 Formation of Polymersomes

Polymersomes are hollow vesicles formed from block copolymers that mimic phospholipids that form vesicles in nature. Polymersomes are formed in aqueous conditions by utilising the hydrophobic effect. Using a block copolymer consisting of a hydrophobic part and a hydrophilic part means that when in contact with water the polymers will arrange in a way that shields the hydrophobic blocks from the water and leaves the hydrophilic blocks in contact with the water. The most entropically favourable structure for this is a bilayer with the hydrophobic blocks in the centre of the bilayer and the hydrophilic blocks either side. However a single bilayer leaves the end hydrophobic molecules exposed therefore the bilayer curves into more complex structures (Smart *et al.*, 2008). Various different shapes can be formed such as hollow spherical vesicles as well and cylindrical and spherical micelles that do not have a hollow core. Many intermediate structures can also be formed. The propensity for a certain shape or structure to be formed is determined by various conditions including polymer concentration and rate of formation which can be controlled by temperature. The main factor influencing the structure formed upon self-assembly of block-copolymers is the relative sizes of the two blocks. In the formation of polymersomes the size of the block-copolymer affects how closely it can pack together and therefore the degree of curvature of the membrane and thus the article size generated. This enables the size of the particles produced to be controlled by controlling the block-copolymer length however there is usually still a relatively large size distribution of particles.

Polymersomes can be produced by two general methods, solvent switch or film-rehydration. The first method uses a solvent that both blocks of the copolymer can dissolve in, then the solvent is switched to an aqueous solvent in which only the hydrophilic polymer can be dissolved, driving the formation of vesicles. The second method uses a thin film of polymer which is then rehydrated by stirring of an

aqueous solvent. As polymer comes into contact with the solution bits of polymer breaks off into solution and vesicles are formed. Following polymersome production there are various techniques employed to reduce polydispersity and select polymersomes of a particular size. These methods include sonication, gel permeation chromatography and hollow fibre filtration.

1.3.1.2 Polymersome Characteristics

The advantage of using polymers to form vesicles is the large array of characteristics that can be inferred on the vesicle through polymer chemistry. An interesting and particularly useful property of polymersomes is the toughness of the membrane formed. Polymers used to make polymersomes are much longer than phospholipids used to make liposomes with a higher molecular weight. This means that when the polymersome membrane is formed the polymer chains interdigitate and tangle with each other (Battaglia & Ryan, 2006). This causes polymersomes to have much stronger membranes than liposomes meaning they are less likely to break and are less permeable, therefore they hold their cargo better (Discher *et al.*, 1999).

The most important characteristic of polymersomes for *in vivo* applications is being able to avoid protein adsorption due to their hydrophilic bush exterior. Low protein adsorption enables polymersomes to avoid clearance from the blood stream by avoiding the immune system. Some polymers are known to have low protein adsorption, the most famous being poly(ethylene glycol) (PEG), also known as poly(ethylene oxide) (PEO) (Alcantar *et al.*, 2000). Poly(2-(methacryloyloxy)ethyl phosphorylcholine) (PMPC) also has a very low non-fouling profile, suggesting that polymersomes made of this hydrophillic polymer will be non-toxic (Lewis, 2000; Chen *et al.*, 2005b). By engineering polymersomes with a corona made up of a nonfouling polymer such as PEO or PMPC polymersomes can avoid detection by the immune system and have relatively high circulation times as well as low toxicity.

Polymersomes can also be made to be responsive to their environment by incorporating responsive polymers. The pH sensitive polymer poly(2-(diisopropylamino)ethyl methacrylate) (PDPA) has been used to produce polymersomes that break up at low pH enabling endosomal escape of encapsulated cargo (Du *et al.*, 2005). PDPA is a hydrophobic polymer that becomes deprotonated on the tertiary amine at low pH. Interestingly it has a pKa of around 6.6 and is therefore hydrophobic at physiological pH but becomes hydrophilic at pH5 causing rapid dissociation of the polymersomes. Other polymers have been used to create polymersomes that are sensitive to temperature, oxidative species or hydrolysis. Liquid crystalline polymersomes have been shown to undergo controlled release of cargo upon increasing temperature to around 55˚C however this is unlikely to have any *in vivo* applications. Controlled release can also be achieved by forming polymersomes with hydrolysable polymers that are degraded over a matter of hours or days (Ahmed & Discher, 2004a). Similarly forming polymersomes using a block copolymer with a hydrophobic block that can be oxidised to a hydrophilic block can also enable controlled release of encapsulated cargo. Photo-responsive polymersomes have also been created through encapsulation of dextran. These particles undergo membrane rupture upon exposure to UV light however the biological application for this is unclear (Kamat *et al.*, 2010).

Further to choosing polymers with specific characteristics to produce polymersomes, polymers can be decorated with functionalities that can confer other properties to the polymersomes. The hydrophilic polymer can be conjugated with various molecules either directly or through biotin-avidin interaction. Direct conjugation of a fluorophore to the block copolymer enables polymersomes to be fluorescently labelled to assist tracking of these particles *in vitro* and *in vivo* (Madsen *et al.*, 2011). Functionalizing polymers with biotin enables polymersomes to be formed which can be tagged with a variety of different moieties without changing the polymer chemistry (Weiss *et al.*, 2007).

Peptides can be added to the surface of polymersomes through conjugation to the hydrophilic polymer to affect the uptake profile of polymersomes. By attaching

peptides to the surface of polymersomes that recognise specific cell receptors, cell specific targeting can be achieved. This suggests that polymersomes can be targeted towards specific areas of interest and could enable crossing of the blood brain barrier to achieve CNS delivery. Tissue specific targeting of polymersomes would be very useful for gene therapy as this would reduce the risk of off-target affects and make therapy more specific. Furthermore polymersomes can be decorated with other peptides to improve their stealth properties and increase *in vivo* circulation times (Egli *et al.*, 2011; Rodriguez *et al.*, 2013).

1.3.1.3 Biological Applications

Polymersomes have a wide range of biological applications due to the flexible design and varied characteristics outlined above. Encapsulation of both hydrophilic and hydrophobic particles in the aqueous core and polymer membrane respectively allows polymersomes to be used as a delivery vehicle for many biomacromolecules such as antibodies and drugs as well as nucleic acids for gene therapy. Polymersomes have been used to encapsulate a combination of hydrophilic and hydrophobic cancer drugs with impressive tumour shrinking results (Ahmed *et al.*, 2006a; Ahmed *et al.*, 2006b; Li *et al.*, 2007; Chen *et al.*, 2010b). Proteins and antibodies have also been encapsulated within polymersomes (Wang *et al.*, 2012; Canton & Battaglia, 2013). Polymersomes can also be used for diagnostic purposes and *in vitro* applications through the delivery of fluorophores.

1.3.1.4 Polmersomes for Gene Therapy

Polymersomes can readily enter cells by endocytosis and can encapsulate nucleic acids in their aqueous core making them a promising vehicle for gene therapy. Antisense oligonucleotides and siRNA have been successfully encapsulated into polymersomes and have been delivered to cells leading to transduction (Kim *et al.*, 2009; Jin *et al.*, 2010). Plasmid DNA has been encapsulated within PMPC-PDPA

polymersomes with an estimated 20% of DNA added to the solution being retained within the polymersomes (Lomas *et al.*, 2007). Interestingly at weakly acidic pH the protonated tertiary amine groups of the PDPA block interact with the phosphate groups of DNA. This is thought to aid encapsulation by complexing the DNA to the block copolymer, before the pH is increased to form polymersomes. When the pH is increased to a neutral pH the formation of vesicles is unaffected by the relatively weak binding of DNA to PDPA and the DNA is trapped inside the lumen of these vesicles. Importantly these pH-sensitive polymersomes release around 90% of the encapsulated DNA when pH is dropped to around 6 and then increased again to neutral pH (Lomas *et al.*, 2010). Poly(oligo(ethylene glycol) methacrylate) (POEGMA) has also been used to make a block copolymer with PDPA to form polymersomes. POEGMA-PDPA polymersomes have also been used to encapsulate plasmid DNA, and have been incorporated into large layer-by-layer capsules in order to achieve delivery of a large number of particles at one time (Lomas *et al.*, 2011). Encapsulation and delivery of plasmid DNA by PMPC-PDPA polymersomes has resulted in efficient transfection of Chinese hamster ovary and human dermal fibroblast cells with a GFP reported plasmid (Lomas *et al.*, 2007).

1.4 Aims of the Project

The aim of this project was to develop potential therapies for SMA by investigating different viral and non-viral gene therapy vectors. Furthermore the effect of two potential disease-modifying genes was investigated. This project used 3 AAV vectors and polymersomes to investigate gene therapy for SMA. The project aimed to optimise encapsulation of DNA within polymersomes and assess their ability to mediate transfection. The ability of AAV5 to transduce CNS tissue following neonatal intravenous injection was investigated to determine whether this vector could be used for SMA gene therapy. AAV6 was used to overexpress hnRNP R in a mouse model of SMA with the aim of investigating whether this could rescue the disease phenotype. The effect of PTEN silencing on SMA through AAV9 expression of siRNA was also investigated to determine whether PTEN silencing could improve survival in SMA.

The aims of the project can be summarised as follows:

i. Optimise and validate polymersomes as a gene delivery vehicle to be used to express SMN plasmid DNA *in vitro*.
ii. Assess the ability of AAV5 to transduce CNS tissue following neonatal intravenous delivery in wild-type mice.
iii. Investigate whether AAV6-mediated overexpression of hnRNP R could ameliorate the phenotype of an *in vivo* mouse model of SMA.
iv. Determine whether silencing PTEN through AAV9-mediated expression of siRNA could increase the lifespan of a mouse model of SMA.

Chapter 2

MATERIALS & METHODS

2.1. Materials

2.1.1. Polymer Synthesis

Poly(2-(methacryloyloxy)ethyl phosphorylcholine)$_{25}$-*b*-poly(2-(diisopropylamino)ethyl methacrylate)$_{70}$ (PMPC-PDPA) and rhodamine 6G labelled PMPC-PDPA (Rhd-PMPC-PDPA) were kindly synthesized by Dr Jeppe Madsen and Dr Nicholas Warren by atom transfer radical polymerisation as previously reported (Du & Armes, 2005; Madsen *et al.*, 2011).

2.1.2. DNA Preparation

pCS2+hSMN and pGL4.13[luc2/SV40] (Promega) plasmids were prepared using Qiagen mega prep kit (Qiagen). They were further desalted before use with polymersomes by ethanol precipitation.

2.1.3. PTEN siRNA

To silence PTEN a 19 nucleotide sequence targeting exon 1 of mouse PTEN was used to generate a stem-loop-stem shRNA. The sequences used were as follows:

- siPTEN: 5'-AGATGAGAGACGGCGGCGG-3'
- scrambled-siPTEN: 5'-CCCTCTATCGCGCCCTGCT-3'

2.1.4. Viral Vectors

The production of all viral vectors used for *in vivo* studies was out-sourced; details of companies used and viral titres are as follows:

Table 2.1 List of viral vectors used

Virus	Promoter	Production Company	Titre
AAV6-hnRNP R-HA	CMV	Virapur	4.0E12 vp/ml
AAV6-GFP	CMV	Virapur	1.2E13 vp/ml
AAV5-CMV-hrGFP	CMV	AMT Biopharma	1.23E13 gc/ml

AAV5-CAG-GFP	CAG	AMT Biopharma	3.30E12 gc/ml
AAV9-siPTEN	CMV	University of North Carolina	1.5E12 vp/ml
AAV9-scrambled-siPTEN	CMV	University of North Carolina	2.0E12 vp/ml

vp - virus particles, gc – genome copies

2.1.5. Protein Extraction and Analysis

Lysis of cells was performed using cytoplasmic and nuclear lysis buffer containing 50mM Tris-HCl, 150mM NaCl, 2mM EDTA (ethylenediaminetetraacetic acid, Melford), 1% Igepal CA630 (Sigma) and 0.1% SDS (sodium dodecyl sulphate, Sigma). Extracted protein samples were added to loading buffer (10ml 4x stock: 4ml glycerol (Sigma), 2ml 10% SDS, 0.25mg bromophenol blue (Sigma), 2.4ml stacking gel 4x buffer (see below), and 0.5ml b-mercaptoethanol (Invitrogen)) before being denatured. Polyacrylamide gels were prepared using 4x separating gel buffer (1.5 M Tris base, 13.87mM SDS, pH 8.8) and 4 x stacking gel buffer (0.5 M Tris base, 13.87 mM SDS, pH 6.8), along with 30% acrylamide (Geneflow), ammonium persulfate (Sigma) and TEMED (tetramethylethylenediamine, Sigma). Transfer buffer used for the transfer of proteins onto a polyvinylidene difluoride (PVDF) membrane (Millipore) contained 25mM Tris, 192mM Glycine and 10% v/v methanol. Membrane washes were carried out in TBS-T (0.137 M NaCl, 25.92 mM Tris base, 0.1% Tween20 (Sigma), pH 7.6 and membranes were incubated in blocking solution before addition of antibodies (TBS-T with 5% w/v dried skimmed milk).

2.1.6. Antibodies

Table 2.2 List of antibodies used

Target Protein	Host	Supplier	Cat No.	Use
Primary Antibodies				
SMN	Mouse	BD	610646	WB + IF
α-Tubulin	Mouse	Calbiochem	CP06	WB
GFP	Rabbit	Invitrogen	A11122	IHC + IHF
NeuN	Mouse	Millipore	MAB377	IHF
GFAP	Mouse	Sigma	G3893	IHF
PTEN	Mouse	Santa Cruz	sc-7974	IHF
CGRP	Mouse	Abcam	Ab47027	IHF
GFP-TRITC	Goat	Acris	R1091T	IHF
Secondary Antibodies				
Mouse-HRP	Goat	Bio-Rad	170-6516	WB
Rabbit-FITC	Goat	Jackson	111-095-003	IF + IHF
Mouse-A594	Goat	Invitrogen	A1105	IF + IHF
Mouse-A350	Goat	Invitrogen	A11045	IHF

WB - Western blot, IHC – immunohistochemistry, IF - Immunofluorescence, IHF - immunohistofluorescence.

2.1.7. Spectrophotometry

Assays requiring microplate reader for UV/Vis absorbance measurements or luminescence measurements were performed using a FLUOstar Omega plate reader (BMG Labtech). Fluorescence measurements were recorded using a Varian Cary Eclipse spectrofluorimeter.

2.2. *In Vitro* Experimental Methods

2.2.1. Cell Lines and Cell Culture

HEK293T cells (human embryonic kidney cell line immortalized by the adenoviral E1A/E1B protein and expressing the SV40 large T antigen) were used for uptake assay, toxicity assay and transfection. GM03813 fibroblasts derived from an SMA type 1 patient (Coovert *et al.*, 1997) (Coriell Cell Repository) were also used for transfection. For HEK293T cells, Dulbecco's Minimum Essential Medium (DMEM with 4.5 g/L Glucose, L-glutamine, without Na Pyruvate, Lonza) was used and for fibroblast cell line Minimum Essential Medium Eagle (MEME without L-glutamine, Sigma M5650) was used. Both were supplemented with 10% fetal calf serum (FCS, Biosera), and 100 U/ml of penicillin and 100 µg/ml streptomycin (penicillin G sodium and streptomycin sulphate in 0.85% saline, Invitrogen). MEME was also supplemented with 1% L-glutamine (200mM, Sigma).

2.2.2. Polymersome Production

First $PMPC_{25}$-$PDPA_{70}$ polymer was weighed and dissolved in pH2 PBS to make a starting polymer concentration of 10mg/ml, usually a starting volume of between 4ml and 6ml of polymer solution was used to produce polymersomes. The solution was then filter sterilised and sonicated for 15 minutes to ensure complete dissolution of the polymer. A syringe pump was used to increase the pH by addition of 0.5M NaOH with constant stirring. Plasmid DNA was then added at pH6 again using the syringe pump, to give a final DNA concentration of 50µg/ml, before further addition of 0.5M NaOH until pH7.4 was reached. At this point the solution would appear turbid due to the formation of polymersomes. The solution was then sonicated for 30 minutes in order to reduce polydispersity.

To purify polymersomes by size the solution was separated into 1ml aliquots and centrifuged at various speeds for 20 minutes before re-suspending the pelleted polymersomes in PBS. To separate different sized polymersomes (section 3.2.1.4) the polymersome solution was first centrifuged for 20 minutes at an r.c.f of 500 x *g,* the supernatant was then removed and centrifuged again for 20 minutes at an r.c.f of 2000 x *g*. This process of removing the supernatant and centrifuging again

was repeated at an r.c.f of 5000, 10000, 15000 and 20000 x *g*, all for 20 minutes (table 2.3). Following each centrifugation the pelleted polymersomes were re-suspended in PBS and polymer concentration, DNA concentration and particle size was measured.

Table 2.3 Centrifugations to separate polymersomes by size

	Sample	Centrifuge Speed (r.c.f)	Time (mins)
1	Initial solution of polymersomes	500 x *g*	20
2	First supernatant	2000 x *g*	20
3	Second supernatant	5000 x *g*	20
4	Third supernatant	10000 x *g*	20
5	Fourth supernatant	15000 x *g*	20
6	Fifth supernatant	20000 x *g*	20

2.2.3. Polymersome Characterisation

To characterise the size of nanoparticles produced the polymersome solution was diluted in PBS and size was measured using dynamic light scattering (DLS) (Malvern Zetasizer Nano ZS). To measure concentration fluorescence of rhodamine-labelled polymer was measured using a Varian Cary Eclipse spectrofluorimeter. A calibration curve was made using serial dilutions of Rhodamine-PMPC-PDPA. Each sample was diluted before measuring fluorescence with excitation at 540nm and measurement at 560nm.

2.2.4. Encapsulation Assessment

PicoGreen assay (Quant-iT PicoGreen, Invitrogen) was used to measure the concentration of plasmid DNA encapsulated within the polymersomes as to the manufactures guidelines. For calibration curve serial dilutions of the original sample before purification was used. Polymersomes were centrifuged at an r.c.f of either 5000, 10000 or 20000 x *g* (section 3.2.1.3) and the pelleted polymersomes were re-suspended in PBS in order to remove any free DNA. In the presence of DNA the PicoGreen reagent fluoresces. Fluorescence was measured at 520nm after excitation

at 485nm. To determine levels of DNA encapsulation in different sized polymersomes (section 3.2.1.4) polymersomes were centrifuged as outlined in section 2.2.2, and PicoGreen assay was performed following re-suspension of pelleted polymersomes.

2.2.5. Toxicity Assay

Reduction of 3-(4,5-dimethylthiazol-2-yl)-2,5-diphenyl tetrasodium bromide (MTT, Sigma) by cellular dehydrogenases was used to quantify the number of living cells. MTT (pale yellow substrate) is reduced in metabolically active cells to form insoluble purple formazan crystals. Cells were grown in 24 well plates, when they came to be assayed the growth media were removed, 1ml of 5mg/ml MTT was added to each well and the cells were incubated at 37ºC for 45 minutes. The MTT solution was then removed and 100µl acidified isopropanol was added to solubilize the formazan crystals. The plate was shaken for two minutes before the solution was transferred to a 96 well plate to measure the absorbance. Absorbance was determined at 540 nm and referenced at 630nm.

2.2.6. Luciferase Assay

Cells were grown in 24-well plates and transfected with luciferase. When they were to be assayed the cell growth media was removed, the cells were washed and then resuspended in 100µl PBS. The cell solution was transferred to a 96-well plate and 100µl Luciferin substrate was added (Bright-Glo Luciferase Assay System, Promega) and luminescence was recorded using a FLUOstar Omega plate reader (BMG Labtech).

2.2.7. Real-time Quantitative-PCR

Cells were harvested at the appropriate time and RNA was extracted using the SV-total RNA extraction system (Promega) to the manufacturer's guidelines. The concentration of extracted RNA was then measured using NANODROP1000. cDNA was synthesized from the RNA by reverse transcription using the super-script III first-strand synthesis system (Invitrogen). For QPCR 12.5ng cDNA was added to 10µl 2x SYBR Green Master Mix (Aligent) along with the appropriate forward and reverse primers and H_20 to make a final volume of 20mL. MX3000-P Real-time PCR system was used to perform the QPCR using the following program:

- 95˚C 10 minutes
- 95˚C 30 seconds
- 60˚C 1 minute

} 40 cycles

- 95˚C 1 minute
- 60˚C 30 seconds
- 95˚C 30 seconds

} Dissociation curve

Signal intensity was analysed using the MX3000 software and expression values were normalized to GAPDH.

Table 2.4 Primers used for QPCR

Gene	Primer Sequence	Concentration
SMN	Forward – 5' TGCTGGCTGCCTCCATTT 3'	150 nM
	Reverse – 5' GCATCATCAAGAGAATCTGGACAT 3'	150 nM
GAPDH	Forward – 5' GGAAGCTCACTGGCATGGC 3'	300 nM
	Reverse – 5' TAGACGGCAGGTCAGGTCCA 3'	300 nM

2.2.8. Western Blot

Protein lysates were collected at the appropriate time using nuclear and cytoplasmic lysis buffer supplemented with complete protease inhibitor cocktail (Roche). Protein concentration was then determined by Bradford assay. For HEK cell transfection 5µg protein per sample was used, for SMA fibroblast transfection 15ug protein per

sample was used. Protein samples were denatured in loading buffer by heating at 95ºC for 5 minutes before being loaded on to a 10% SDS-polyacrylamide gel. The gels were electrophoresed in Tris/Glycine/SDS running buffer at 50V for 30 minutes then 1-1.5 hours at 120V. For immunodetection proteins were transferred onto a PVDF membrane (Millipore). The membrane was placed in 100% methanol before being immersed in transfer buffer. The proteins were transferred onto the membrane in cold transfer buffer at 250mA for 1 hour, or at 40mA overnight at 4ºC. Membranes were then blocked in blocking buffer for 30 minutes at room temperature with agitation before being probed with antibodies. Primary antibody solutions were prepared in blocking buffer and secondary antibody solutions were prepared in TBST. Mouse primary antibodies against SMN and α-tubulin were diluted at 1:5000 and incubated at room temperature for two hours with agitation. A goat secondary anti-mouse-HRP antibody was used at a dilution of 1:2000 and incubated for 1 hour at room temperature with agitation. Between antibody incubations the membranes were washed three times for ten minutes in TBST at room temperature with agitation to remove any un-bound antibody. The proteins were visualized using the ECL Plus chemiluminescence detection kit (GE Healthcare) for HRP (horseradish peroxidase). The chemiluminescence was visualized using the G-BOX Image Capture System (G:BOX, Syngene), this was also used for image capture and densitometric analysis using the GeneSys software (GeneSnap and GeneTools, GeneSys software, Syngene).

2.2.9. Immunofluorescence

Immunofluorescence staining was performed on fibroblasts after transfection with SMN plasmid DNA to investigate transfection by polymersomes. Cells were plated onto glass coverslips in 6-well plates at a density of $5x10^4$ cells per well. 72 hours after transfection, the cells were fixed by incubating them in 4% PFA in PBS at room temperature for 15 minutes. Cells were washed with PBS then incubated with blocking solution (0.5% Triton TX-100 (Sigma), 5% normal goat serum in PBS) for 30 minutes at room temperature. Blocking solution was then removed and cells were incubated with anti-mouse SMN antibody (BD, 610646) diluted at 1:1000 in

PBS for 2 hours. After 3x 10 minute PBS washes the cells were incubated with anti-mouse fluorescent secondary antibody with an Alexafluor 594 conjugate (Invitrogen A1105) diluted at 1:200 in PBS for 1 hour at room temperature in the dark. Cells were washed a further 3 times for 10 minutes in PBS and were then mounted on glass slides using Vectashield mounting medium with DAPI. Images were taken with a fluorescence microscope (ZEISS) using OpenLab software (Improvision) at 63x magnification and were analysed using ImageJ software.

2.3. *In Vivo* Experimental Methods

2.3.1. Breeding and Genotyping of Transgenic Mice

For all *in vivo* studies, FVB.Cg-Tg(SMN2*delta7)4299Ahmb Tg(SMN2)89Ahmb *Smn1*^{tm1Msd}/J SMNΔ7 mice (The Jackson Laboratory stock 005025) were used. These are triple mutant mice on a FVB background; they have two transgenes inserted, the full-length human SMN2 gene and a second copy of the human SMN gene lacking exon 7. The mice are also lacking the murine Smn gene (Le *et al.*, 2005). All mice were maintained in a controlled facility in a 12-hour dark-light photocycle with free access to food and water. All *in vivo* experimental work was performed in accordance to the UK Home Office Animals (Scientific Procedures) Act 1986.

Carrier animals were used for breeding, and the offspring were genotyped immediately after birth by PCR to detect presence of the transgene. Tail clips were taken at the day of birth and incubated in 15µl DNA extraction buffer (DNA extraction solution 1.0. Epicentre Biotechnologies) for 1 hour at 65ºC and then inactivated at 98ºC for 5 minutes. The PCR reaction was then performed using this DNA. Three primers were used recognizing Smn with two different reverse primers specific for either the wild-type gene, or the mutated gene.

Table 2.5 Primers used for genotyping

Primer	Sequence	Concentration
Smn Forward	5' CTCCGGGATATTGGGATTG 3'	1.34 µM
Smn Wild-Type Reverse	5' TTTCTTCTGGCTGTGCCTTT 3'	1.34 µM
Smn Targeted-Mutation Reverse	5' GGTAACGCCAGGGTTTTCC 3'	0.5 µM

The PCR reaction consisted of 1ul of template, 1.34µM of forward primer and 1.34µM or 0.5µM of either Wild-type or Targeted-Mutation reverse primer, 5µl PCR

Mix (5x FIREPol Master Mix, Solis BioDyne) and H_2O to a final volume of 25µl. The PCR program was as follows:

- 95˚C 3 minutes
- 95˚C 30 seconds ┐
- 52˚C 30 seconds ┘ 35cycles
- 72˚C 30 seconds
- 72˚C 7 minutes
- 10˚C forever

The PCR product was electrophoresed on a 1.5% agarose gel with 0.5µg/uL ethidium bromide at 140V for 30 minutes. Wild-type animals were expected to have one band at 800bp. Homozygous transgenic animals were expected to have one band at 500bp and hemizygous carriers were expected to have two bands, one at 800bp and one at 500bp. Bands were visualised on a GENi imaging system (Syngene).

2.3.2. Recruiting Experimental Mice

For the AAV6-hnRNP R study (chapter 4) and the AAV9-siPTEN study (chapter 6) litter mates were split equally between treatment groups when possible. For the AAV5-GFP study (chapter 5) wild-type litter mates of the SMNΔ7 mice were used. The sex of the recruited mice was not matched between groups as this was not possible without further PCR which time constraints did not permit prior to injections at post-natal day one.

Power analysis was performed using GraphPad StatMate 2 software to determine the cohort size for the AAV6-hnRNP R study and the AAV9-siPTEN study. This analysis indicated a total sample size of 10 per group was necessary to detect effects of 25% on survival (two-tailed) with a power of 80%. However for the AAV6-hnRNP R

study the experiment was curtailed at n=7 for the AAV6-hnRNP R group and n=5 for the AAV6-GFP group due to the initial findings.

2.3.3. Viral Vector Delivery

Animals were injected in the facial vein the day after birth (post-natal day 1) under gas anaesthesia (IsoFlo, 100% w/w isoflurane inhalation vapour, liquid, Abbott) using anaesthesia apparatus (Burtons). A 10µl 33-gauge Hamilton syringe (ESS Lab) was used to inject 10µl of viral vector solution to each animal (see table 2.5 for dose administered). After injection animals were left a few minutes to recover before being rolled in sawdust from their cage and returned to the cage with their mother.

Table 2.6 Viral vector dose administered

Virus	Titre	Dose
AAV6-hnRNP R-HA	4.0E12 vp / ml	4.0E10 virus particles
AAV6-GFP	1.2E13 vp / ml	1.2E11 virus particles
AAV5-CMV-hrGFP	1.23E13 gc / ml	1.23E11 genome copies
AAV5-CAG-GFP	3.30E12 gc / ml	3.30E10 genome copies
AAV9-siPTEN	1.0E12 vp / ml	1.0E10 virus particles
AAV9-scrambled-siPTEN	1.0E12 vp / ml	1.0E10 virus particles

2.3.4. Behavioural and Clinical Assessment

Mice were weighed and assessed for motor ability daily as well as being scored for signs of distress. Motor ability was assessed using tests characterised previously (El-Khodor *et al.* 2008). Righting reflex was assessed by placing animals on their backs and assessing whether they could turn-over onto their front within 30 seconds. For distress scoring four parameters were taken into account and scored, these scores were then combined to give an overall distress score. The parameters were as follows: appearance, provoked behaviour, percentage weight loss from peak body weight and hind-limb score.

2.3.5. Tissue Collection

Mice were euthanized by intraperitoneal injection of 500mg/kg of sodium pentobarbital (sodium pentobarbital, 20% w/v solution for injections, JML) when the mice were deemed ready for sacrifice.

For histological analysis intracardiac perfusion of cold PBS containing 5 units/mL Heparin (2000 units/mL heparin, Sigma) was immediately performed followed by perfusion with 4% PFA using an *in vivo* perfusion system (AutoMate Scientific). Organs were then collected and incubated overnight in 4% PFA at 4ºC. Spinal cords and brains were further incubated in 30% sucrose in PBS for at least one day before being cryoembedded in optimum cutting temperature medium (OCT, Dako). Muscle tissue was stored in PBS with NaN_3 before being paraffin embedded and sectioned at 8µm.

2.3.6. Histological Analysis

Lumbar spinal cords were sectioned at 20µm and brains were sectioned at 40µm using a Lycia cryostat and mounted onto slides. To analyse AAV5 transduction efficiency 1 in 5 slides were taken throughout the brain and lumbar spinal cord for analysis. This equated to between 10 and 30 lumbar spinal sections being analysed per animal and 13-16 brain sections analysed per animal.

2.3.6.1. Immunohistochemistry

For the AAV6-hnRNP R study (chapter 4) total motor neuron counts were determined by staining sections for Nissl. Sections were incubated in xylene for 5 minutes before being hydrated through 100%, 95% and 70% ethanol. Sections were then washed in H_20 before being incubated in 0.1% Cresyl Fast Violet (BDH). After a brief wash in H_20 sections were differentiated in 95% ethanol for up to 15 minutes (depending on the intensity of staining). The sections were then dehydrated in

100% ethanol for 1 minute and then incubated in xylene for 5 minutes before being mounted onto cover slips using DPX. The motor neurons were counted under a light microscope with help from Dr. K. Ning who was blinded to the treatment groups. Motor neurons were identified by their size and morphology.

Transduction of cells of the brain and spinal cord were assessed by immunohistochemistry to detect cells expressing GFP protein. Vectastain ABC kit (Vector) was used for blocking solutions and secondary antibodies whilst DAB peroxidase substrate kit (Vector) was used to visualise the staining. Tissue was first incubated in 2% hydrogen peroxide in methanol for 20 minutes to block endogenous peroxidase. Sections were then washed in H_20 for 1 minute followed by TBS for 5 minutes. Slides were then incubated with normal serum in TBS for 30 minutes at room temperature to block any non-specific binding. Slides were then incubated with a polyclonal rabbit antibody against GFP (Invitrogen) at a dilution of 1:500 in TBS for 1 hour at room temperature. After this incubation sections were washed twice for 5 minutes with TBS before being incubated with the biotinylated secondary antibody for 30 minutes at room temperature. Cells were then washed again for 2x 5 minutes in TBS before being incubated with the ABC reagent for 30 minutes at room temperature. The slides were washed again for a further 2x 5 minutes in TBS then incubated in diaminobenzidine (DAB) at room temperature for 10 minutes. Finally cells were washed in H_20 for 5 minutes before being dehydrated through 70%, 95% and absolute ethanol, and then placed in xylene before being mounted with coverslips using DPX. Slides were then analysed using an Olympus BX61 microscope with Cell^R (Olympus) software.

2.3.6.2. Immunofluorescence

Immunofluorescence was used to stain for neuronal or astrocyte markers (NeuN and GFAP respectively) as well as for GFP and PTEN. Slides were washed 3 times for 10 minutes with PBS before being incubated with 5% normal goat serum (NGS) and 0.5% Triton X-100 (Sigma) in PBS for 2 hours at room temperature. For the AAV5-

GFP study (chapter 4) two primary antibodies were then incubated together, rabbit antibody against GFP (Invitrogen) alongside either a mouse antibody against GFAP (Sigma) or mouse antibody against NeuN (Millipore), all diluted 1:500 in PBS and incubated overnight at 4ºC. Sections were then washed three times in PBS before secondary antibodies were added. Secondary antibodies used were a goat FITC-conjugated anti-rabbit antibody (Jackson), and a goat Alexafluor 594-conjugated anti-mouse antibody (Invitrogen). Secondary antibodies were diluted 1:200 in PBS and incubated at room temperature for 1 hour before being washed in PBS 3 times for 10 minutes.

For the AAV9-siPTEN study (chapter 5) spinal cord sections were stained with a rabbit primary antibody against CGRP diluted at 1:500 and a goat Alexa-Fluor594-conjugated anti-mouse antibody as described above. CGRP-positive motor neurons were counted with help from Dr. Ke Ning who was blinded to treatment groups. To assess transduction and PTEN depletion in the spinal cord triple immunofluorescence was performed. Sections were stained with a mouse antibody against PTEN (Santa Cruz), a goat antibody against GFP with a TRITC conjugate (Acris) and a rabbit antibody against CGRP (Abcam). These primary antibodies were diluted 1:200 and incubated overnight at 4ºC. Secondary antibodies used were a goat Alexafluor 350-conjugated anti-mouse antibody (Invitrogen) and a goat FITC-conjugated anti-rabbit antibody (Jackson). These secondary antibodies were diluted 1:200 and incubated at room temperature for 1 hour. Washing and blocking steps were performed as detailed above.

Slides were mounted with Vectashield hard-set mounting medium with DAPI (Vector laboratories). Images were taken with a fluorescence microscope (ZEISS) using OpenLab software (Improvision) at 63x magnification and were analysed using ImageJ software. Confocal microscope images were taken using a Leica SP5 microscope system.

RESULTS

Chapter 3

Polymersomes as Gene Therapy Vectors

3.1 Introduction

Polymersomes are designed to mimic vesicles found in nature using block copolymers rather than phospholipids to create a sphere consisting of a polymer membrane and a hollow core (Discher *et al.*, 1999). Vesicles form in aqueous conditions when a block copolymer consists of a hydrophilic block and a hydrophobic block. The hydrophobic block minimises contact with water molecules by being in close proximity to other hydrophobic blocks, whilst the hydrophilic block repels other blocks in order to be in contact with water (Tanford, 1979). This behaviour causes a membrane to be formed, with the need for the hydrophobic blocks at the end of the membrane to be shielded from water causing curvature of the membrane, forming vesicles, spherical micelles and tubular micelles (Discher & Eisenberg, 2002). The propensity of block copolymers to form spherical or tubular micelles or vesicles is determined by the ratio between the soluble and insoluble blocks, or the hydrophilic and hydrophobic blocks. Therefore the structures formed can effectively be tuned by controlling the respective lengths of each part of the copolymer. The block-copolymers used to form polymersomes have a higher molecular weight than phospholipids, and the long polymer chains naturally interlink with each other (Battaglia & Ryan, 2005) therefore the particles produced have more resilient membranes than liposomes, creating improved mechanical properties (Discher *et al.*, 1999).

As well as affecting the structure formed changing the polymers used to make up the block-copolymer can change how polymersomes can react to or interact with their environment. Polymersomes can be made to be responsive to various external stimuli such as hydrolysis (Ahmed & Discher, 2004b), oxidative species (Napoli *et al.*, 2004), temperature (Agut *et al.*, 2010; Hocine *et al.*, 2013) and pH (Du *et al.*, 2005; Giacomelli *et al.*, 2006). Furthermore the nature of the polymer used can affect how it interacts with cells and the circulation half-life of polymersomes *in vivo*. Here we use block-copolymer with a hydrophilic poly(2-(methacryloyloxy)ethyl phosphorylcholine) (PMPC) block which has impressive nonfouling properties (Lewis,

2000), coupled with a hydrophobic poly(2-(diisopropylamino(ethylmethacrylate) (PDPA) block that is pH sensitive (Du *et al.*, 2005).

PMPC-PDPA polymersomes have been shown to enter many cell types by endocytosis (Massignani *et al.*, 2009). Once endocytosed the pH sensitive nature of these polymersomes causes disassembly in the acidic environment of the endosome (Lomas *et al.*, 2008; Massignani *et al.*, 2009). This dissociation of the polymersome into individual block-copolymer units releases approximately 1700 copolymer chains (for a 200nm polymersome) as well as any encapsulated cargo into the endosome, causing osmotic shock and disruption of the endosome (Lomas *et al.*, 2008). This enables encapsulated molecules to escape the endosome and be released into the cytoplasm. The aqueous core of polymersomes enables the encapsulation of various biomacromolecules including antibodies, drugs, and nucleic acid (Ahmed *et al.*, 2006b; Lomas *et al.*, 2007; Kim *et al.*, 2009; Canton *et al.*, 2013). Moreover the hydrophilic polymer brush of the polymersomes can be decorated with ligands such as peptides that can influence uptake and targeting to specific cell types ((Broz *et al.*, 2005; Weiss *et al.*, 2007; Egli *et al.*, 2011)). Furthermore this hydrophobic membrane allows the encapsulation and delivery of hydrophobic molecules (Ahmed *et al.*, 2006b; Li *et al.*, 2007).

The most efficient method of gene therapy is generally considered to be through the use of viral vectors. Viruses have evolved to enter cells and use the machinery of the nucleus to express their own genes therefore they are an ideal candidate for delivery of therapeutic genes. Although viral vectors used for gene therapy have modified genomes making them non-pathogenic and unable to replicate, they can still be detected by the immune system (Xiao *et al.*, 2000). Furthermore since viral vectors are based on naturally occurring viruses many people harbour antiserum against certain serotypes of adeno-associated viruses (Chirmule *et al.*, 1999). The presence of antiserum against a viral vector can reduce transgene expression and may cause unwanted side effects. Furthermore generation of antibodies following administration of viral vector mediated gene therapy will reduce the effect of repeat delivery (Mastakov *et al.*, 2002). Therefore it may be useful to develop non-viral

methods of delivering gene therapy that can avoid immune response. Polymersomes have previously been used to encapsulate DNA and deliver it to cells to cause efficient transduction (Lomas *et al.*, 2007).

Polymersomes are a relatively new technology with only a limited amount of research published regarding plasmid DNA encapsulation. Therefore, much optimisation is required to achieve a standardised method of production of nanoparticles with high encapsulation efficiency. Various methods of polymersome production were trialled before deciding on the method detailed in section 3.2.1.1 using a syringe pump and magnetic stirrer. The ability of these nanoparticles to efficiently encapsulate plasmid DNA and cause transfection then needed to be verified and optimised. Therefore various methods of encapsulating plasmid DNA and improving encapsulation and transfection efficiency were tested before using the purification by centrifugation method detailed below.

This aim of this section was to optimise encapsulation and transfection efficiency of $PMPC_{25}$-$PDPA_{70}$ polymersomes and test their ability to deliver gene therapy for SMA. Here centrifugation was used to sort polymersomes by size and investigate the effect of particle size on encapsulation. Furthermore polymersomes were used to deliver a reporter luceriferase gene in HEK293T cells and to deliver SMN plasmid DNA to an *in vitro* model of SMA.

3.2 Results

3.2.1 Polymersome Characterisation

3.2.1.1 Cell Viability Following Incubation with Polymersomes

Polymersomes were produced by pH switch. Briefly the $PMPC_{25}$-$PDPA_{70}$ copolymer was dissolved at pH2 before being raised to pH6 using a syringe pump to control addition of NaOH whilst the solution was stirred using a magnetic stirrer. At pH6 plasmid DNA was added to the solution; at this point the polymers are still completely dissolved. NaOH was again added until the solution reached pH7.4 by which point the PDPA block would become deprotonated and thus become hydrophobic, resulting in polymersome formation. All characterisation experiments were performed with polymersomes encapsulating luciferase plasmid DNA. This is to control for any affect the plasmid may have on the polymersome formation, size distribution or toxicity. Furthermore all characterisation experiments were performed using polymersomes containing 10% rhodamine-labelled PMPC-PDPA, which enabled the polymer concentration to be easily measured, as well as uptake to be assessed by fluorescent microscopy.

We first aimed to assess how polymersomes affected cell viability and to ascertain the ideal working concentration to use. To this end we carried out an MTT assay following incubation of HEK293T cells with polymersomes. Rhodamine-labelled PMPC-PDPA polymersomes encapsulating luciferase DNA were produced as described earlier and HEK293T cells were treated with six different concentrations of polymersomes. 48 hours later MTT assay was performed to measure cell viability. As polymer concentration increased cell viability decreased (fig. 3.1), becoming statistically significant at 1.0mg/ml (one-way ANOVA, Dunnett's multiple comparison test). Cell viability of 80% was seen for a final polymer concentration of 0.5mg/ml,

therefore this was chosen as the maximum concentration to be used for further experiments.

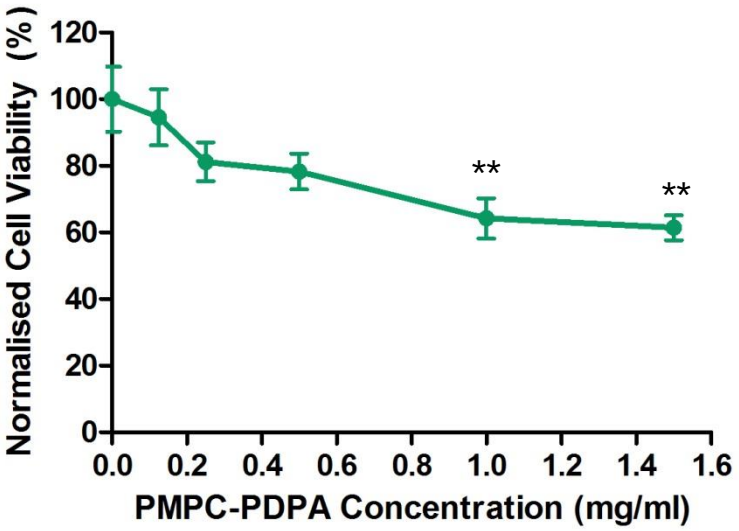

Figure 3.1 HEK293T cell viability after treatment with Rhd-PMPC-PDPA. HEK293T cells were incubated for 48 hours with different amounts of Rhd-PMPC-PDPA polymersomes before MTT assay was performed. Cell viability decreased with high levels of polymersomes. n=3 ** $p<0.01$ versus untreated control, one-way ANOVA with Dunnett's multiple comparison test.

3.2.1.2 Uptake of Rhodamine-labelled Polymersomes by HEK293T Cells

It has been shown that many cell lines can easily uptake PMPC-PDPA polymersomes, with the only cell type not displaying any uptake being red blood cells (Massignani *et al.*, 2009). To demonstrate the uptake of polymersomes by HEK293T cells the cells were incubated with 0.5mg/ml of polymersomes containing 10% rhodamine-tagged PMPC-PDPA. 48 hours later cells were washed and fixed with 4% PFA before being imaged by fluorescence microscopy. This study revealed that approximately 100% of cells displayed fluorescence following treatment with fluorescent polymersomes, showing that these polymersomes are readily internalised by the cells (fig. 3.2). Furthermore fluorescence appeared to be spread throughout the cytoplasm with much less fluorescence seen in the nucleus. Uptake of rhodamine-labelled polymersomes has previously been extensively studied, therefore this was

not further investigated here (Lomas *et al.*, 2008; Massignani *et al.*, 2009). Confocal microscopy of single HDF cells using pH-sensitive and non-pH-sensitive polymersomes demonstrated that PMPC-PDPA polymersomes are efficiently endocytosed and the fluorescent polymer is spread throughout the cytoplasm following endocytosis (Massignani *et al.*, 2009).

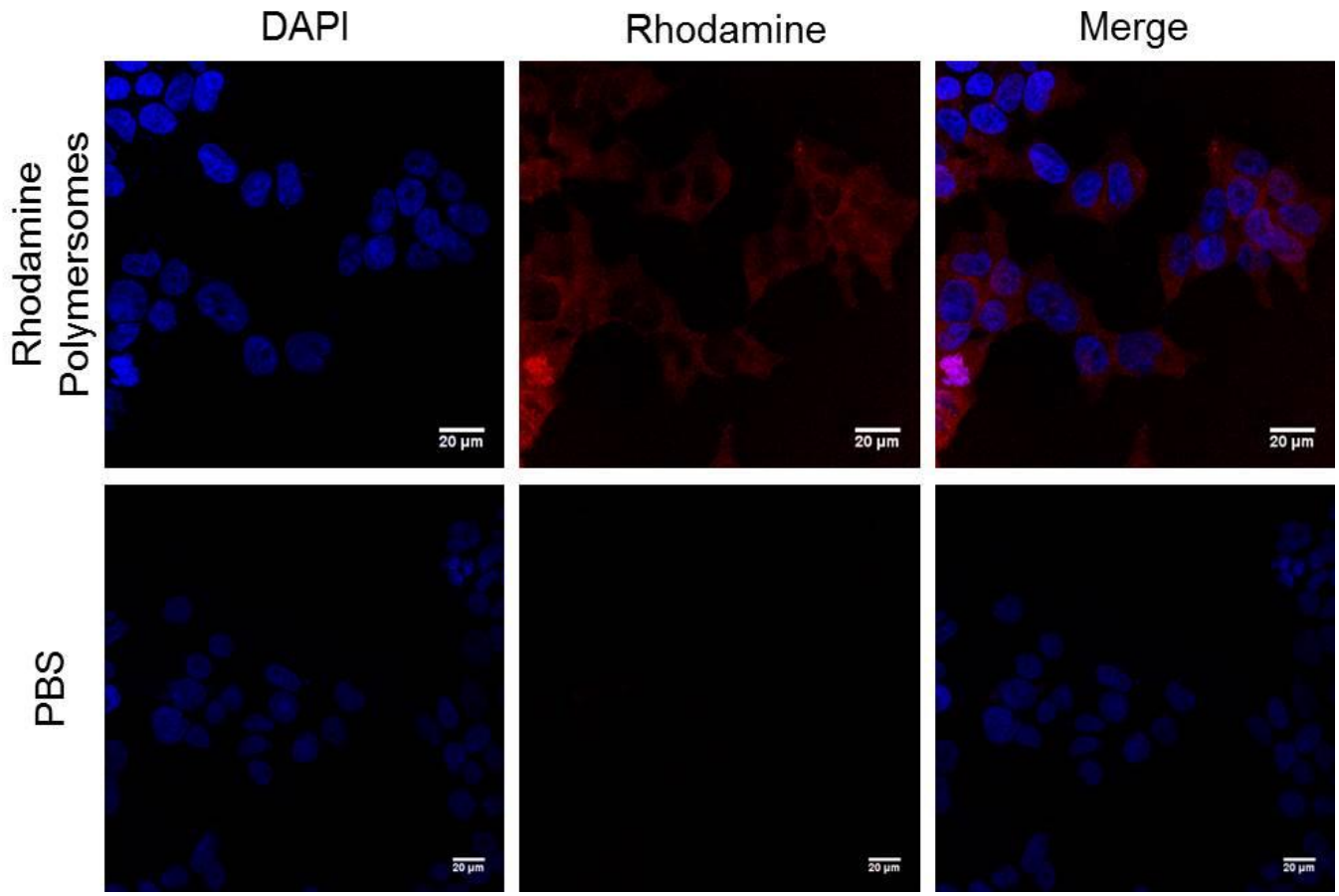

Figure 3.2 Uptake of rhodamine-labelled polymersomes in HEK293T cells. HEK293T cells were incubated with Rhd-PMPC-PDPA polymersomes for 48 hours before being fixed with 4% PFA and imaged for fluorescence. Cells treated with rhodamine-labelled polymersomes display fluorescence following uptake of the polymersomes. Scale = 20µm.

3.2.1.3 Encapsulation of Plasmid DNA in Polymersomes

Production of polymersomes by the method detailed above (section 3.2.1.1) results in a polydisperse solution with a wide size distribution. Due to the relatively large size of plasmid DNA to the polymersome core we suspected that there may be polymersomes that are too small to encapsulate DNA, as well as micelles that are unable to encapsulate DNA due to their lack of lumen. Moreover we hypothesized that larger polymersomes would contain greater amounts of plasmid DNA. We thus sought a simple way of separating size fractions of polymersomes and hypothesized that in doing so we may also be able to select only the polymersomes containing high amounts of plasmid DNA.

To test this hypothesis we first centrifuged polymersomes at an r.c.f of either 5000, 10000 or 20000 x *g*. We then collected the resulting pellet of polymersomes, re-suspended it, and measured the polymer concentration and DNA concentration. One advantage of centrifuging the polymersomes is that any free plasmid DNA remains in the supernatant, so the amount of encapsulated DNA can be easily measured. Furthermore the tough nature of polymersomes means that they are not damaged by centrifugation at high speeds. A third advantage of centrifugation is that it efficiently removes any micelles, which cannot contain DNA.

Analysis of polymer concentration showed that at higher speed more polymer was pelleted, as expected (fig. 3.3 A). There was also an increase in the concentration of pelleted DNA (fig. 3.3 B), however when normalised to the amount of polymer pelleted the overall concentration of encapsulated DNA falls (fig. 3.3 C). A significant difference in the amount of encapsulated DNA was seen in polymersomes collected following centrifugation at an r.c.f of 5000 x *g* compared to those collected following centrifugation at an r.c.f of 20000 x *g* ($p<0.01$, one-way ANOVA) Therefore the polymersomes collected following centrifugation at slower speeds contain more DNA. The effect seen here was modest but significant and showed that plasmid DNA could be efficiently encapsulated within polymersomes and led us to investigate further the possibility of using centrifugation to separate polymersomes by size.

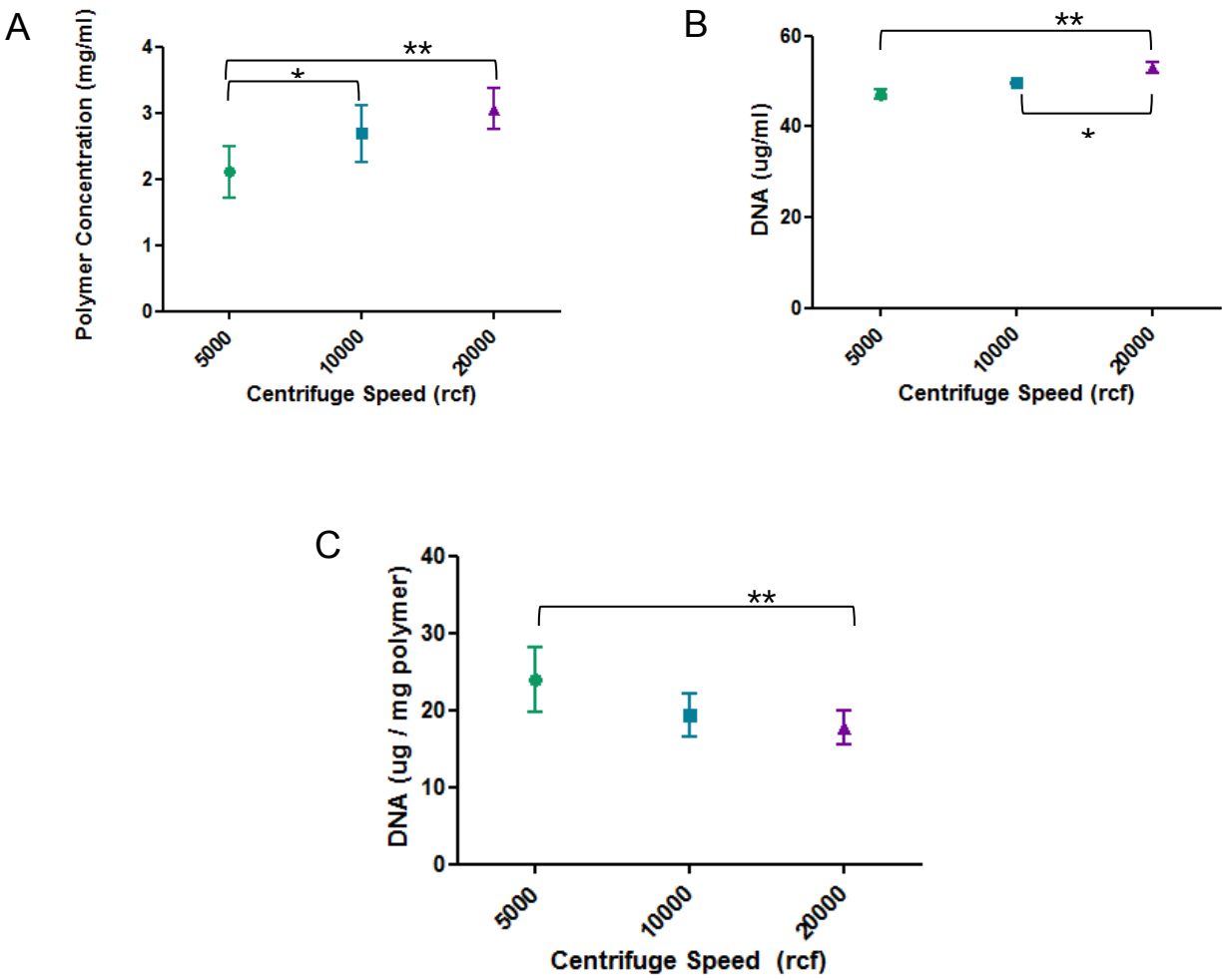

Figure 3.3 Encapsulation of plasmid DNA in polymersomes. Following polymersome formation, they were centrifuged at three different speeds. The polymer concentration **(A)** and DNA concentration **(B)** in the pelleted polymersomes was measured and used to calculate the amount of encapsulated DNA in each sample **(C)**. n=3. * $p<0.05$, ** $p<0.01$, one-way ANOVA, Tukey's multiple comparison post-hoc test.

3.2.1.4 Using Centrifugation to Sort Polymersomes by Size

To investigate further the use of centrifugation to separate different sized polymersomes we again made rhodamine-labelled polymersomes encapsulating plasmid DNA. The polymersome solution was centrifuged at an r.c.f of 500 x *g*, the supernatant removed and centrifuged again at an r.c.f of 2000 x g. The supernatant was removed and went through four further centrifugations at increasing speeds. Following each centrifugation the pelleted polymersomes were fully re-suspended and the particle size was measured by dynamic light scattering (DLS). Unfortunately the DLS software could not accurately determine the size of polymersomes collected following the first centrifugation at 500rcf. This may be due to the

presence of particles that are settling due to their large size, or due to the presence of non-spherical particles.

Size distribution datashowed a decrease in size distribution following each centrifugation (fig. 3.4 A). Furthermore the mean particle diameter of polymersomes collected after centrifugation at an r.c.f of 2000 x *g* was significantly higher than the mean diameter of particles collected following centrifugation at an r.c.f of 10000 x *g* ($p<0.01$, one-way ANOVA) (fig. 3.4 B). Therefore centrifugation is able to separate polymersomes by size, with the earlier, slow centrifugations pelleting polymersomes with higher average diameters than particles collected from later, faster centrifugations (fig. 3.4 B).Centrifugation does not completely separate size fractions in the solution but there is a clear shift towards smaller sized particles with higher speed centrifugations, suggesting that a high proportion of the largest particles have been removed following slow speed centrifugation.

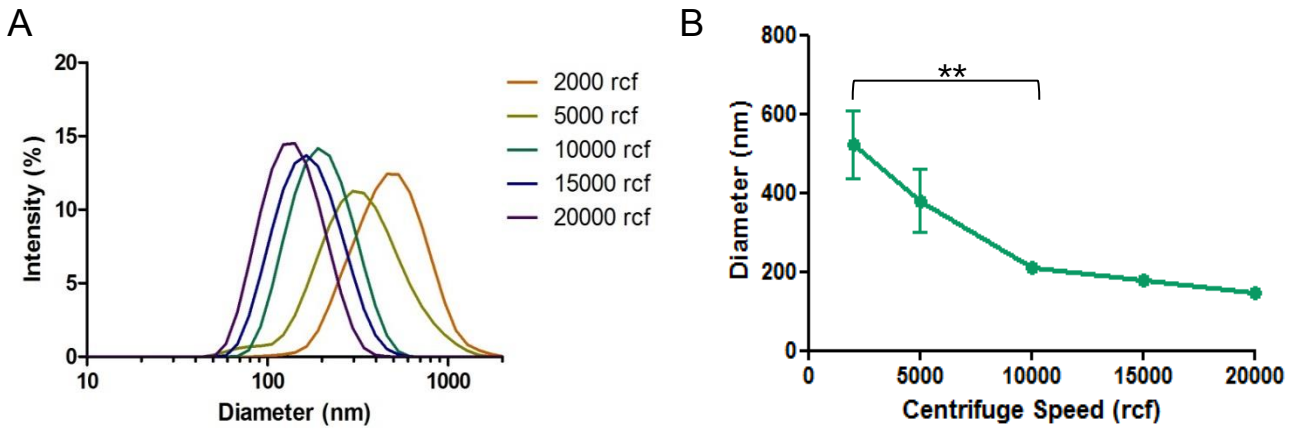

Figure 3.4 Size sorting of polymersomes by centrifugation. Polymersomes were centrifuged at increasing speeds from 500 to 2000g. After each centrifugation step the supernatant was removed and centrifuged again at a higher speed. The polymersomes pelleted after each centrifugation were re-suspended and size was measured by DLS. **A:** size distribution by intensity for each centrifuge fraction. **B:** average particle diameter for each centrifuge fraction. Data shows mean diameter (nm) ± SEM. n=3. ** $p<0.01$ One-way ANOVA, Tukey's multiple comparison post-hoc test.

3.2.1.5 Size Dependent Encapsulation of DNA

Once we had ascertained that centrifugation could separate different sized polymersomes we used the different polymersome fractions collected to assess how particle size affected the amount of encapsulated luciferase plasmid DNA. Using the same set-up described above (section 3.2.1.1), the polymersomes collected from each round of centrifugation were assessed for polymer concentration and DNA concentration. Analysis revealed that the amount of encapsulated DNA, when normalised to polymer concentration, was by far superior in the polymersomes centrifuged at the slowest speed (fig. 3.5 A). The concentration of encapsulated DNA then decreased in polymersomes collected after further centrifugation of the supernatants at increasing speeds. When the amount of encapsulated DNA (normalised to polymer concentration) is plotted against the average diameter of polymersomes measured above, a clear relationship can be seen between polymersome diameter and the amount of DNA that is encapsulated (fig. 3.5 B).

Note that as in figure 3.4 the data from polymersomes collected after centrifugation at 500 rcf is not included in figure 3.5 as the size distribution data could not be accurately calculated (as mentioned in section 3.2.1.4). Furthermore there was a large amount of polymer left in the supernatant following the final centrifugation at 20000 rcf that has been excluded from this analysis, this is expected to contain mainly micelles and small polymersomes as well as free DNA.

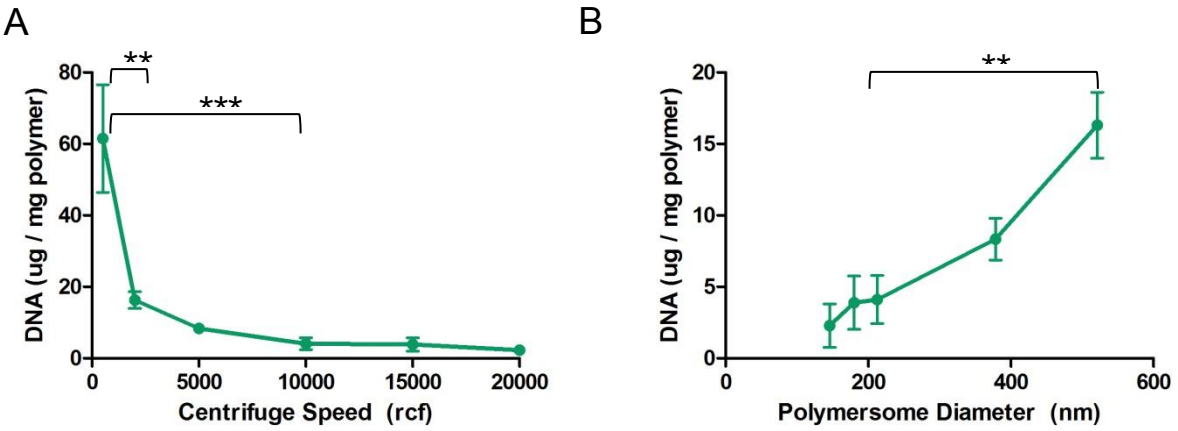

Figure 3.5 Encapsulation of DNA in different polymersome fractions. Polymersomes encapsulating luciferase DNA were centrifuged at increasing speeds. After each centrifugation the DNA and polymer concentration of the pelleted polymersomes was measured **(A)**. The amount of encapsulated DNA for each fraction was compared to the average particle diameter for that fraction **(B)**. n=3. ** p<0.01, *** p<0.001, one-way ANOVA with Tukey's multiple comparison post-hoc test.

3.2.2 Polymersomes as DNA Delivery System

3.2.2.1 Luciferase Transfection with Polymersomes Sorted by Centrifugation

To assess the transfection efficiency of encapsulated DNA, HEK293T cells were incubated with polymersomes collected following size sorting by centrifugation. The cells were incubated for 48 hours with 0.5 mg/ml of polymersomes collected after each centrifugation. Luciferin substrate was then added and luminescence was detected. The highest level of luminescence was seen in cells transfected with polymersomes collected following the slowest centrifugation (fig. 3.6 A). The amount of luminescence detected then decreased as the centrifuge speed used to collect the polymersomes increased. Moreover when luminescence was plotted against the amount of encapsulated DNA measured in each sample of polymersomes used there is a linear relationship between the amounts of encapsulated DNA and the level of transfection seen (fig. 3.6 B).

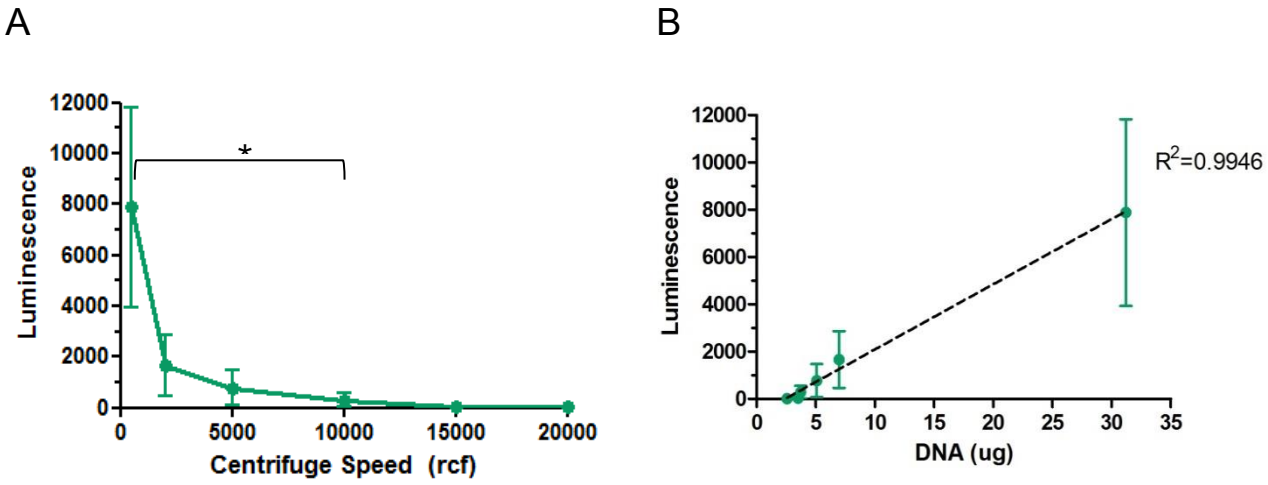

Figure 3.6 Luciferase transfection with different polymersome fractions. Polymersomes collected following each centrifugation were used to transfect HEK293T cells. The cells were incubated with the 0.5mg of various polymersome fractions for 48 hours before luciferin substrate was added and luminescence was detected **(A)**. Luminesce detected was plotted as a function of the amount of encapsulated DNA in each fraction used **(B).** n=3. * $p<0.05$ One-way ANOVA with Turkey's multiple comparison post-hoc test.

3.2.2.2 Using Polymersomes to Overexpress SMN

Following successful transfection of HEK cells with luciferase reporter plasmid we further investigated whether polymersomes could be used to deliver SMN gene therapy for SMA. We therefore prepared polymersomes encapsulating plasmid DNA encoding the human SMN gene. The polymersomes were then centrifuged at an r.c.f of 10000 x *g* to collect the majority of DNA containing polymersomes and exclude empty polymersomes. The pelleted polymersomes were used to transfect HEK293T cells. After incubating the cells for 48 hours the cells were harvested for protein and mRNA for Western blot and QPCR analysis respectively. Cells were also transfected with SMN plasmid DNA alone using calcium phosphate as a positive control. Western blot was performed on protein samples (fig. 3.7 A) and densitometric analysis revealed a 2.6-fold increase in SMN protein levels following transfection with polymersomes compared to untransfected controls (fig. 3.7 B, n=3, $p<0.05$, t-test). For comparison calcium phosphate transfection resulted in a 7.8-fold increase in SMN protein expression. Real-time QPCR was performed on mRNA extracted from transfected HEK293T cells and revealed a 38-fold increase in SMN mRNA following transfection with SMN plasmid DNA-loaded polymersomes (fig. 3.8, n=3, $p<0.05$, t-test). This compares to a 158 fold increase in SMN mRNA following transfection using calcium phosphate.

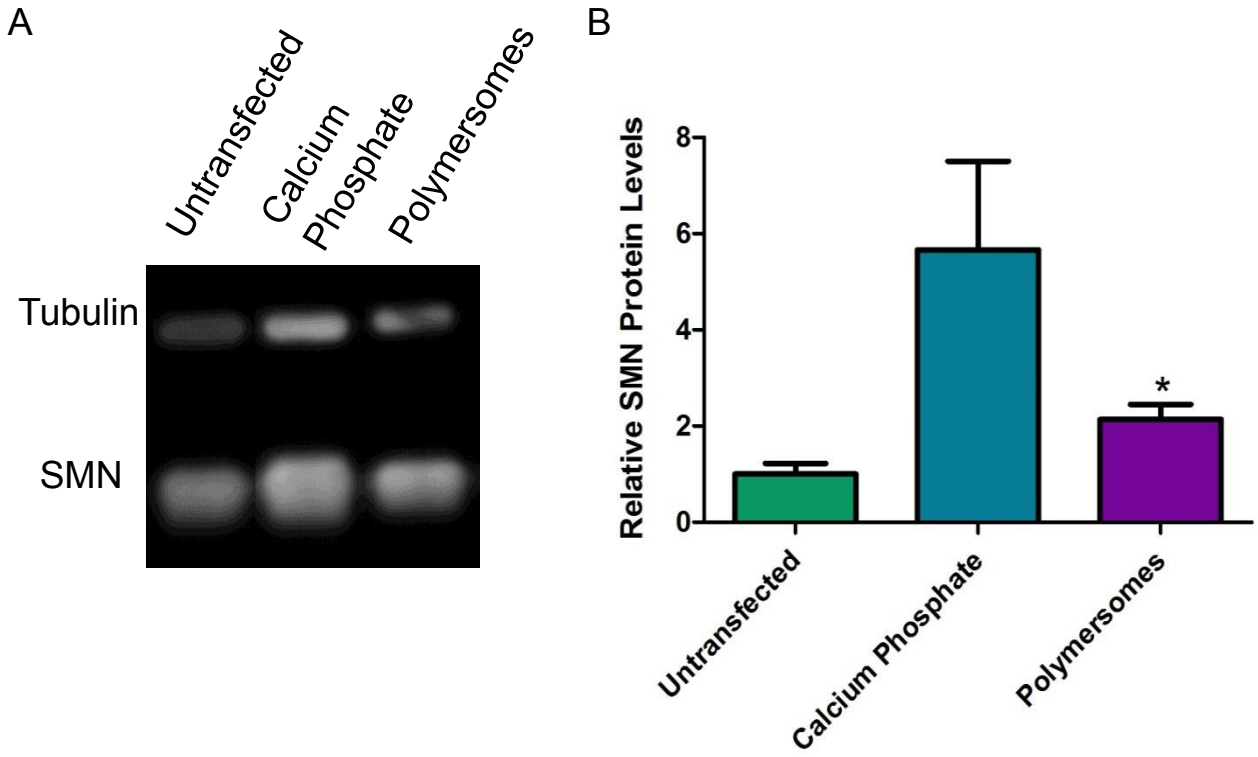

Figure 3.7 Polymersome-mediated SMN transduction in HEK293T cells. HEK293T cells were incubated with polymersomes encapsulating SMN plasmid DNA for 48 hours and protein levels were assessed by Western blot **(A)**. Densitometric analysis **(B)** revealed SMN levels were increased by an average of 2.1-fold following transfection with polymersomes compared to untransfected cells. n=3. * p<0.05 t-test versus untransfected.

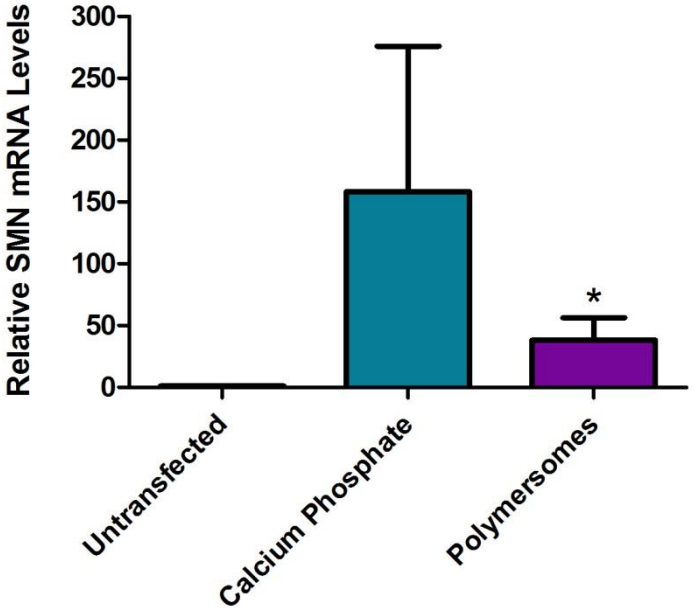

Figure 3.8 Increased levels of SMN mRNA following transfection by polymersomes. HEK293T cells were incubated with polymersomes loaded with SMN plasmid DNA. 48 hours post transfection mRNA levels were measured using QPCR. Data represents ddCt values relative to GAPDH and normalised to untransfected cells. Transfection with polymersomes increased SMN mRNA levels by 35.8 fold compared to untransfected. n=3. * p<0.05 t-test versus untransfected with Mann-Whitney post-hoc test.

3.2.2.3 Overexpression of SMN in an *In Vitro* Model of SMA

We used a fibroblast cell line derived from a SMA type 1 child to establish a proof-of-concept for SMN replacement using polymersomes Polymersomes encapsulating SMN plasmid DNA were incubated with the cells for 72 hours before mRNA was extracted. QPCR revealed a 367-fold increase in SMN mRNA when normalised to GAPDH mRNA expression following treatment with polymersomes (fig. 3.9, n=3, $p<0.05$, t-test). Again transfection using calcium phosphate was used for comparison which led to an increase in SMN mRNA expression of 2378-fold (fig. 3.9).

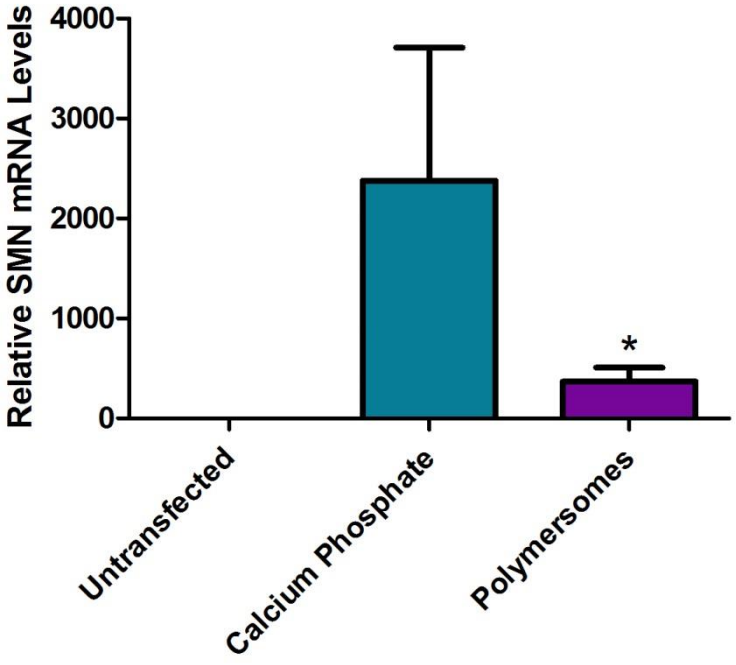

Figure 3.9 Polymersome-mediated SMN gene replacement in type I SMA fibroblasts. SMN-deficient fibroblasts were transfected with polymersomes loaded with SMN plasmid DNA. 72 hours later mRNA was extracted, RT-PCR was performed and the resulting cDNA was used for QPCR. Analysis revealed an increase in SMN mRNA of over 600-fold compared to untransfected cells. n=3 * $p<0.05$ t-test versus untransfected with Mann-Whitney post-hoc test.

SMA fibroblasts isolated from a type 1 SMA child have low levels of SMA and therefore do not display the characteristic SMN gems that are seen in wild-type cells. Immunofluorescence was used to investigate whether transfection using polymersomes could restore protein levels by observing the presence of SMN. Furthermore immunofluorescence enabled us to analyse the transfection efficiency of polymersomes *in vitro*. Cells were incubated with polymersomes encapsulating SMN plasmid DNA for 72 hours before being fixed and stained using mouse antibody against SMN. Cells transfected with SMN plasmid using calcium phosphate were used as a positive control in this study.

Microscopy analysis revealed an increase in SMN fluorescence in cells transfected using polymersomes as well as in cells transfected using calcium phosphate. Following transfection with calcium phosphate quite a low percentage of cells were transfected (approximately 10%), however, cells that were transfected displayed a very high level of SMN fluorescence (fig. 3.10). Cells transfected by calcium phosphate displayed SMN gems throughout the cytoplasm as well as in the nucleus, this has previously been reported following lentiviral-mediated overexpression of SMN (Azzouz *et al.*, 2004). It is expected that the presence of SMN gems in the cytoplasm is due to unusually high levels of SMN protein being expressed. Interestingly following transfection using polymersomes a higher percentage of cells appeared to be transfected (fig. 3.10). Although the SMN was not as highly expressed as with calcium phosphate cells transfected with polymersomes did display restored SMN gems in the nucleus. This demonstrates that polymersomes can be used to transfect cells and cause restoration of functional protein in an *in vitro* model of SMA.

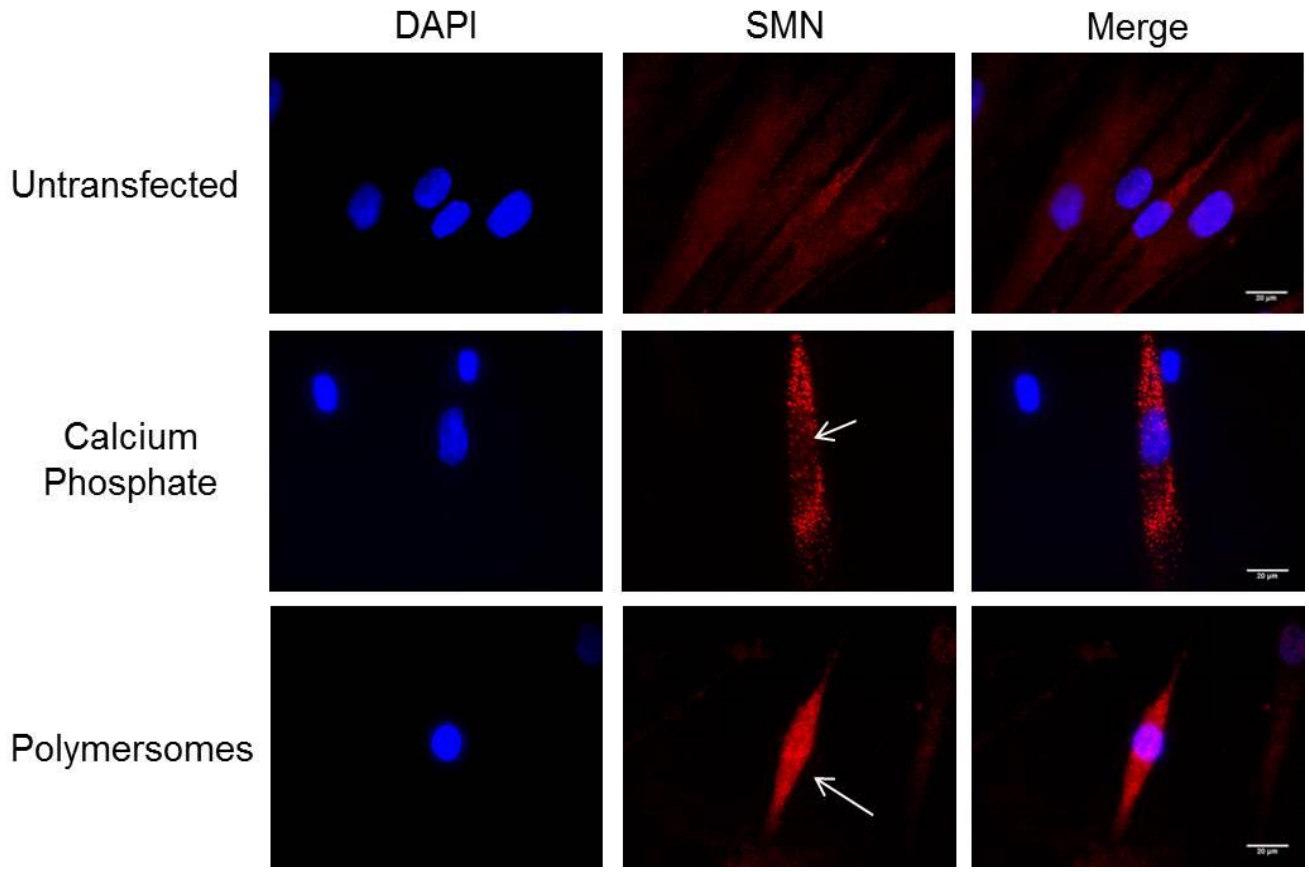

Figure 3.10 Polymersome-mediated SMN replacement in type I SMA patient fibroblasts. SMN deficient fibroblasts were incubated with polymersomes loaded with SMN plasmid DNA for 72 hours before being fixed and stained for SMN. Following polymersome-mediated transduction cells displayed increased fluorescence. Scale = 20µm. n>100 cells analysed for SMN fluorescence per group.

3.3 Discussion

Polymersomes composed of PMPC-PDPA have been shown to enter many cell types with very low levels of toxicity (Massignani *et al.*, 2009). We have used a rhodamine-labelled $PMPC_{25}$-$PDPA_{70}$ polymersomes to confirm uptake in a human cell line (HEK293T cells). These cells display a decrease in viability following incubation for 48 hours with high polymersome concentrations, however the concentration used for further *in vitro* experiments (0.5mg/ml) only caused a small reduction in cell viability as assessed by MTT assay. Fluorescent microscopy revealed that incubation with this concentration of polymersomes for 48 hours led to uptake in almost all cells, with the majority of fluorescence localising in the cytoplasm. The even distribution of fluorescence throughout the cytoplasm suggests that these pH sensitive polymersomes break up in the acidic environment of the endosome following endocytosis and the polymer becomes dispersed throughout the cell, as previously reported (Massignani *et al.*, 2009).

Polymersomes have previously been used to deliver nucleic acids including DNA to cells leading to transfection. To investigate the possibility of using polymersomes as a delivery vehicle for gene therapy to treat SMA we first wanted to improve the encapsulation efficiency, or find a way of sorting polymersomes to remove those that have not encapsulated any DNA. Theoretically the size and shape of structures formed from amphiphilic block-copolymers in an aqueous environment can be controlled by changing the size of each block. However there is a wide distribution of particle sizes within the solution of polymersomes produced with $PMPC_{25}$-$PDPA_{70}$, including micelles of <40nm, and vesicles of >400nm. We hypothesized that we could increase the percentage of polymersomes that contained DNA by removing polymersomes that were unlikely to have encapsulated DNA due to their small size, and thus in effect enhance encapsulation efficiency.

To investigate how centrifugation could affect the amount of encapsulated DNA in the polymersome formulation, polymersomes encapsulating luciferase plasmid DNA were centrifuged at an r.c.f of either 5000, 10000 or 20000 x *g*. When the amount of encapsulated DNA was calculated, normalised to polymer concentration for each

sample there was a trend towards higher DNA concentration at lower centrifuge speeds.

To check how well particle size could be separated by centrifugation at different speeds polymersomes were produced encapsulating luciferase plasmid DNA and centrifuged at increasing speeds. The particle size of polymersome collected after each centrifugation was measured which revealed that the slower rounds of centrifugation removed many of the largest particles. There was a clear shift towards smaller sized particles collected after faster centrifugations. However the size distribution curves for the different polymersome fractions overlapped which demonstrates that the method of sorting particle size by centrifugation is not totally effective. The pelleting of polymersomes by centrifugation also enables the concentration of the polymersome solution to be controlled by varying the volume that the pellet is re-suspended in. Furthermore pelleting polymersomes and removing the supernatant led to exclusion of unencapsulated DNA.

It may be possible to separate different sized particles by other methods such as by gel permeation chromatography or using a hollow fibre filtration system. Gel permeation chromatography was initially tested to purify polymersomes using a column of sepharose by size however this was inefficient and difficult to accurately control. Furthermore this method of gel permeation chromatography was unable to separate free plasmid DNA from polymersomes due to their similar size. Hollow fibre filtration systems are useful for excluding particles below a certain size from a solution however it may be difficult to use this method to generate a series of particle fractions of different size. Centrifuge columns could also be used to more accurately separate different sized particles using centrifugation, however due to time constraints this possibility was not explored.

The different polymersome fractions collected following centrifugation at increasing speeds were then analysed to measure the amount of encapsulated DNA in the polymersomes collected after each centrifugation. Remarkably there was a large difference between the concentrations of DNA encapsulated in the polymersomes collected after different centrifugations. The amount of DNA encapsulated in

polymersomes collected following the first centrifugation was higher than in any other fraction collected thereafter. The amount of encapsulated DNA then decreased in polymersomes collected following each round of centrifugation. When plotted against the average particle diameter for each solution it was observed that as average particle diameter increases so does the amount of encapsulated DNA.

To check that the improvement in encapsulation efficiency through selection of the largest particles can translate to improvement in transduction efficiency we then used these polymersomes to transfect HEK293T cells. Assessing the luciferase activity 48 hours post-transduction revealed that the polymersomes collected after the first centrifugation at the slowest speed did indeed generate the highest level of luminescence. Furthermore when the luminescence detected was plotted against the amount of DNA encapsulated in the polymersomes used for each transfection there was a linear relationship between the amount of encapsulated DNA and the level of luminescence detected.

We show here that by removing empty polymersomes transfection efficiency can be improved. Another benefit of this approach is improving reliability of the transfection. Without purifying polymersomes the solution contains polymersomes that have encapsulated little or no DNA as well as polymersomes that contain a high concentration of DNA. Using a small sample of this solution for transfections is likely to cause a large variation in the amount of transfection seen between, or even within experiments.

Following successful transfections with a luciferase reporter plasmid we investigated how well polymersome transfection could lead to SMN gene transfer. Western blot analysis revealed a 2.6 fold increase in SMN protein expression following transfection by polymersomes encapsulating SMN plasmid DNA. Furthermore QPCR analysis revealed an increase in SMN mRNA of 38 fold. Since HEK293T cells are an embryonic cell line they express a high level of SMN protein, therefore an increase in expression by over 2 fold could be considered a significant outcome. The overexpression following transfection by polymersomes was not as high as seen for calcium phosphate however a direct comparison between the two methods

cannot be made. Calcium phosphate is known to be toxic to cells therefore the cell growth media is removed after 6 hours and replaced with fresh media. If calcium phosphate had been incubated with the cells for as long as the polymersomes we would expect to see a large amount of cell death. Furthermore the amount of DNA used for calcium phosphate transfection differs from the amount encapsulated in the polymersomes used.

To further investigate the possibility of using polymesomes to deliver gene therapy for SMA we tested the ability of polymersomes to overexpress SMN in an *in vitro* model of SMA. A fibroblast cell line derived from a type 1 SMA patient was used which displays low levels of SMN. We first transfected these cells with polymersomes containing plasmid DNA expressing the human SMN1 gene and assessed the mRNA levels by QPCR. This revealed an increase in SMN mRNA of over 300 fold. Immunofluorescence of SMN-deficient fibroblasts transfected with polymersomes encapsulating SMN plasmid DNA revealed an increase in SMN protein levels.

The work here shows that polymersomes can be used to encapsulate plasmid DNA to cause transfection as reported previously (Lomas *et al.*, 2007). Furthermore the data here shows that polymersomes encapsulate DNA in a size dependent manner. Increase of SMN mRNA and protein levels in an *in vivo* model of SMA demonstrates that polymersomes could potentially be used as a non-viral gene therapy vector for SMA. As mentioned in the introduction to this section polymersomes are a new technology that needed optimisation of production, encapsulation and transfection before using the methods detailed in this section. Therefore the time spent on optimisation meant it was not possible to go on to test this non-viral vector system *in vivo*. It would be interesting to follow-up this research by testing the transfection efficiency of polymersomes *in vivo* and ultimately delivering SMN plasmid DNA to an *in vivo* model of SMA.

Chapter 4

AAV5-mediated Transduction in the CNS

4.1 Introduction

To achieve effective gene therapy for disorders of the central nervous system (CNS) it is important to develop vector systems capable of widespread gene transfer in the brain and spinal cord. To do this a gene delivery vector must be able to pass the blood-brain barrier (BBB) and enter the CNS. Different AAV serotypes have been shown to have different tropisms for tissues leading to different transduction profiles (Zincarelli *et al.*, 2008). We decided to investigate whether AAV5 could enter the CNS following intravenous injection of neonatal mice.

AAV5 genome sequencing revealed some similarity to AAV2 with a level of sequence consensus of around 50% (Bantel-Schaal *et al.*, 1999; Chiorini *et al.*, 1999). However sequencing demonstrated that AAV5 is a distinct serotype with a high degree of heterogeneity seen in the region encoding capsid proteins. Analysis of RNA generated following viral infection of AAV5 also revealed significant differences in transcription profiles compared to AAV2 (Qiu *et al.*, 2002).

AAV5 can transduce both neurons and astrocytes following direct injection of this vector system to the CNS (Davidson *et al.*, 2000). Interestingly following direct injection to the striatum AAV5 caused extensive spread of transduction through much of the injected hemisphere. In comparison AAV2 and AAV4 mediated a more localized pattern of transduction and a much lower level of transgene expression (Davidson *et al.*, 2000). However when delivered to the right lateral ventricle transduction by this vector system was predominantly localized to the ependyma. Furthermore AAV5-mediated transduction increased between 3 and 12 weeks, whereas AAV4 transduction remained constant and AAV2 transduction was lost by 12 weeks. Self-complementary AAV5 (scAAV5) has also been injected directly into the retina of a mouse model of a severe form of retinal dystrophy (Leber's congenital amaurosis-2). Remarkably scAAV5-mediated expression of the target gene restored visually evoked behaviour to photoreceptors and prevented degeneration of cone cells (Pang *et al.*, 2010).

Systemic delivery of various AAV serotypes has previously been performed to assess transduction levels in adult mice (Zincarelli *et al.*, 2008). Bioluminescence analysis following intravenous (IV) administration of various AAV serotypes to adult mice revealed AAV5 caused lower overall expression than AAV1, 6, 8, 7 and 9. Tissue analysis showed that transgene expression was mainly confined to the liver following AAV5 administration. Viral genome copy number however revealed $>10^4$ copies/µg of genomic DNA in the brain, kidney and lung at 100 days post injection. Recently the efficiency of different AAV serotypes to transduce the CNS following IV injection of neonates has been assessed using the CAG promoter with tissue taken at 21 days (Zhang *et al.*, 2011). At 21 days AAV5 and AAV2 were found to generate much lower levels of transgene expression than other vectors. Image analysis revealed that AAV5 caused low transgene expression the brain and spinal cord. However analysis of the efficiency of AAV5 to transduce motor neurons was not reported. Intraperitoneal (IP) injection of AAV5 has also been investigated in neonates (Ogura *et al.*, 2006). Overall transgene expression was higher following IP injection than IV injection. Transgene expression was high and long lasting however it was confined to the peritoneum, therefore IP injection would not be sufficient to treat CNS disorders such as SMA.

Comparison of the transduction efficiency of different AAV serotypes in the brain of young adult rats has previously been performed (Blits *et al.*, 2010). The red nucleus of the rat brain has projections through the spinal cord and was injected directly with different AAV serotypes. At one week post injection AAV5 transduced fewer neurons than AAV6 however the number of neurons transduced by AAV5 increased over time whilst the number of AAV6 neurons remained constant. Interestingly as with intrastriatal injection (Davidson *et al.*, 2000) AAV5 transduction spread to neurons outside the red nucleus, unlike other AAV serotypes (Blits *et al.*, 2010).

Direct injection of different AAV serotypes into the dorsal root ganglia was performed to assess how efficiently these sensory neurons were transduced (Mason *et al.*, 2010). The highest level of transduction was obtained with AAV5, followed by AAV6 and AAV1. The percentage of cells transduced by AAV5 increased over time

from 1 week to 12 weeks. At 12 weeks transduction was also seen in fibres of the sciatic nerve and axons in the dorsal roots and entering the spinal cord.

The aim of this section is to undertake a small pilot study to assess the efficiency of AAV5 transduction in the CNS following intravenous injection in neonate mice. Furthermore the ability of two different promoters to drive transgene expression in the CNS will be analysed. The two promoters used in this study are the cytomegalovirus (CMV) promoter and the CAG promoter which is a combination of the CMV early enhancer element and the chicken β-actin promoter. Both of these promoters have been used previously to drive transgene expression in the CNS (Gray *et al.*, 2011; Zhang *et al.*, 2011). CNS tissue was extracted at 4 and 8 weeks following intravenous injection of the vectors at post-natal day 1 in order to assess whether transgene expression changed over time.

4.2 Results

4.2.1 AAV5-mediated GFP Transduction in the Brain

4.2.1.1 Transduction of Neurons and Astrocytes in the Brain

We compared two AAV5 viral vectors expressing green fluorescent protein (GFP) or humanised recombinant GFP (hrGFP) under the control of a CAG or a CMV promoter respectively. Wild-type mice were intravenously injected with 10µl ($3.3x10^{10}$ vector genomes (vg)) of AAV5-CAG-GFP (n=6) or 10µl ($1.23x10^{11}$ vg) of AAV5-CMV-hrGFP (n=6) at postnatal day one. Note that two slightly different amounts of vector genomes were injected due to different vector concentrations. The vectors were not diluted to matching concentrations as we wanted to deliver as much vector as possible for each group and did not expect this small difference in concentration to affect transduction.

GFP expression in the brain and spinal cord was assessed by performing immunohistochemistry on brain and spinal cord sections at 4 weeks (n=3) or 8 weeks (n=3) post vector administration. In the AAV5-CAG-GFP treatment group a modest amount of transduction of both neurons and astrocytes or glial cells was seen throughout the brain (fig. 4.1). Fig. 4.1 shows that GFP-positive neurons display co-localisation with staining against NeuN (fig. 4.1 D&E) and astrocytes display co-localisation with GFAP positive cells (fig. 4.1 B). Moreover many GFP-positive fibres were seen that appeared to be axons, without any visible cell body transduced (fig 4.1 C). Almost no transduction was detected in the AAV5-CMV-hrGFP treatment group therefore the following sections will only summarise the data obtained with AAV5-CAG-GFP.

4.2.1.2 Quantification of Transduced Astrocytes and Neurons in the Brain

The number of transduced astrocytes and neurons in brain sections was determined following injection of AAV5-CAG-GFP. The amount of transduced cells per section was counted per animal and the cell type (either neuronal or glial) was determined by the morphology of the transduced cell. When grouped together the results suggest that there is a higher level of transduction after 8 weeks than after 4 weeks (fig. 4.2 A) although this is not significant (two-way ANOVA). Looking at the individual data (fig. 4.2 B) it is obvious that these results are skewed by one animal which is transduced more than any other. Furthermore there was one animal in the 8 weeks group with no transduction detected and one animal in the 4 weeks group with only one transduced cell observed. It is clear that there is variability in the levels of transduction observed in different animals. Among the 6 animals in the CAG promoter group there were one animal with a moderate level of GFP expression, 3 animals low transgene expression and two animals with almost no GFP expression (fig. 4.2 B).

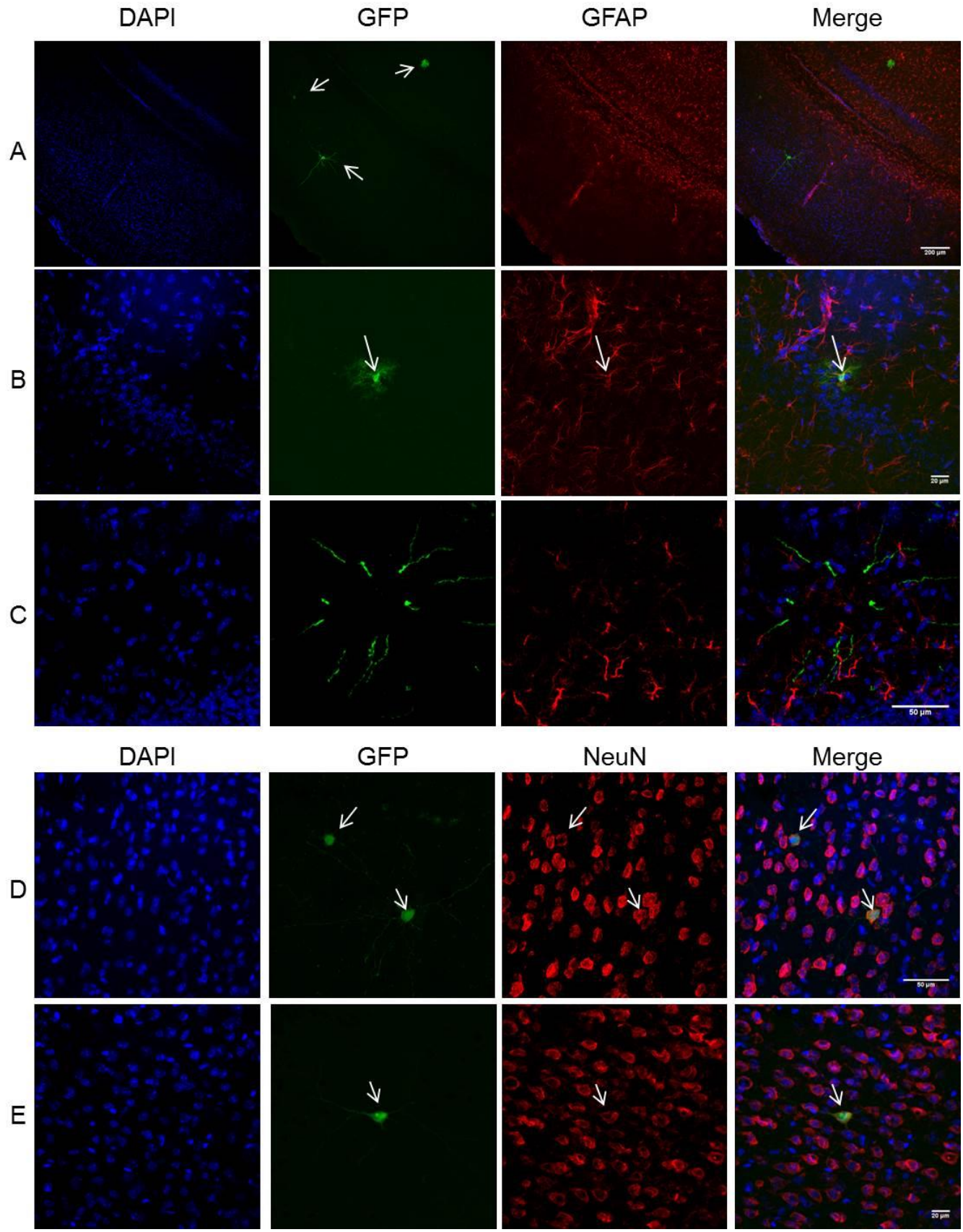

Figure 4.1 AAV5-mediated GFP expression in the brain. Wild-type mice were injected at postnatal day 1 with AAV5-CAG-GFP, brains were extracted at 4 or 8 weeks post-injection, sectioned and stained for DAPI (blue), GFP (green), GFAP (red; **A, B & C**) or NeuN (red; **D & E**). **A:** transduced astrocytes and a neuron at 8 weeks in the cerebral cortex (scale = 200µm), **B:** transduced astrocyte in the cortex at 4 weeks (scale = 20µm). **C:** transduced fibres in the cortex which appear to be axons at 8 weeks (scale = 50µm). **D & E:** transduced neurons within the striatum which co-localise with NeuN

A

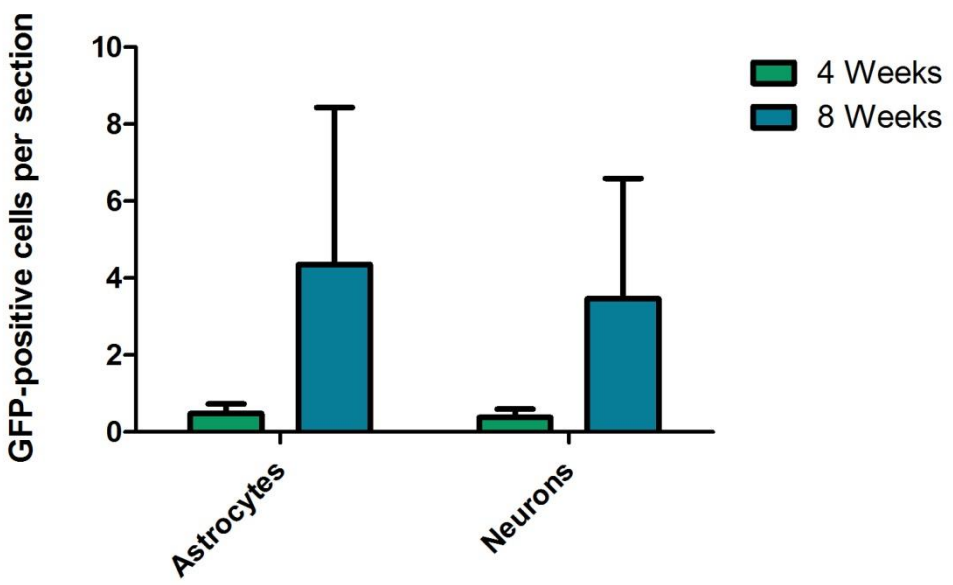

B

	Mouse ID	Astrocytes per section	Neurons per section
4 weeks	*209*	0.94	0.75
	208	0.076	0
	508	0.43	0.36
8 weeks	*210*	0.57	0.71
	227	0	0
	228	12.5	9.7

Figure 4.2 Quantification of astrocytes and neurons transduced in the brain. A: number of GFP-positive astrocytes and neurons per brain section at 4 or 8 weeks post-injection of AAV5-GFP (n=6). Data shows mean ± SEM from between 13 and 16 sections per animal. No significant difference between cell types transduced or between 4 weeks and 8 weeks (two-way ANOVA). **B:** average number of astrocytes and neurons transduced per brain section for each mouse.

Unfortunately the high variability and poor transduction efficiency in this pilot study means it is challenging to compare the two time points. However the presence of one animal with a relatively good level of transduction at 8 weeks demonstrates that the transduction with AAV5-CAG-GFP can be long lasting. The table (fig. 4.2 B) shows that there was little difference between the number of astrocytes and the number of neurons transduced for each mouse.

4.2.1.3 Transduction of the Cerebellum

As mentioned above there were many fibres that appeared to be axons that were transduced, without any visibly transduced cell body (fig. 4.1 C). Some transduction of tracts within the cerebellum was also identified (fig. 4.3). This transduction was mainly confined to distinct bundles in the white matter and was found throughout the cerebellum.

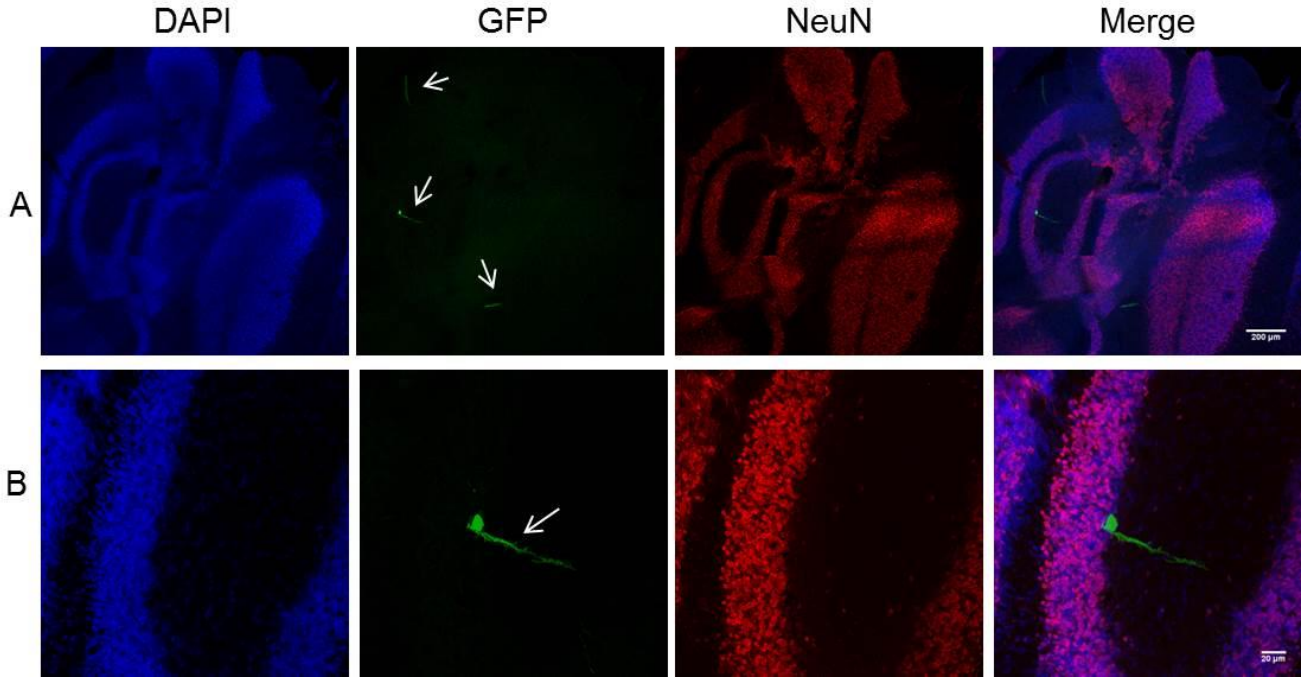

Figure 4.3 Transduction in the cerebellum. Staining of brain sections for GFP (green), NeuN (red) and DAPI (blue) revealed transduction of fibres in the cerebellum. **A:** low magnification image of the cerebellum with arrows highlighting transduced fibres, scale = 200µm. **B:** higher magnification image of **(A)**, scale = 20µm. Images from tissue taken at 8 weeks.

4.2.1.4 Transduction within the Ventricles

By far the highest area of transduction seen in the brain was within the ventricles, which is most likely to be the choroid plexus (fig. 4.4 A & B). The choroid plexus is involved in the production of cerebrospinal fluid (CSF) and therefore does not contain such a tightly regulated BBB as the rest of the brain. This would explain why this area would be more easily transduced following intravenous injection of AAV5. Interestingly it was observed that areas of the brain surrounding the ventricles were also transduced where high levels of transduction in the ventricles were seen (fig. 4.4 A). This may suggest a route of entry for AAV to transduce the brain. Furthermore transduction of the pineal gland was seen in one animal, which is also outside of the BBB (fig. 4.5 A). The transduction of surrounding axons and astrocytes also suggests that viral vectors may have been able to take advantage of the lack of BBB in this area. The level of transduction found in the ventricles correlated with the level of transduction in the rest of the brain; the animal with the highest level of astrocytes and neurons transduced also had the highest level of ventricular transduction. This suggests that the animals with a lower level of transduction received a lower load of viral vectors. It could be argued that the choroid plexus is outside the blood brain barrier and therefore the high level of transduction seen here suggests that the AAV5 vector does not easily pass the BBB.

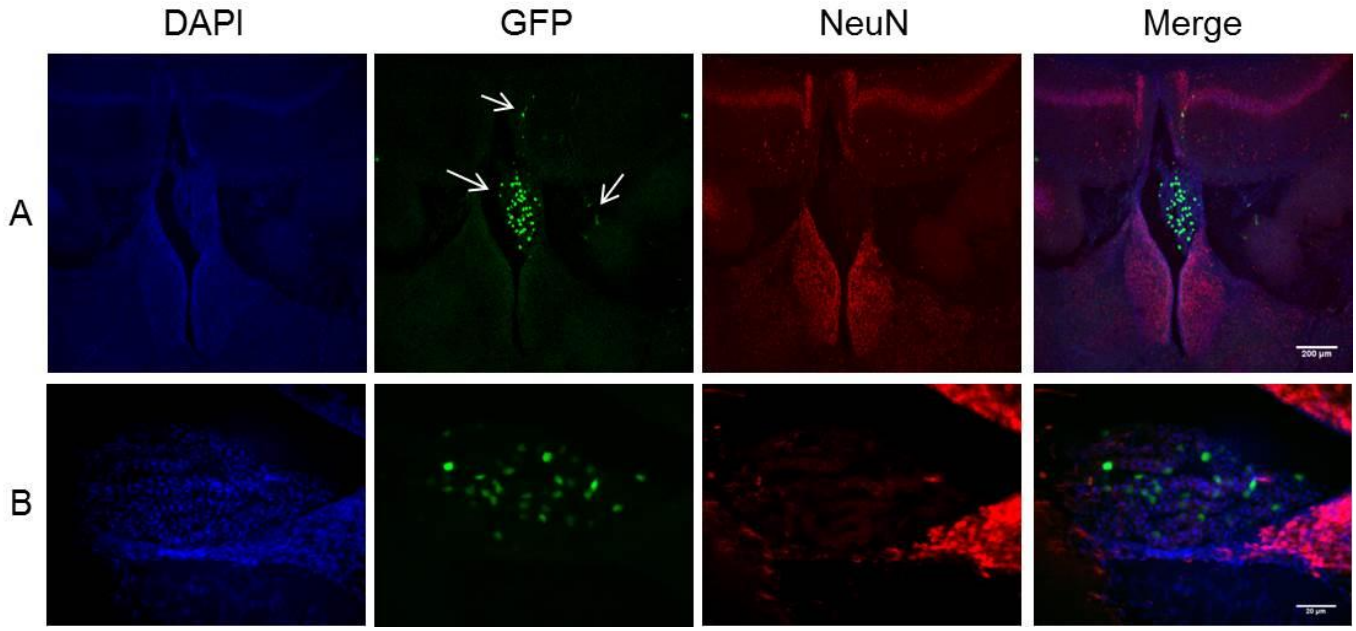

Figure 4.4 Transduction within the 3rd ventricle. Staining of brain sections for DAPI (blue), GFP (green) and NeuN (red) revealed a high amount of transduction within the 3rd ventricle. **A:** transduction of the choroid plexus (bottom left arrow) within the third ventricle and transduction of the periventricular region (top arrow and right arrow). Scale = 200µm. **B:** high magnification image of transduction of the choroid plexus. Scale = 20µm. Images from tissue taken at 8 weeks.

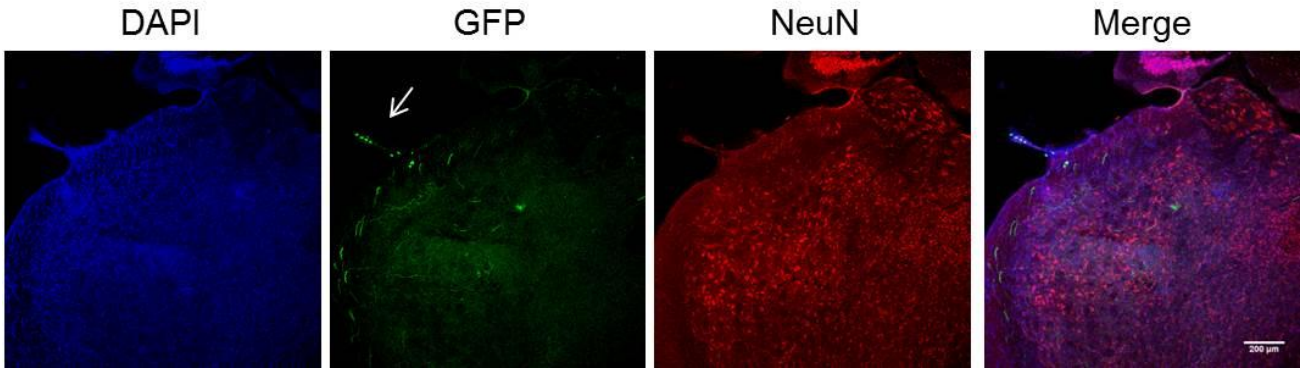

Figure 4.5 Transduction of the pineal gland and surrounding area. A brain sectioned 8 weeks post-injection of AAV5-GFP and stained for DAPI (blue), GFP (green) and NeuN (red) revealed GFP transgene expression in the pineal gland (arrow). A high level of transduction of cells and axons in the surrounding area was also seen. Scale = 200µm. Image from tissue taken at 8 weeks.

4.2.2 AAV5-mediated Transduction in the Spinal Cord

4.2.2.1 Transduction of Spinal Cord Neurons

The main interest of this chapter is to investigate whether AAV5 is a suitable vector system to treat SMA. To successfully treat SMA with gene therapy the vector must be able to transduce motor neurons in the lumbar spinal cord. Spinal cords were collected from mice at 4 and 8 weeks following IV injection of AAV5-GFP and 20µm sections were stained with anti-GFP alongside a neuronal marker (NeuN) (fig. 4.6). Very few transduced neurons were observed in the spinal cord which appeared to be less transduced than the brain (fig, 4.6). Furthermore only a small number of transduced neurons were found in the ventral horn region with the morphology of motor neurons (fig. 4.6 C). Therefore AAV5 did not readily transduce neurons in the lumbar spinal cord. Interestingly many GFP-positive fibres were observed in the spinal cord (fig. 4.6 D). These transduced fibres appeared to be axons and were similar to those found to be transduced in the brain (fig. 4.1 C).

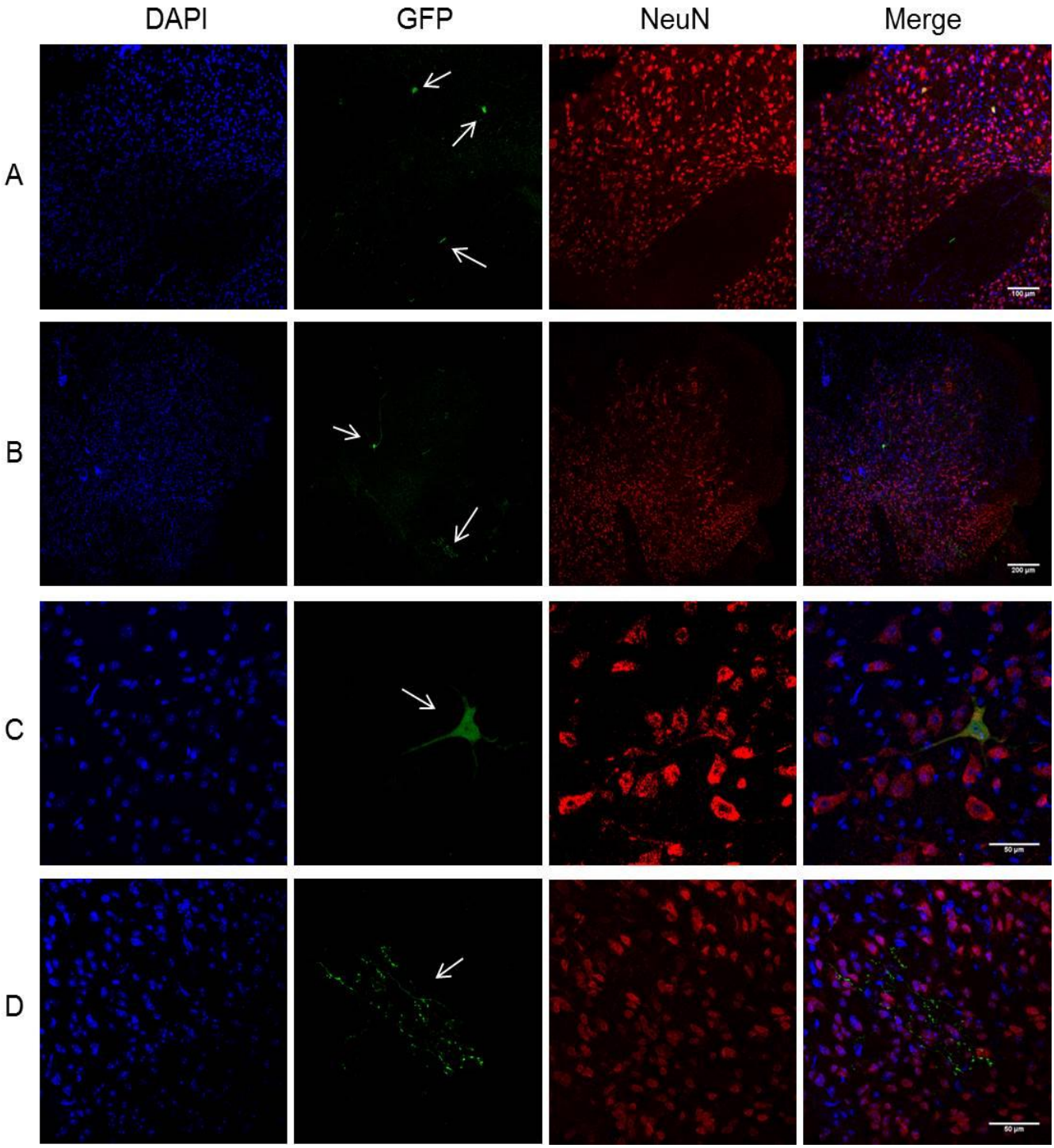

Figure 4.6 Neuronal transduction in the lumbar spinal cord. 4 or 8 weeks following IV injection of AAV5-GFP spinal cords were extracted, sectioned and stained for DAPI (blue), GFP (green) and NeuN (red). **A:** transduced neurons and transduction in the ventral column at 4 week. Scale = 100µm. **B:** transduced neuron and axons at 8 weeks. Scale = 200µm. **C:** high magnification image of a transduced neuron at 8 weeks. **D:** high magnification image of transduced axons seen in **(B)**. Scale = 50µm

4.2.2.2 Transduction of Astrocytes in the Spinal Cord

Further to investigating levels neuronal transduction in the spinal cord following intravenous injection of AAV5 spinal cords were also analysed for the presence of transduced astrocytes. Spinal cord sections were stained with GFP and GFAP to identify transduced astrocytes. Only a small number of cells were found to express GFP which co-localised with GFAP staining (fig. 4.7). This shows that AAV5 is able to transduce some astrocytes in the spinal cord but with low efficiency.

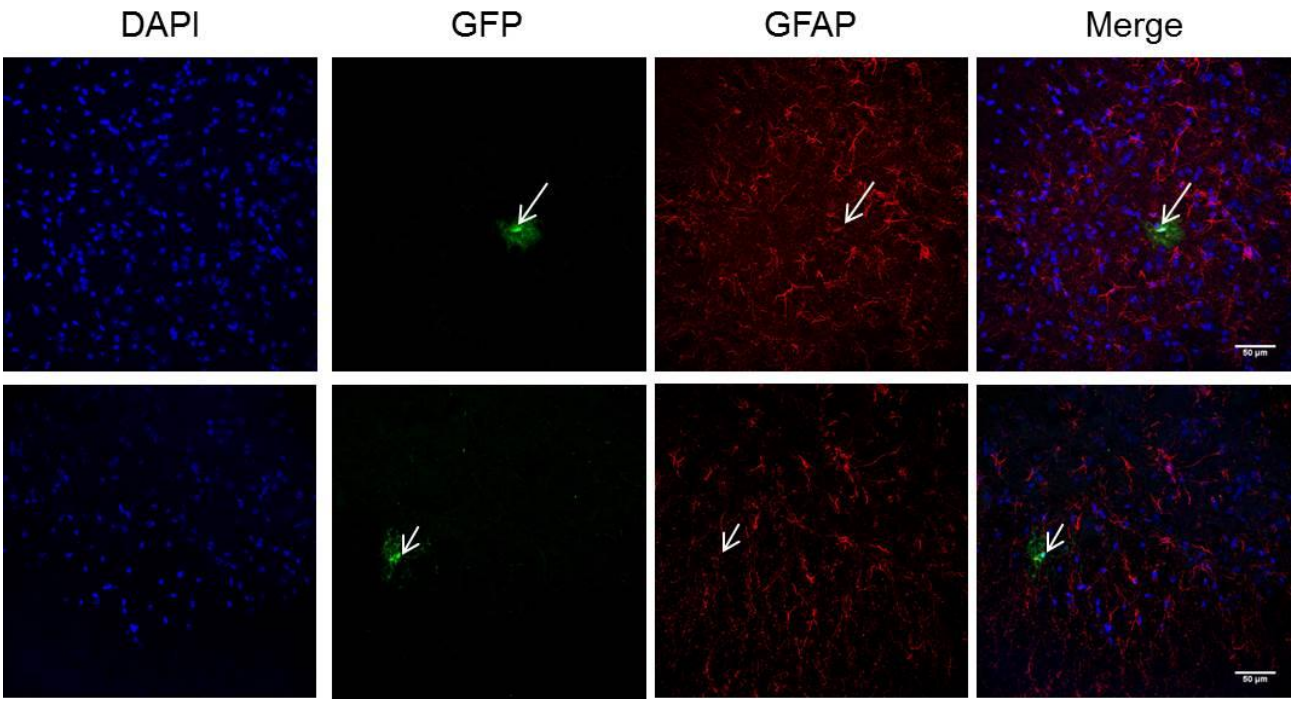

Figure 4.7 AAV5-mediated transduction of astrocytes in the spinal cord. Spinal cords of mice were extracted from mice 4 weeks and 8 weeks after vector delivery and were sectioned and stained for DAPI (blue) GFP (green) and GFAP (red). This revealed a small number of transduced astrocytes in the spinal cord. Scale = 50µm. Images from tissue extracted at 8 weeks.

4.2.2.3 Quantification of Transduction in the Spinal Cord

To assess the level of transduction within the spinal cord following intravenous injection of AAV5-GFP the number of GFP-positive astrocytes and neurons was counted (fig. 4.8). As with the brain the variation between animals coupled with the low level of transduction meant that it was difficult to ascertain any strong conclusions from this quantification. Overall there were more GFP-positive neurons than astrocytes within the spinal cord, however this is not statistically significant (t-test) and only two of the five spinal cords sectioned displayed any transduced astrocytes and neurons. As mentioned above there was a high number of GFP-positive axons seen within the spinal cord (fig. 4.6 D). Interestingly transduced axons were observed in many of the spinal cord sections that displayed no GFP-positive neurons or astrocytes. The percentage of sections containing GFP-positive axons was calculated revealing that approximately 30% of spinal cord sections displayed some transduction of axons in tissue taken at 8 weeks (n=3, data not shown).

A

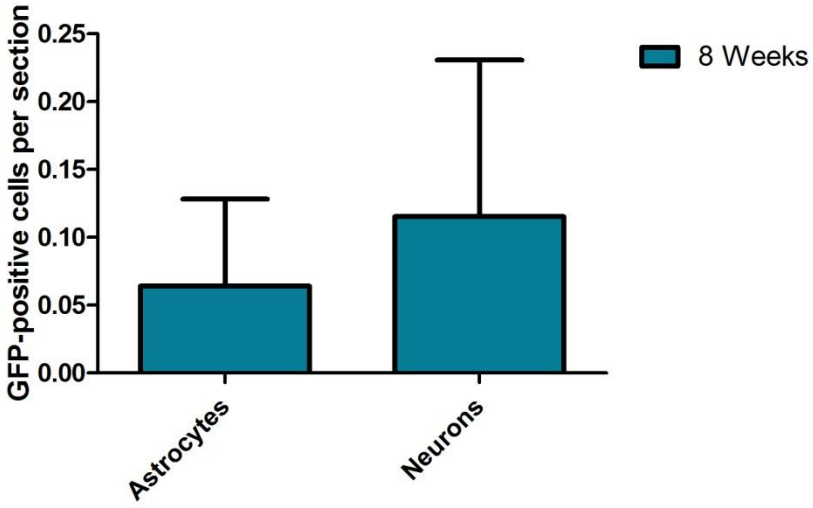

B

	Mouse ID	Astrocytes per section	Neurons per section
4 weeks	*209*	0.1	0.8
	208	0	0
8 weeks	*210*	0	0
	227	0	0
	228	0.19	0.35

Figure 4.8 Quantification of neurons and astrocytes transduced in the spinal cord. Spinal cord sections were assessed for the presence of GFP-positive astrocytes and neurons. **A:** average number of GFP-positive astrocytes and neurons per spinal cord section extracted at 8 weeks post injection. Data shows mean ± SEM, from between 10 and 30 sections per animal, n=3. No significant difference between cell types (t-test). **B:** average number of astrocytes and neurons transduced for each mouse.

4.2.2.3 Transduction of Dorsal Root and White Matter

Spinal cords extracted following AAV5-GFP administration were sectioned and stained to analyse GFP expression. Some spinal cord sections contained the dorsal root alongside the spinal cord. The dorsal root connects the spinal cord to the dorsal root ganglion which contains sensory neurons that innervate the muscles of the lower limb. The dorsal root areas were found to be highly transduced (fig. 4.9 A&B). It is therefore likely that this area is transduced via retrograde transport of viral vectors from the muscle. Transduction through retrograde transport would explain why this area is more highly transduced than the rest of the spinal cord as this route avoids crossing the BBB. Furthermore sections close to the dorsal root displayed high levels of transduction of cells and fibres (fig. 4.9 B). Transduction of cells in areas of the spinal cord near the dorsal root suggests transduction in the spinal cord may be mediated through retrograde transport rather than through the BBB. Consistent with previous reports investigating the transduction profile of AAV5 in adult mice (Zincarelli *et al.*, 2008), no transduction was seen within the gastrocnemius muscle (data not shown). The white matter areas of the spinal cord also displayed high levels of transduction (fig. 4.9 C). The high levels of transduction found in the dorsal root coupled with the transduction seen in the white matter and fibres in the spinal cord suggest a tropism of AAV5 for white matter areas rather than for astrocytes or neurons.

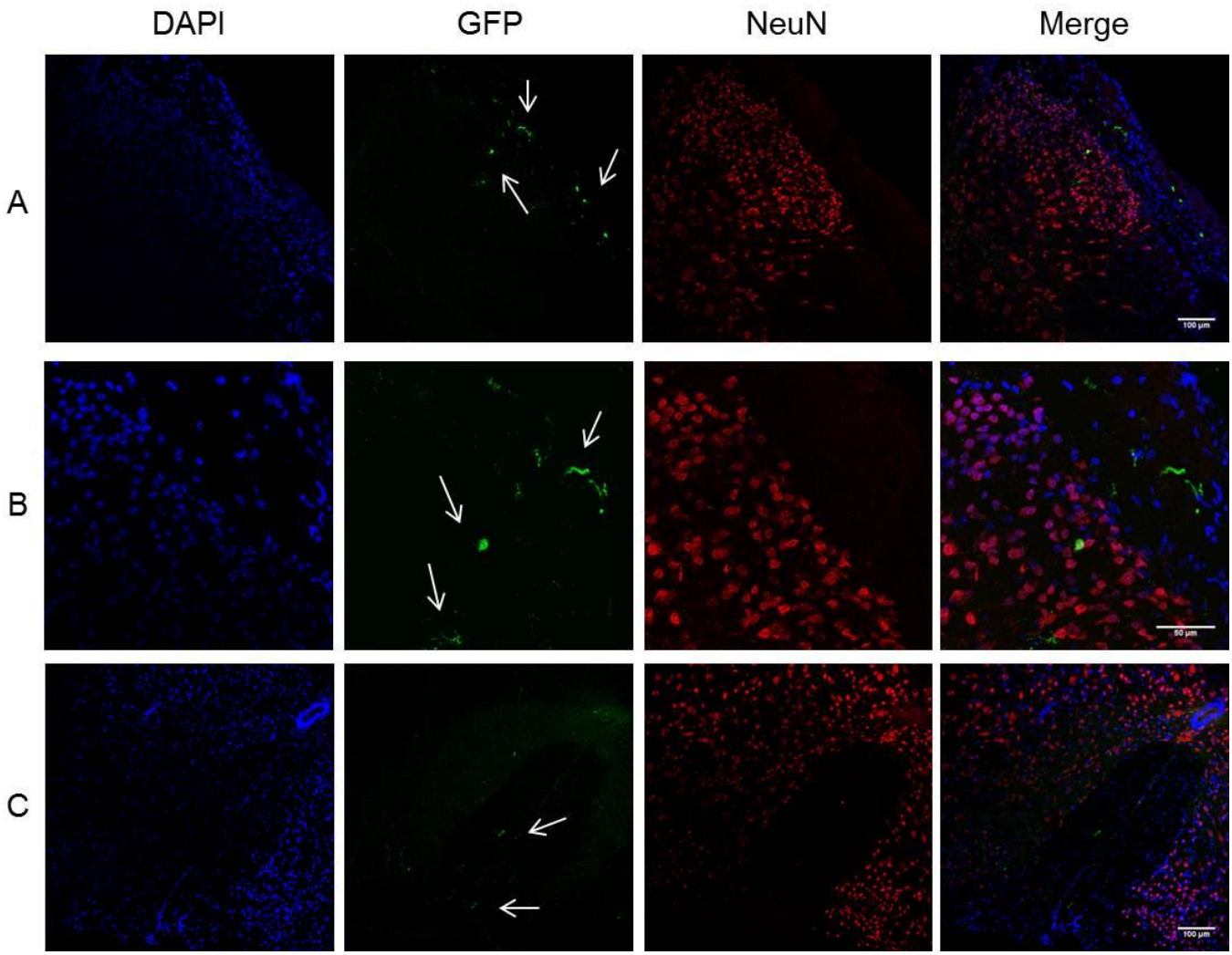

Figure 4.9 AAV5-mediated transduction in spinal cord white matter. Spinal cords were sectioned and stained for DAPI (blue), GFP (green) and NeuN (red). **A:** GFP transgene expression in the dorsal root and of nearby tissue. Scale = 100µm. **B:** higher magnification image of **(A)** (scale = 50µm), highlighting transduction in the dorsal root and nearby tissue. **C:** transduction in the ventral column. Scale = 100µm. Images from tissue extracted at 8 weeks.

4.3 Discussion

To ascertain whether AAV serotype 5 would be a good candidate for a gene therapy vector to treat CNS disorders, in particular SMA, we injected neonatal wild-type mice with 10µl AAV5 expressing GFP. This equates to $1.23x10^{11}$vector genomes for AAV5-CMV-GFP, and $3.3x10^{10}$ vector genomes for AAV5-CAG-GFP. Two different GFP vectors were used under the control of different promoters (CMV and CAG), and CNS tissue was extracted at two different time points to assess the level of transduction by immunofluorescence. The aim was to compare which promoter provided the highest level of GFP expression *in vivo* and whether transduction was highest at 4 weeks or 8 weeks post-injection.

The brains and spinal cords of injected mice were sectioned and stained using an antibody against GFP alongside other antibodies against neuronal and glial markers (NeuN and GFAP respectively). Analysis of the immunofluorescence in the brain revealed a modest level of transduction with AAV5-CAG-GFP, with transduced cells appearing to be spread randomly throughout the brain. There was a similar amount of astrocytes and neurons transduced in the brain, with fine fibres also transduced that were assumed to be axons. Some of the transduced fibres resembled oligodendrocytes, however it was not possible to confirm the cell type from the staining performed. It would have possible to confirm this by co-immunolabelling with an oligodendrocyte marker such as an anti-CNPase antibody. A distinct pattern of transduction of bundles within the cerebellum was also observed. The highest level of transduction in the brain was seen in structures within the ventricles. The transduced cells within the ventricles make up the choroid plexus and circumventricular organs.

In the spinal cord a low number of astrocytes and neurons were found to be transduced by AAV5-CAG-GFP, with very few motor neurons expressing GFP. However there was a high amount of GFP positive fibres observed which appear to be axons. Furthermore transduction was also seen in white matter areas of the lumbar spinal cord such as the ventral and dorsal column. Some spinal cord sections also

contained parts of the dorsal root which displayed a much higher level of transduction than in the spinal cord.

As mentioned above we aimed to compare the difference in expression between two different promoters, CMV and CAG. Almost no transduction was seen in brains and spinal cords of mice injected with AAV5-CMV-GFP, therefore only the transduction in animals injected with AAV5-CAG was quantified. It is not clear why the vector with the CMV promoter transduced so few cells since this promoter is used routinely to drive expression of genes in viral vectors. It must be noted that the two viral vectors used do not express exactly the same gene; the vector using CAG expresses wild-type GFP whereas the vector using CMV expresses humanised renilla GFP (hrGFP) however this should not negatively affect expression.

The level of transduction seen in the CNS of animals injected with AAV5-CAG-GFP varied widely between animals. It was therefore difficult to assess how expression may change between 4 and 8 weeks. The highest level of transduction was seen from an animal in the 8 weeks post-injection group. However the variability within the group means we cannot say for certain that transduction increases over time; however it shows that transduction can be maintained for up to 8 weeks. The variation seen within the CAG group may be due to a technical issue regarding the variability of injecting neonatal animals. It may also be natural variation in the amount of viral vectors that was able to enter the brain and spinal cord. One way to test this would be to assess the level of transduction in an organ that is highly transduced such as the liver. If there was also a large variation in transduction levels in the liver then the variation is likely to be due to human error. If a similar level of transduction was seen in the livers of all animals then the variation seen in the CNS is likely to have resulted from natural variation between animals.

The data presented here is generally in agreement with previously published results from a study that investigated the transduction efficiency of AAV5 following intravenous injection in neonatal mice (Zhang *et al.*, 2011). AAV5 was reported to generate low levels of transduction in the brain, which has also been shown here. Interestingly the pattern of transduction of the choroid plexus within the ventricles

of the brain shown here has been also reported for other AAV serotypes (Zhang *et al.*, 2011). Furthermore Zhang *et al.*, demonstrated that transduction of the spinal cord by AAV5 was low, however did not report whether AAV5 could specifically transduce motor neurons. The data here adds to this by showing that this vector system does not efficiently transduce neurons in the lumbar spinal cord.

AAV5-mediated transduction has previously been investigated in CNS tissue extracted at 21 days (Zhang *et al.*, 2011). Here later time points of 4 weeks and 8 weeks have been used. Studies have shown that AAV5-mediated transgene expression increases over time and that AAV5 can cause transgene expression for up to 200 days post-injection (Zincarelli *et al.*, 2008; Mason *et al.*, 2010). However it is difficult to conclude from the data here whether transgene expression in the CNS increases between 4 and 8 weeks. The observations made here that AAV5-mediated transduction appears to spread from transduced dorsal root to cells in the spinal cord supports previously published data showing that direct injection of the dorsal root ganglia can cause some transduction in the spinal cord (Mason *et al.*, 2010).

The low level of transduction in the brain and spinal cord following systemic delivery of AAV5 suggests that this serotype cannot easily pass the blood brain barrier. This is compounded by the fact that areas outside of the BBB such as circumventricular organs and the choroid plexus in the brain and the dorsal root in the spinal cord express high levels of GFP. Furthermore it was observed that areas of the brain and spinal cord close to highly transduced areas such as the dorsal root and choroid plexus displayed higher levels of transduction. It can therefore be postulated that AAV5 viral vectors may enter the brain through the CSF and enter the spinal cord through retrograde transport. Interestingly there appeared to be tropism of AAV5 for white matter in the CNS demonstrated by transduction of bundles in the cerebellum, and transduction in the ventral and dorsal column and the dorsal root. Furthermore the presence of GFP positive fibres was seen throughout the brain and spinal cord more often than transduced cell bodies. These fibres appear to be axons suggesting that axons express GFP following AAV5 transduction more than cell bodies.

This small pilot study showed that AAV5 mediated poor gene transfer in the CNS following IV delivery in neonate mice. It is possible that some particles may enter the CNS through the CSF and by retrograde transport however the low level of transduction suggests that AAV5 cannot pass the BBB. Therefore AAV5 is not thought to be an appropriate vector for gene therapy to treat SMA. For this reason the decision was taken not to expand this study further and increase the number of animals used.

Chapter 5

AAV6-mediated Expression of hnRNP R

5.1 Introduction

hnRNP R was identified in 1998 as a protein of 633 amino acids (Hassfeld *et al.*, 1998). This protein contains three adjacent RNA binding domains in the central part of the protein as well as an RGG box, another type of RNA binding domain, towards the *C*-terminal. hnRNP R was further identified by a yeast two hybrid screen as a binding partner of Smn (Rossoll *et al.*, 2002). However it is not able to bind to Smn mutants that reflect mutations seen in SMA suggesting the function of hnRNP R is compromised in SMA. Expression of hnRNP R is widespread and is expressed most highly during embryogenesis and was shown to be able to bind to RNA, as the structural analysis would suggest.

This protein was observed to co-localise with SMN in the axons of cultured motor neurons suggesting it may be involved in the axonal role of SMN. Furthermore motor neurons from $Smn^{-/-}$;SMN2 mice show a reduction of hnRNP R staining in distal axons and growth cones (Rossoll *et al.*, 2003). An hnRNP R mutant has also been generated that is lacking the ability to bind to SMN, when over expressed in differentiated PC12 cells this protein localises more in the nucleus rather than in neuritic processes as wild type hnRNP R does (Rossoll *et al.*, 2003). Together this suggests that Smn is involved in translocation of hnRNP R to axons.

Furthermore hnRNP R can bind directly to the 3'UTR of actin and these two proteins colocalise in axon terminals of primary mouse motor neurons (Glinka *et al.*, 2010). However mutant hnRNP R that cannot bind SMN also has a lower affinity for actin. This suggests that these three proteins work in conjunction with each other. Growth cones of $Smn^{-/-}$;SMN2 mice have a reduced number of actin mRNA positive growth cones and reduced actin staining in these areas, as well as reduced hnRNP R staining (Rossoll *et al.*, 2003).

SMN over-expression in differentiated PC12 cells has been shown to increase axon length; the same result was also seen following over-expression of hnRNP R. However, over-expression of hnRNP R mutants that lack either SMN binding domains

or mRNA binding domains had no effect on axon length (Rossoll *et al.*, 2003). This suggests that hnRNP R could be a modifier of SMA axon phenotype through SMN and mRNA binding. Similarly, knockdown of hnRNP R in primary motor neurons reduced axon length and calcium channel activity, which replicates SMN knockdown (Glinka *et al.*, 2010). Furthermore this was replicated in zebrafish where injection of morpholinos targeted against hnRNP R caused shortening of axons and increased axon branching, again replicating the effect of silencing SMN.

These data suggest that hnRNP R is involved in actin binding through interactions with SMA. Interestingly hnRNP R knockdown causes similar effects to SMN knockdown and hnRNP R overexpression can compensate for lack of SMN.

Work by our collaborators has furthered this by showing that hnRNP R is enriched in the growth cone of cultured motor neurons of wild-type mice compared to the rest of the axon. Conversely in growth cones of axons from $Smn^{-/-}$;SMN2 mice there is 50% less hnRNP. It was also shown that depletion of hnRNP R in purified motor neurons reduces actin levels to a similar amount as SMN depletion does. Furthermore overexpression of hnRNP R restores actin mRNA levels in $Smn^{-/-}$;SMN2 growth cones to almost wild type levels. hnRNP R overexpression was also able to rescue the reduction in axon length seen in $SMN^{-/-}$;SMN2 motor neurons. We therefore hypothesized that overexpression of hnRNP R in SMNΔ7 mice would have a similar effect to SMN over expression and ameliorate their SMA phenotype.

Adeno-associated virus serotype 6 was isolated as a contaminant of adenovirus stock and is thought to have arisen from a mutation of AAV1 (Rutledge *et al.*, 1998) or a natural recombination of AAV1 and AAV2 (Xiao *et al.*, 1999) as the sequence of AAV6 is very similar to both. AAV2 is the most widely characterised serotype of AAVs however there is a large presence of neutralising antibodies towards this virus in the human population. It would therefore be advantageous to use other serotypes for gene therapy. For example AAV6 can transduce cells in the presence of serum from animals exposed to AAV2. AAV6 has previously been shown to transduce motor neurons by retrograde transduction (Salegio *et al.*, 2012). It was

hypothesized that AAV6 may be able to pass the neonatal blood brain barrier and effectively transduce motor neurons after systemic delivery via facial vein injection.

We therefore decided to use AAV6 to express hnRNP R in neonatal SMNΔ7 mice and hypothesized that this would ameliorate the phenotype of these mice. We injected 10ul of viral vectors to the facial vein at post-natal day one which is considered to be presymptomatic. We injected 7 mice with AAV6-hnRNP R and injected 5 mice with AAV6-GFP as controls. To determine the effect of hnRNP R expression on disease phenotype the mice were monitored daily for signs of overall health and for motor ability, they were then sacrificed when they showed signs of severe ill health. Furthermore histological analysis was performed to determine levels of transduction in the spinal cord in order to evaluate the efficiency of AAV6 to transduce the CNS.

5.2 Results

5.2.1 *In Vivo* Assessment

5.2.1.1 Body Weight

SMNΔ7 mice, a well-established model of SMA, were used to assess the efficacy of AAV6 mediated hnRNP R expression on body weight, functional motor activity, motor neuron survival and lifespan of treated animals. AAV6-hnRNP R (n=7) or AAV6-GFP (n=5) vectors were injected systemically into the facial vein of postnatal day 1 SMNΔ7 mice.

These mice are characterised by progressive muscle weakness and die on average 2 weeks after birth (El-Khodor *et al.*, 2008).The body weight of all mice was monitored daily throughout the study as a measure of overall health. There was no significant difference between the weights of AAV6-hnRNP R treated mice and AAV6-GFP treated mice at any time point ($p>0.05$ two-way ANOVA) (fig. 5.1).

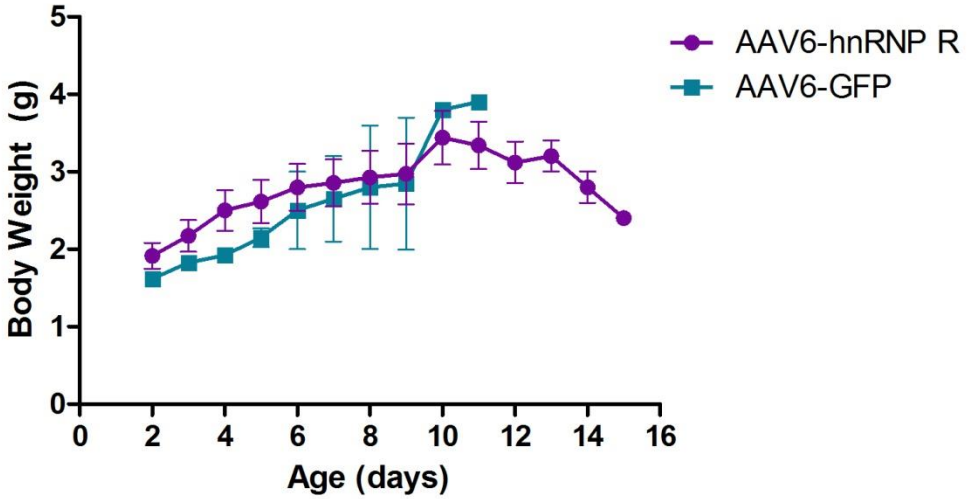

Figure 5.1 Body weight assessment. Change in body weight over duration of life span. AAV6-hnRNP R n=7, AAV6-GFP n=5. Data points represent mean weight in grams for each group with standard error of mean. Statistical analysis ($p>0.05$, 2-way ANOVA, Bonferroni post-hoc test) revealed no significant difference in weight at any day between day 2 and 11.

5.2.1.2 Righting-reflex

To test the general motor ability of these mice we performed a righting reflex test daily. This test assessed the success or failure of the mice to reposition themselves within 30 seconds after being placed on their back. The functional test revealed that overall more AAV6-hnRNP R treated mice were able to successfully complete the righting-reflex test when compared to AAV6-GFP mice at all time points (Fig 5.2, P<0.001, two-way ANOVA). However righting-reflex monitoring revealed variability within groups and between days. Variation between days meant that ability to self-right on one day was not predictive of being successful the following day. However a general trend of reduction in successful mice with time was seen in both groups.

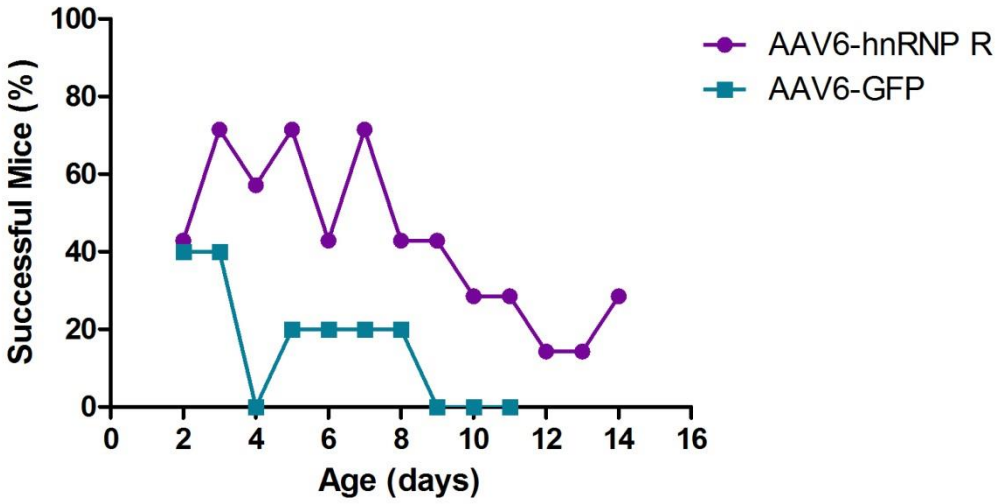

Figure 5.2 Righting reflex assessment. The ability of mice to re-orientate themselves after being placed on their back was assessed over the duration of their lifespan. AAV6-hnRNP R n=7, AAV6-GFP n=5. Data points represent percentage of mice in each group that were able to complete the test within 30 seconds. Statistical analysis revealed significant difference overall between the treatment with AAV6-hnRNP R and controls ($p<0.001$) but no significant difference at any individual time point (two-way ANOVA, Bonferroni post-hoc test).

5.2.1.3 Survival

The first mouse to die in the AAV6-GFP group did so at the age of 3 days whereas the first mouse to be sacrificed in the AAV6-hnRNP R group occurred at the age of 10 days. This trend continued throughout the study with the median survival of AAV6-GFP treated mice being 6 days whilst the median survival of the AAV6-hnRNP R group being 14 days. Furthermore the oldest mouse lived for 15 days after treatment with AAV6-hnRNP R whereas the longest surviving mouse after treatment with AAV6-GFP lived for 12 days (fig. 5.3 A). Mean survival for the AAV6-hnRNP treatment group was 13.0±0.76 days compared to 7.20±1.53 days for that of the AAV6-GFP treated group (fig. 5.3 B, $p<0.01$ t-test). Kaplan-Meier analysis revealed that treatment of SMNΔ7 mice with AAV6-hnRNP R caused a marginal but significant increase in survival compared to treatment with AAV6-GFP ($p<0.01$, Log-rank (Mantel-Cox) test).

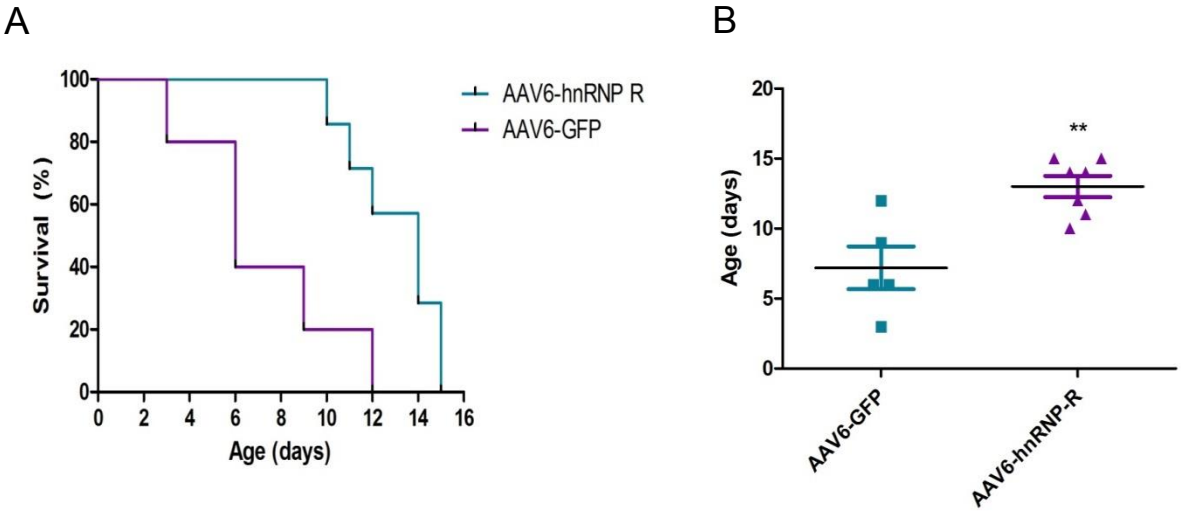

Figure 5.3 Survival analysis of SMNΔ7 mice. A: Kaplan-Meier cumulative survival curves comparing lifespan of AAV6-hnRNP R injected animals (n=7) and AAV6-GFP injected animals (n=5), $p<0.01$, log-rank (Mantel-Cox) test. **B:** Comparison of mean survival across the two groups ($p<0.01$, t-test).

5.2.2 Histological assessment

5.2.2.1 Motor Neuron Survival

To assess whether expression of hnRNP R could increase survival of spinal motor neurons we labelled and quantified motor neurons of the lumbar spinal cord. Lumbar spinal cord was taken from end-stage mice, cut into sections and stained for Nissl (cresyl violet). Motor neurons were identified by their location within the anterior horn of the spinal cord as well as their size and morphology. Nissl staining highlights RNA in the endoplasmic reticulum and causes dark staining of motor neurons. Motor neurons were counted under a light microscope by Dr K. Ning after being blinded to treatment groups. No significant difference was seen between groups, although AAV6-hnRNP R treated animals had a slightly higher mean motor neuron count than AAV6-GFP injected.

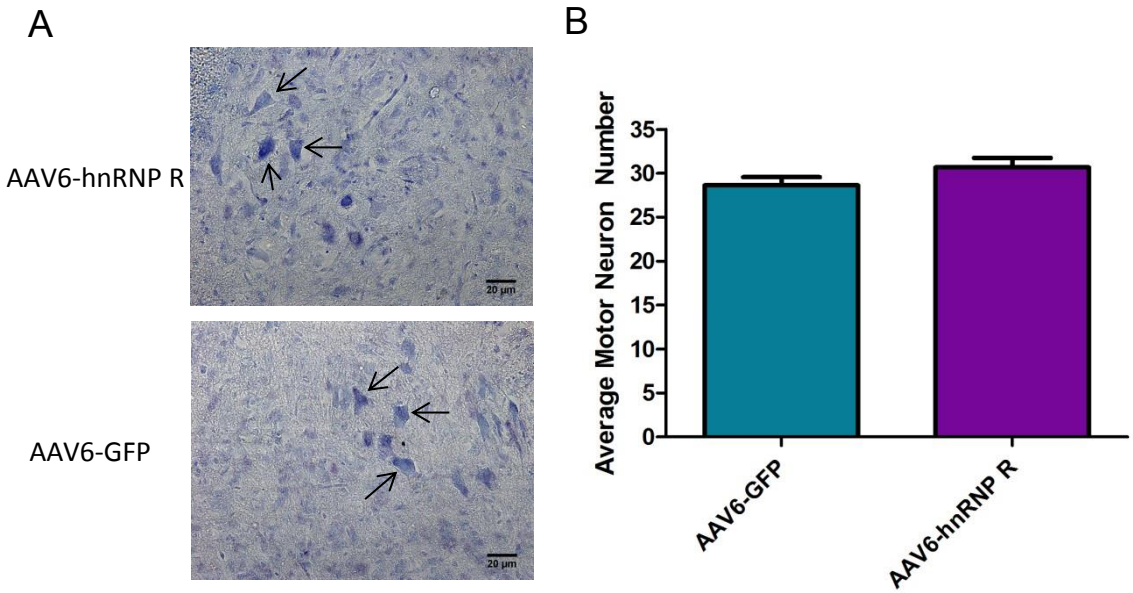

Figure 5.4 Quantification of lumbar spinal cord motor neurons. A: Representative images of lumbar spinal cord sections after Nissl staining. Arrows indicate motor neurons. Scale = 20µm. **B:** Quantification of motor neurons in the lumbar spinal cord. Data represents the mean number of motor neurons per section for each group. AAV6-hnRNP R n=3, AAV6-GFP n=2. No significant difference between AAV6-hnRNP R treatment and AAV6-GFP controls ($p>0.05$, t-test).

5.2.2.2 Transduction Efficiency of AAV6

To assess transduction efficiency of AAV6-GFP transduction in SMNΔ7 mice, lumbar spinal cord sections were stained with antibodies against GFP. Sections were then analysed using a light microscope to assess levels of transduction in the lumbar spinal cord. Staining showed the presence of GFP-positive neurons as well as GFP-positive astrocytes in the ventral horn of the lumbar spinal cord (fig. 5.5). The top and bottom panel (fig 5.5.) show GFP-positive neurons, the cell type was detmined by the relative large size of the cell body and presence of protruding axons. The transduced cell in middle panel (fig 5.5) is thought to be an astrocyte due to the round morphology and presence of small processes. However the total number of transduced cells within the spinal cord was very low. To further assess the efficacy of AAV6 muscle sections were analysed as AAV6 is known to transduce skeletal muscle with high efficiency. Transverse sections of gastrocnemius muscles were stained using an antibody against HA (with which hnRNP R was tagged) and a fluorescent secondary antibody was used. Analysis of sections under a fluorescent microscope showed a large amount of HA-positive muscle fibres (fig. 5.6). Untransduced fibres were also present in the muscle sections (fig 5.6, top arrows), which demonstrates the specificity of the HA staining. Spinal cord sections were also stained using an antibody against HA however no HA-positive cells were observed in the stained spinal cord sections. This suggests that the virus is able to successfully transduce muscle tissue despite the low transduction efficiency seen in the spinal cord.

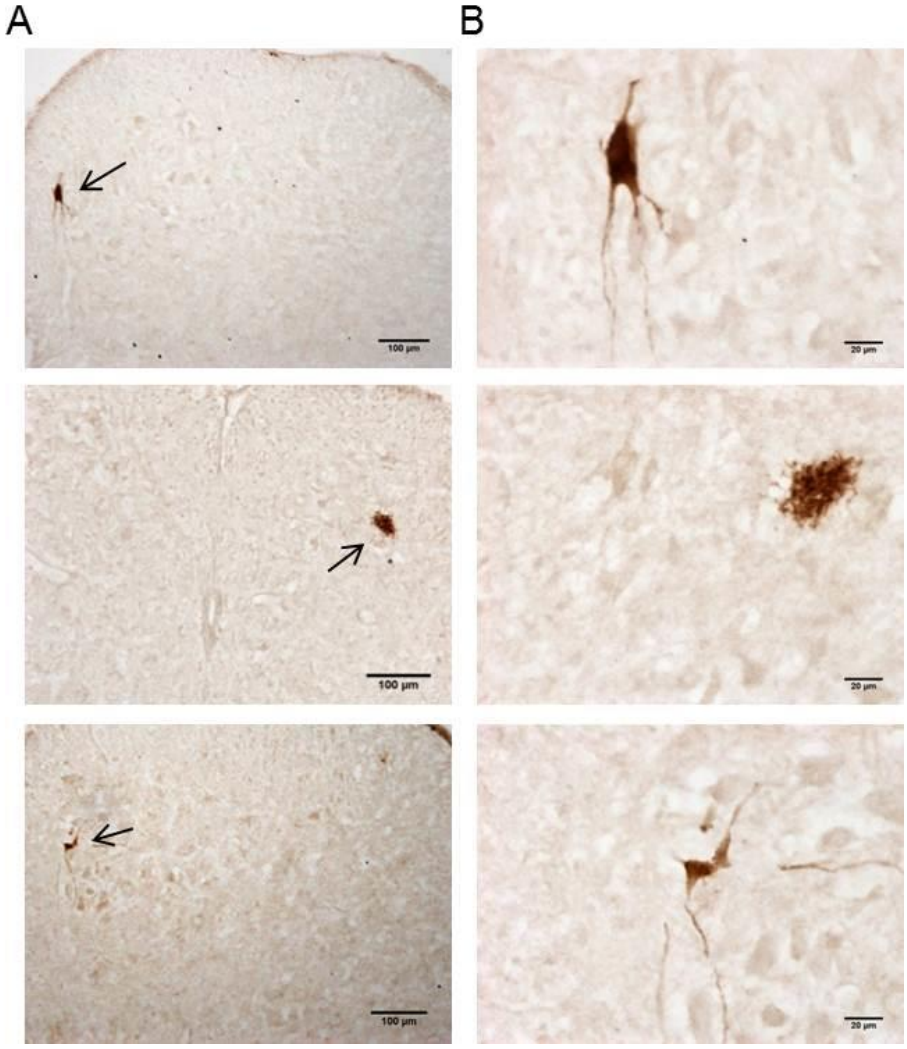

Figure 5.5 AAV6-mediated GFP transduction of lumbar spinal cord in SMNΔ7 mice. A: Spinal cord sections stained for GFP show a small number of motor neurons and astrocytes are transduced by AAV6-GFP. Scale = 100µm. **B:** High magnification images of **(A)**, scale = 20µm.

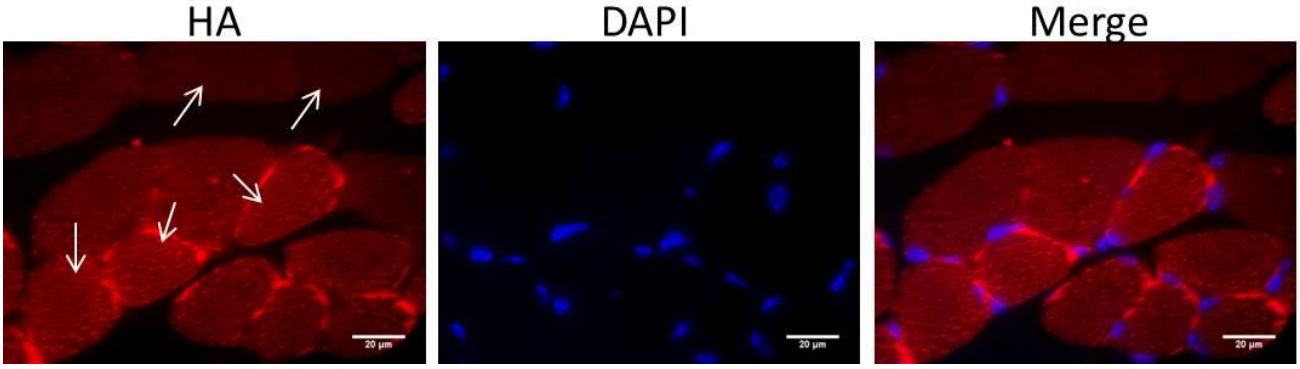

Figure 5.6 AAV6-hnRNP R transduction of gastrocnemius muscle in SMNΔ7 mice. Muscle sections stained for HA (red) and DAPI (blue) show effective transduction of muscle fibres by AAV6-hnRNP R. Scale = 20µm. The top arrows show untransduced fibres as contrast to the transduced fibres indicated by the bottom three arrows.

5.3 Discussion

hnRNP R was identified by our collaborator Michael Sendtner as a direct binding partner of SMN and a modifier of SMA phenotype *in vitro*. We therefore hypothesized that overexpression of hnRNP R would rescue the SMA phenotype in an *in vivo* SMA mouse model.

AAV6-hnRNP R treatment induced a small and marginal effect of survival of SMNΔ7 mice. Kaplan-Meier survival analysis revealed mean survival of 13.0±0.76 days and 7.20±1.53 days for AAV6-hnRNP R and AAV6-GFP treated mice respectively. However it is worth stating that AAV6-hnRNP R mice did not live any longer than the reported lifespan of this knock-out mouse model (average 2 weeks) (Le *et al.*, 2005). It is therefore unclear why the mean lifespan of the AAV6-GFP group was only 7.20±1.53 days. It would have been useful to include a cohort of uninjected SMNΔ7 mice as a further control to determine whether the difference in survival between the two groups was due to a positive effect of AAV6-hnRNP R or a negative effect of AAV6-GFP.

Alongside its effects on lifespan of SMNΔ7 mice we investigated motor ability of treated animals by assessing their ability to right themselves, as these animals were too young for other behavioural motor tests such as rotorod or catwalk analysis. The ability to self-right was generally improved in AAV6-hnRNP R injected mice, compared to controls. However there was a lot of variability in ability to complete the test. Variation was seen between mice in the same group and also between days for the same mouse. Therefore success on one day was not predictive of success the next day, and success of one mouse was not predictive of success for another mouse in the same group. This variation was possibly due to the young age of the mice but despite this variation there was a clear trend that AAV6-hnRNP R treated mice were better at performing the righting-reflex compared to AAV6-GFP controls.

Another phenotype of SMNΔ7 mice is their slow increase in weight gain; we therefore monitored growth of mice by daily measurement of their body weight. This

analysis revealed no significant difference between body weight of hnRNP R expressing mice and controls. Both these groups had significantly lower body weight than carrier littermates.

The number of motor neurons in the anterior horn of the lumbar spinal cord is greatly reduced in SMNΔ7 mice (Le *et al.*, 2005). We were therefore interested to assess the impact of hnRNP R gene therapy on spinal motor neuron survival. Cell counts of motor neurons in the lumbar spinal cord revealed that there was no difference in the number of motor neurons between the two treatment groups.

Overall there appears to be a small effect of overexpressing hnRNP in SMNΔ7 mice; however this effect was much less impressive than that seen in previous studies using SMN gene delivery in the SMNΔ7 mouse model (Foust *et al.*, 2010; Passini *et al.*, 2010; Valori *et al.*, 2010). These studies used AAV serotype 9 which has been reported to lead to widespread gene transfer in the CNS when delivered systemically in neonate mice (Foust *et al.*, 2010; Valori *et al.*, 2010). Prior to the start of this study using the hnRNP R gene, it was unclear how efficient the AAV6 vector was in crossing the blood brain barrier in mouse. Gene transfer analysis revealed very low number of GFP expressing motor neurons in the lumbar spinal cord (less than 5 per animal) and a similar number of GFP-expressing astrocytes. hnRNP R expression was also monitored using anti-HA-tag antibodies. Analysis of spinal cord sections revealed no HA-positive staining in motor neurons. In order to demonstrate that the vector can efficiently transduce other tissues muscle tissue was stained with anti-HA. The staining revealed high transduction efficiency of muscle fibres with AAV6-hnRNP. Together this study suggests that AAV6 does not effectively cross the blood brain barrier when administered systemically in neonate mice.

It is possible that the small effect of AAV6-mediated hnRNP R expression was due to very little transduction of lumbar spinal cord motor neurons. The improved survival of AAV6-hnRNP R injected mice compared to AAV6-GFP controls and the superior performance in the righting reflex suggests there was some positive effect of treatment. However this effect was not large enough to alter body weight or

survival. It is possible that some positive effect on phenotype was due to transduction in other tissues. It has been reported that therapy targeted towards SMA needs to affect peripheral tissue as well as the CNS to treat other organs effected by SMA (Hua *et al.*, 2011; Hamilton & Gillingwater, 2013).

In summary the effect of hnRNP R overexpression in SMNΔ7 neonates is inconclusive but hnRNP R still a promising candidate as a modifier of SMA. We have also demonstrated that AAV6 is not efficient at crossing the blood brain barrier in neonate mice. Further work using hnRNP R could be performed using AAV9 as a vector for hnRNP R expression since this has previously been shown to efficiently restore SMN levels in SMNΔ7 mice (Foust *et al.*, 2010; Passini *et al.*, 2010; Valori *et al.*, 2010).

Chapter 6

Effect of PTEN Silencing on SMA

6.1 Introduction

Spinal muscular atrophy is characterised by axon degeneration and subsequent death of motor neurons. The role of PTEN in negatively regulating cell survival, as well as cell size and axon growth suggests that it could be a potential therapeutic target for SMA (Stambolic *et al.*, 1998; Kwon *et al.*, 2001; Ning *et al.*, 2010). Inhibition of PTEN has been shown to confer resistance to apoptosis as well as improve regeneration after nerve injury and in purified motor neurons from an SMA mouse model. We therefore hypothesised that widespread silencing of PTEN in the spinal cord of SMNΔ7 mice may improve survival of motor neurons and possibly enhance axon growth, leading to an overall improvement in survival in this mouse model.

PTEN was first identified as a tumour suppressor gene found mutated in multiple cancers including glioblastomas, prostate, kidney and breast cancers (Li *et al.*, 1997) and was also named MMAC1 (Steck *et al.*, 1997). The protein was shown to contain a tyrosine phosphatase domain and also a region of homology with tensin. Tensin is a protein that links actin filaments to integrin receptors and interacts with tyrosine-phosphorylated proteins and plays an important role in muscle regeneration and cell migration (Lo, 2004). The PTEN protein is made up of 403 amino-acids and contains three domains. A phosphatase domain is situated at the N-terminus, with a C2 domain involved in lipid-binding and a PDZ ligand sequence at the C-terminus (Ross *et al.*, 2001). PTEN also has two PEST sequences that cause proteasomal degradation, leading to rapid protein turnover.

Shortly after identification the protein was shown to be a dual specificity phosphatase due to the ability to dephosphorylate serine/threonine and tyrosine peptides (Myers *et al.*, 1997). Furthermore it was demonstrated that this protein was able to dephosphorylate phosphatidylinositol 3,4,5-triphosphate (PIP3) (Maehama & Dixon, 1998; Stambolic *et al.*, 1998). This was consolidated by the finding that PKB/Akt is hyperphosphorylated in cells lacking PTEN. PKB/Akt is a promoter of cell survival, and activation is dependent on levels of PIP3. In short PTEN inhibits PIP3 mediated activation of PKB/Akt by dephosphorylating PIP3 to PIP2 (fig. 6.1).

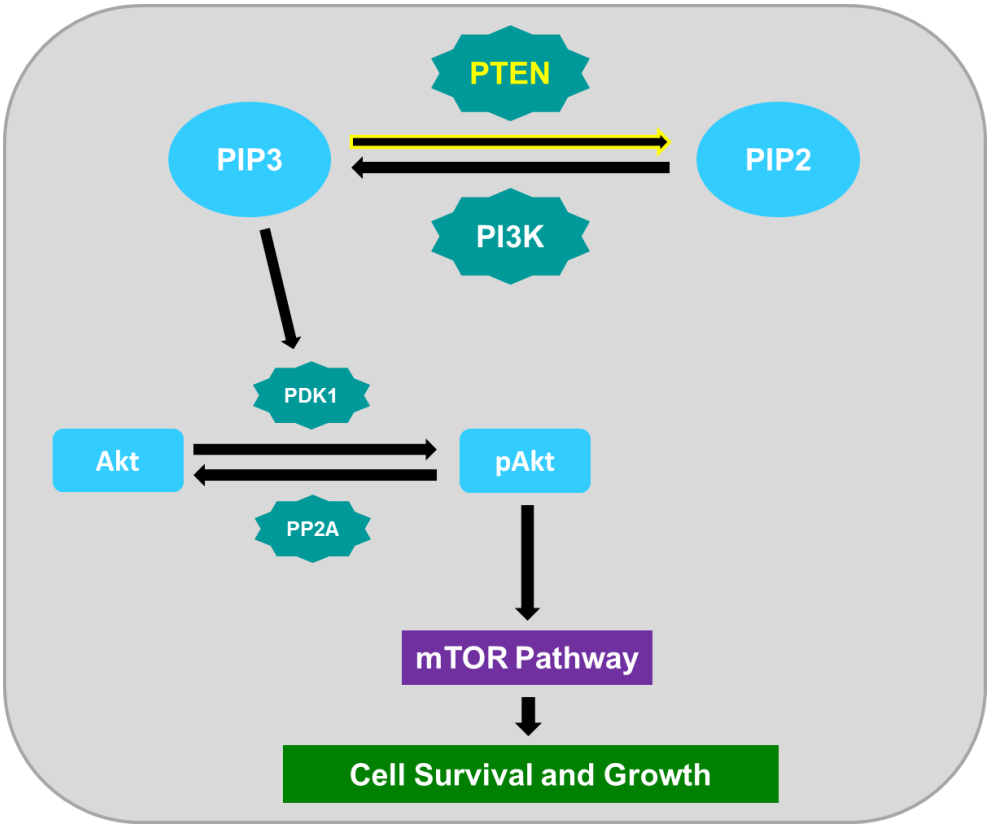

Figure 6.1 PTEN function in the PI3K / Akt pathway. PTEN negatively regulates the PI3K / Akt pathway by dephosphorylating PIP3 to PIP2. PI3K activates PDK1 to phosphorylate Akt, activating the mTOR pathway (among others) to promote cell survival and growth.

Tissue specific knockdown of PTEN in the brain has been used to investigate the function of this protein during brain development. The brains of these mice were significantly larger than controls and neurons displayed increased soma size (Backman *et al.*, 2001; Kwon *et al.*, 2001). The mice appeared healthy at birth but developed seizures and ataxia at the age of 9 weeks. There is some disagreement as to whether PTEN knockdown in the brain affects proliferation as some groups suggested proliferation was increased (Groszer *et al.*, 2001; Li *et al.*, 2002) but others found no difference (Backman *et al.*, 2001; Kwon *et al.*, 2001). Furthermore PTEN-null cells display increased resistance to apoptosis when cells were exposed to various apoptosis stimuli (Stambolic *et al.*, 1998), as well as preventing excitotoxic death after exposure to glutamate (Gary & Mattson, 2002).

Conditional knockdown of PTEN in the brain has been used to further elucidate how this protein can affect neurons. PTEN-deficient neurons display increased cell size and dendritic spine density alongside enlargement of projections (Kwon *et al.*, 2006; Fraser *et al.*, 2008; Luikart *et al.*, 2011). Furthermore PTEN knockdown in PC12 cells lead to increased proliferation and survival, and improvement in neurite outgrowth in differentiating PC12 cells (Jia *et al.*, 2010). PTEN silencing also ameliorates the inhibitory effect that myelin-associated glycoproteins have on neurite outgrowth in cortical neurons (Perdigoto *et al.*, 2011). PTEN plays an important role in axon outgrowth; knockdown in muscle-nerve co-cultures from xenopus displayed increased rate of axon outgrowth after contact with muscle cells (Li & Peng, 2012). Enhanced axon outgrowth was also seen in PTEN-null neurons in mice (Kwon *et al.*, 2006).

Interestingly PTEN-knockdown has been shown to improve axon regeneration following nerve injury. Conditional PTEN deletion improved axon regeneration in injured corticospinal neurons (Liu *et al.*, 2010), injured adult retinal ganglion cells (Park *et al.*, 2008) and drosophila sensory neurons (Song *et al.*, 2012). Furthermore when PTEN-null dopaminergic neurons were transplanted into the brains of a mouse model of Parkinson's disease they displayed improved survival and fibre outgrowth (Zhang *et al.*, 2012). PTEN depletion was also able to rescue the shortened axons of cultured motor neurons purified from SMNΔ7 mice (Ning *et al.*, 2010). PTEN depletion in these SMN-null motor neurons also improved survival, increased growth cone size and restored levels of β-actin in growth cones. Improvement in survival of cultured motor neurons was also translated to improvement in survival of motor neurons in vivo following a single injection of AAV6 expressing siPTEN into the gastrocnemius muscle of SMNΔ7 mice (Ning *et al.*, 2010).

To ensure efficient delivery of siRNA against PTEN to the CNS of SMNΔ7 mice we used the adeno-associated vector serotype 9 (AAV9) which has been shown to rapidly and effectively transduce cells of the CNS after intravenous injection in neonatal mice (Zincarelli *et al.*, 2008; Foust *et al.*, 2009; Miyake *et al.*, 2011). Data from several independent groups indicates that systemic AAV9 delivery causes widespread transduction of neurons and glia in the brain and spinal cord as well as

other cell types in other tissues including heart, muscle and liver (Zincarelli *et al.*, 2008; Foust *et al.*, 2009; Valori *et al.*, 2010). Furthermore administration of scAAV9 delivering SMN protein has extended the life-span and ameliorate motor deficits in a mouse model of SMA (Bevan *et al.*, 2010; Valori *et al.*, 2010; Dominguez *et al.*, 2011). We therefore expected that a scAAV9 vector would be able to provide robust transduction in the spinal cord and thus cause a significant level of PTEN depletion. Self-complementary vectors negate the need for AAV to convert single-stranded DNA into double stranded DNA before transgene expression (McCarty, 2008). This means that self-complementary vectors can express transgenes faster and more efficiently than single-stranded vectors (Wang *et al.*, 2003).

A self-complementary AAV9 construct was designed using the siRNA sequence as previously reported (Ning *et al.*, 2010); this construct also expresses GFP as a reporter gene to assess levels of transduction. The siRNA sequence consists of a 19 nucleotide sequence that target exon 1 of the gene. This sequence generates around 60% reduction in PTEN levels in primary motor neurons (Ning *et al.*, 2010).

6.2 Results

SMNΔ7 mice were injected with 10µl (10^{10} viral particles) of scAAV9-siPTEN (n=10) into the facial vein on post-natal day 1. As a control 10 SMNΔ7 mice were also injected with scAAV9-scrambled-siPTEN, which expresses the same siRNA construct but with the nucleotides in a different order. Untreated SMNΔ7 mice (n=9) and carrier ($Smn^{+/+}$;$SMN2^{+/+}$;$SMN\Delta7^{+/+}$) littermates (n=6) were also included as further controls. The mice were assessed daily throughout their life to determine whether there was any effect on phenotype.

6.2.1 Body Weight

SMNΔ7 is a well-established mouse model of SMA. SMNΔ7 mice are characterised by muscle weakness and die within 2 weeks of age (Le *et al.*, 2005). A major aspect of the phenotype of SMNΔ7 mice is slow growth and body weight decrease from postnatal day 8 (El-Khodor *et al.*, 2008). We therefore measured how the body weight of these mice changed over time. Mice injected with scAAV9-siPTEN displayed slow weight gain, however body weight continued to increase after postnatal day 9 when the body weight of scAAV9-scrambled-PTEN controls began to fall (fig. 6.2 B). scAAV9-siPTEN treated mice had significantly higher bodyweight than scAAV9-scrambled-siPTEN controls from day 12 onwards ($p<0.05$, two-way ANOVA). Body weight measurement revealed that scAAV9-siPTEN treated mice continued to increase steadily throughout their life, but remained approximately half the weight of healthy carriers. Carrier littermates had significantly higher body weights than scAAV9-siPTEN treated animals from day 20 onwards ($p<0.05$, two-way ANOVA).

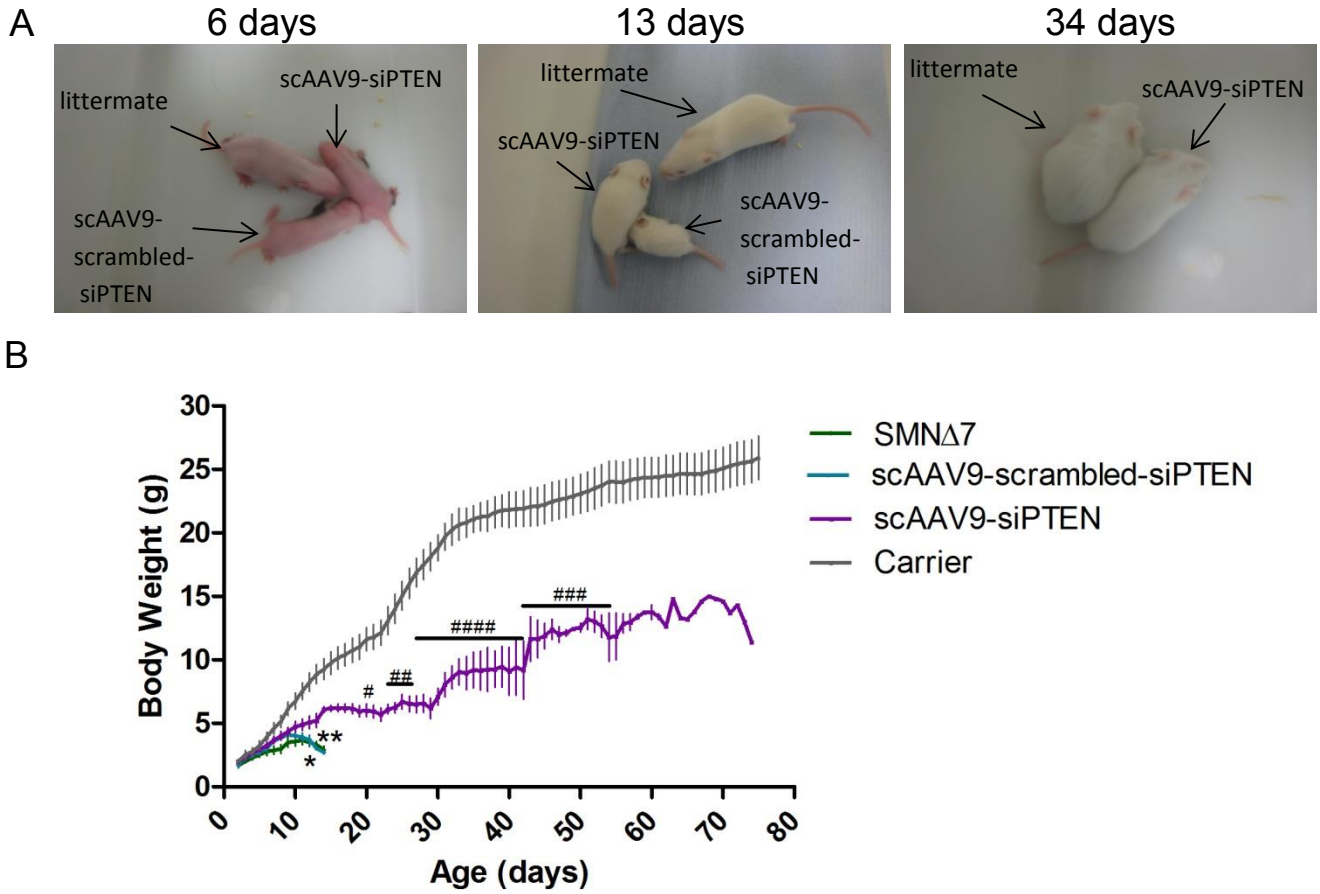

Figure 6.2 scAAV9-siPTEN improves growth in SMNΔ7 mice. A: Pictures showing the same SMNΔ7 pups at different ages, as indicated. A gender-matched carrier littermate is included in each picture for reference. The pups were injected at postnatal day 1 with either scAAV9-siPTEN or scAAV9-scrambled-siPTEN. **B:** Body weight growth in SMNΔ7 injected with scAAV9-siPTEN (n=10) or scAAV9-scrambled-siPTEN (n=10). Untreated and carrier groups were included as controls. * p<0.05, ** p<0.01, scAAV9-scrambled-siPTEN versus scAAV9-siPTEN, # p<0.05, ## p<0.01, ### p<0.001, #### p<0.0001, carrier versus scAAV9-siPTEN, two-way ANOVA with Bonferroni post-hoc test.

6.2.2 Righting Reflex

A righting-reflex test was used to assess the general motor function of treated SMNΔ7 mice. The test was performed daily and assessed whether animals were able to move themselves onto their paws after being placed on their backs. If the animal was able to do this within 30 seconds it was deemed successful (El-Khodor *et al.*, 2008). The number of mice able to successfully right themselves in the scAAV9-siPTEN treatment group increased steadily and reached 100% at 15 days (fig. 6.3). In comparison the scAAV9-scrambled-siPTEN controls were unable to complete the test on the majority of days, with the highest level of success being

20% on two non-consecutive days (fig. 6.3). The number of scAAV9-siPTEN treated animals able to compete the righting-reflex test was significantly higher ($p<0.05$, two-way ANOVA) than scAAV9-scrambed-siPTEN treated animals from day 15. The ability of carrier littermates to complete the test was also assessed and all carriers were able to successfully complete the test from day 2 onwards. There was no significant difference between the ability of scAAV-siPTEN mice to complete the test and the ability of carrier animals to complete the test from day 8 ($p>0.05$, two-way ANOVA).The outcome of this behaviour test demonstrates a robust improvement in the phenotype of mice injected with scAAV9-siPTEN over time.

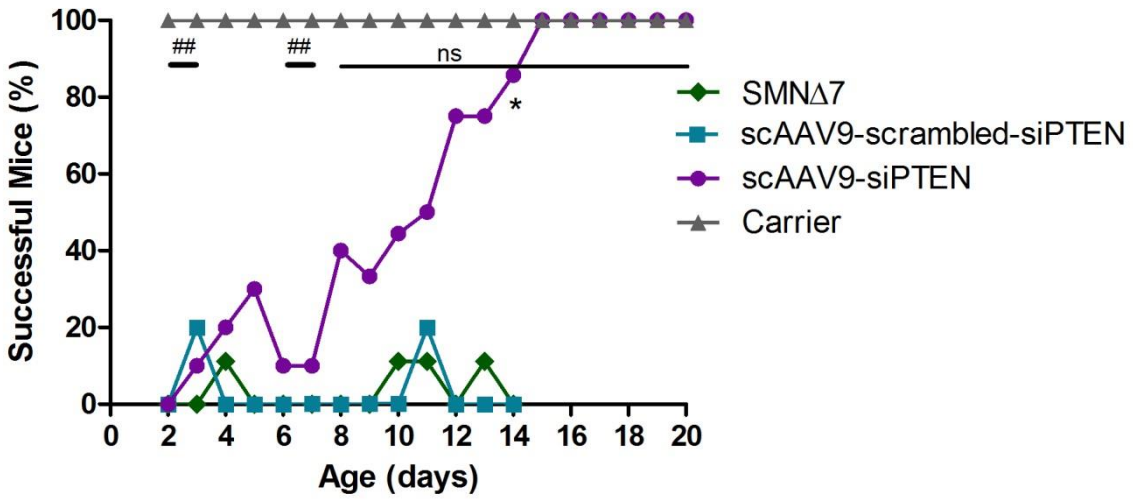

Figure 6.3 Motor function assessment in rescued SMNΔ7 mice. Percentage of mice able to complete the righting reflex test. Mice were placed on their backs and were deemed successful if they were able to re-orientate within 30 seconds. scAAV9-siPTEN injected mice improved gradually over the first 15 days of age. * $p<0.05$, scAAV9-siPTEN versus scAAV9-scrambled-siPTEN, ## $p<0.01$, scAAV9-siPTEN versus carrier, two-way ANOVA with Bonferroni post-hoc test.

6.2.3 Survival

As well as assessing body weight and motor function mice were monitored daily for any signs of ill health. The tails of scAAV9-siPTEN mice were shorter and thicker than healthy littermates and as the animals aged the tails appeared to develop

necrosis. The ears of these mice also became red and inflamed and they too developed necrosis. This has previously been reported in rescued SMNΔ7 mice and is thought to be a secondary phenotype caused by the disease, rather than an effect of the scAAV9 delivery (Narver *et al.*, 2008; Foust *et al.*, 2010; Passini *et al.*, 2010; Valori *et al.*, 2010; Dominguez *et al.*, 2011; Hua *et al.*, 2011).

When treated mice began to exhibit reduced provoked behaviour and lack of grooming alongside a slight reduction in body weight of approximately 10-30% they were humanely culled. They were still successfully able to complete the righting reflex test at this point; however it was observed that some mice dragged their hind-limbs as they walked. Kaplan-Meier analysis was performed to assess the survival time of scAAV9-siPTEN treated mice compared to scAAV9-scrambled-siPTEN treated controls (fig 6.4). This analysis showed a significant increase in lifespan following treatment with scAAV9-siPTEN (fig 6.4), compared to mice injected with scAAV9-scrambled-siPTEN. Mean survival for scAAV9-siPTEN treated mice was 30.4±7.4 days compared to 9.2±1.5 days for scAAV9-scrambled-siPTEN injected mice ($p<0.01$, one-way ANOVA with Tukey's post-hoc test) and 10.56±1.42 for untreated SMNΔ7 mice. The longest surviving treated mouse lived for 74 days, and 60% of mice injected with scAAV9-siPTEN lived for longer than any of the scAAV9-scrambled-PTEN controls. However four scAAV9-siPTEN injected mice did not display any improvement in survival. The data from these animals were still included in the body weight (fig. 6.3) and righting reflex analysis (fig 6.4).

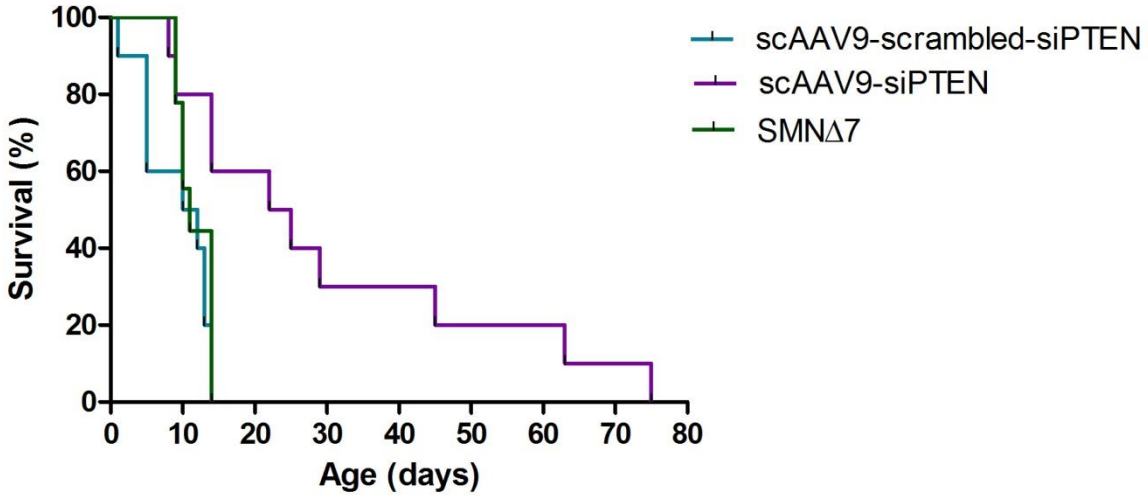

Figure 6.4 Kaplan-Meier survival curve. This graph summarises survival times for scAAV9-siPTEN injected animals (n=10) compared with scAAV9-scrambled-siPTEN (n=10) and uninjected SMNΔ7 controls (n=9). $p<0.01$ scAAV9-scrambled-siPTEN verses scAAV9-siPTEN, log-rank (Mantel-Cox) test. Mice injected with scAAV9-siPTEN lived significantly longer than scAAV9-scrambled-siPTEN ($p<0.01$) and SMNΔ7 controls ($p<0.05$) (one-way ANOVA with Tukey's post-hoc test).

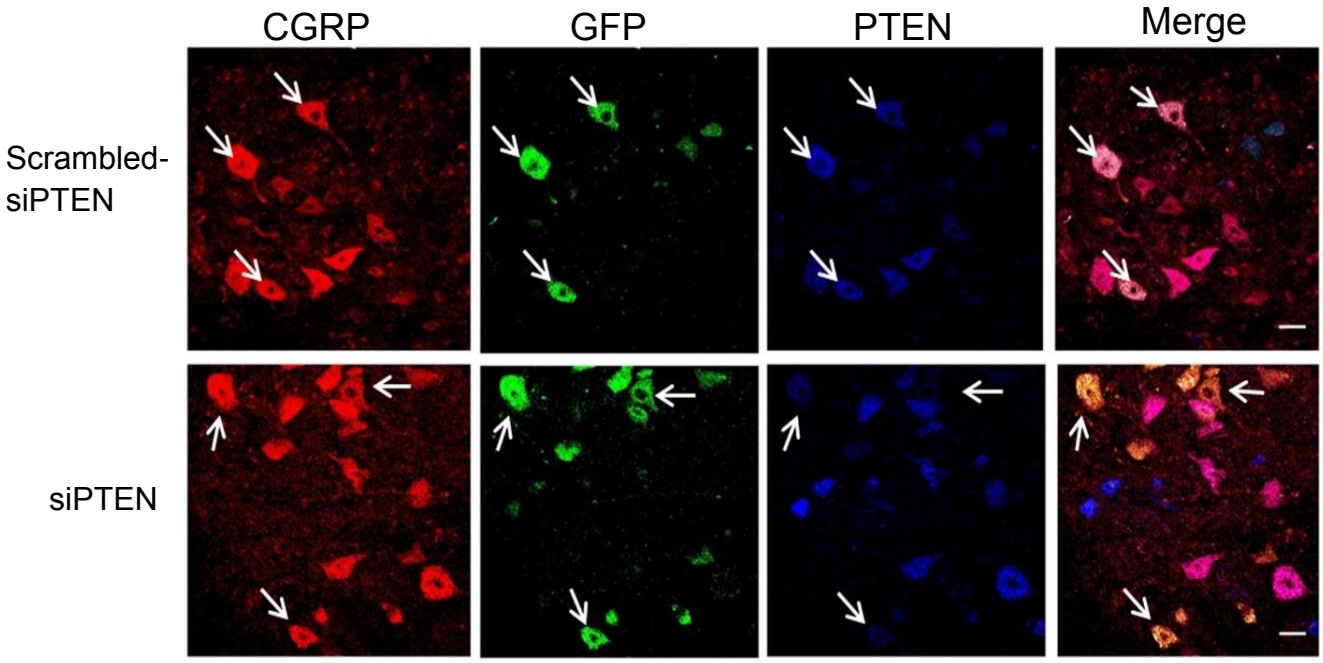

Figure 6.5 scAAV9-siPTEN causes transduction of motor neurons and a reduction in PTEN expression. Immunohistochemistry of lumbar spinal cord sections showing CGRP labelled motor neurons (red), GFP positive cells (green), and PTEN expression (blue). GFP expression demonstrates robust transduction of motor neurons with both vectors used. The staining confirmed PTEN depletion in GFP positive motor neurons of the scAAV9-siPTEN injected group compared to scAAV9-scrambled-siPTEN controls. Scale bars = 20µm

6.2.4 Transduction and PTEN Depletion in Spinal Cord Motor Neurons

We hypothesized that the increased survival observed was due to the effect of PTEN depletion in spinal cord motor neurons. Immunohistochemistry was therefore used to confirm whether spinal cord motor neurons were transduced, and to determine the efficacy of scAAV9-siPTEN in mediating PTEN silencing. The viral vector used also expresses GFP to enable identification of transduced cells. Lumbar spinal cord sections were stained and imaged with help from Dr K. Ning. To assess gene transfer an antibody targeted to GFP was used to detect cells that had been transduced, whilst an antibody against PTEN was used to assess PTEN expression levels. GFP transgene expression was observed in both scAAV9-siPTEN and scAAV9-scrambled-siPTEN injected animals, displaying that both vectors cause transduction (fig 6.5). GFP-positive cells in scAAV9-siPTEN treated animals displayed reduced PTEN fluorescence compared to those in scAAV9-scrambled-siPTEN controls.

6.2.5 Motor Neuron Survival

To investigate whether PTEN knockdown improves the survival of motor neurons in SMNΔ7 mice spinal cord sections were stained for the motor neuron specific marker calcitonin gene-related peptide (CGRP) and positive cells were counted (fig. 6.6 A). Staining and counting was performed with help from Dr K. Ning who was blinded to treatment groups. Because the main aim of this study was to determine whether scAAV9-siPTEN could affect survival the spinal cords used to assess motor neuron survival were from mice of different ages. The three spinal cords from the scAAV9-siPTEN group were from animals aged 25, 29 and 75 days whereas the spinal cords from the scAAV9-scrambled-siPTEN group were from once mouse aged 10 days and two mice aged 13 days. The number of CGRP positive cells per section in the lumbar spinal cord was significantly greater in spinal cord sections of mice injected with scAAV9-siPTEN (n=3), compared to that of scAAV9-scrambled-siPTEN controls (n=3, fig. 6.6 B $p<0.01$).

Furthermore some spinal cord sections were stained with an antibody against GFP alongside CGRP staining and the number of GFP-positive and GFP-negative motor neurons was assessed (fig. 6.6 C). This revealed that the increase in motor neuron numbers can be attributed to increased numbers of GFP-positive cells, as the number of untransduced cells was the same in scAAV9-siPTEN sections and scAAV9-scrambled-siPTEN controls. Therefore the improvement in survival of spinal motor neurons was due to transduction by AAV9-siPTEN. The data suggests that PTEN depletion can reduce cell death in motor neurons of SMNΔ7 mice.

Quantification of GFP-positive motor neurons enabled the transduction efficiency of scAAV9-siPTEN and scAAV9-scrambled-siPTEN to be calculated (fig. 6.6 D). This revealed that 68.22% and 51.05% of spinal motor neurons were transduced by scAAV9-siPTEN and scAAV9-scrambled-siPTEN respectively. The difference in levels of transduction can be attributed to the improved survival of motor neurons transduced with scAAV9-siPTEN compared to scAAV9-scrambled-siPTEN.

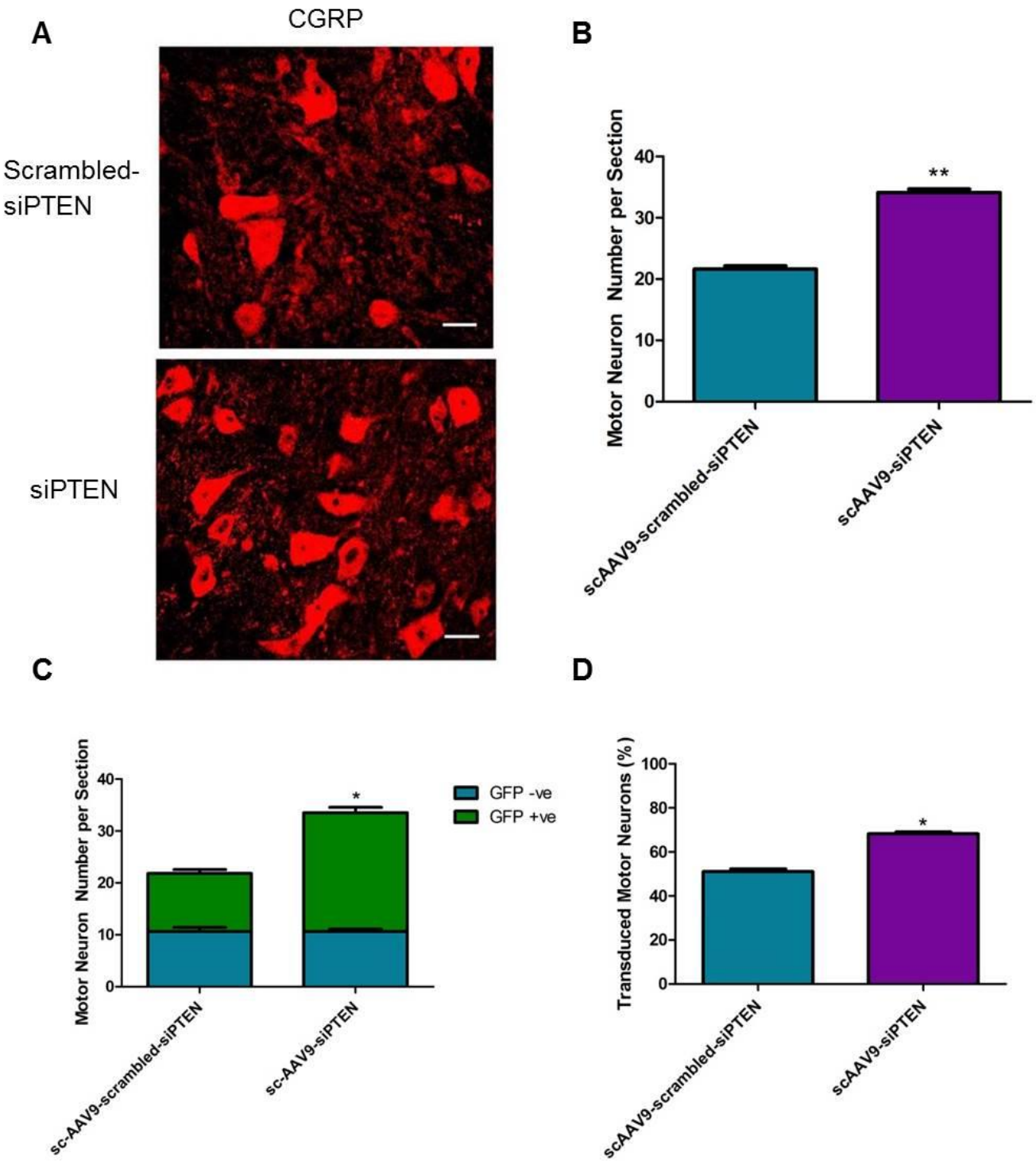

Figure 6.6 Effect of PTEN depletion on motor neuron survival in the spinal cord of SMNΔ7 mice. Lumbar spinal cord sections were stained for CGRP and GFP to quantify motor neuron number and transduction efficiency. **A:** representative images of the ventral horn of the lumber spinal cord of treated animals, stained with anti-CRGP (red). Scale bars = 20µm. **B:** Quantification of mean number of CRGP-positive cells per section. **p<0.01, t-test, n=3. **C:** Quantification of mean number of GFP-positive and GFP-negative spinal motor neurons per section. * p<0.05 (GFP positive cells), t-test, n=3. **D:** Mean percentage of spinal motor neurons that were GFP positive per section. * p<0.05, t-test, n=3.

6.3 Discussion

The data here reveals that a single injection of a scAAV9 expressing siRNA targeted against PTEN is sufficient to reduce PTEN levels in lumbar spinal cord motor neurons and attenuate motor deficits in a mouse model of SMA. PTEN reduction lead to a significant increase in the number of motor neurons in the spinal cord compared to animals injected with scAAV9-scrambled-siPTEN. Furthermore animals treated with scAAV9-siPTEN displayed significantly longer survival times than scAAV9-scrambled-siPTEN controls. Mean lifespan of siPTEN treated mice was 30.4±7.4 days compared to 9.2±1.5 days for animals that received the scrambled-siRNA control vector. The longest surviving mouse lived to 74 days, compared to 14 days for scAAV9-scrambled-siPTEN injected controls, which is an increase in maximum lifespan of 428%, with a mean increase in lifespan of 230%.

Four of the 10 mice injected with scAAV9-siPTEN displayed no improvement in lifespan compared to controls. The reason for this has not been elucidated however it may be due to inefficient gene transfer as previously reported (Valori *et al.*, 2010). This was reasoned to be due to technical failure during intravenous delivery of the vector. Western blot or QPCR could have been used to detect GFP protein or mRNA levels in the organs of mice that showed no improvement following scAAV9-siPTEN injection. This would have determined whether inefficient vector delivery was the cause of this lack of improvement. Due to the small size of mice at postnatal day one, efficient intravenous delivery can be challenging. Therefore it may be necessary to improve intravenous administration technique for further studies. It would be useful to check transduction levels in the mice that displayed no response to treatment to determine how efficient gene transfer was in these mice.

Furthermore within the mice that did show an improvement in lifespan there was variability, with three mice being sacrificed between 22 and 29 days old and three mice living for between 45 and 75 days. Variability in improvement of lifespan was also observed in two other studies that used scAAV9 to express SMN (Valori *et al.*, 2010; Dominguez *et al.*, 2011). Interestingly however there was no observed

difference in transduction efficiency or motor neuron numbers between mice that died at 25, 29 and 75 days. This suggests there may be other external influences on how well these mice thrive and how long they live.

Alongside survival an amelioration of phenotype in rescued animals was observed. PTEN deficient animals displayed robust weight gain, coupled with improved motor function comparable to that of carrier littermates when assessed by righting-reflex test. During early life the scAAV9-siPTEN treated animals were indistinguishable from scAAV9-scrambled-siPTEN controls in terms of size and appearance. By day 10 however the siPTEN treated animals were performing better at the motor function test, and were continuing to gain weight, unlike the control animals, whose weight began to fall. As scrambled-siPTEN controls began to appear moribund, the siPTEN treated animals continued to perform well and looked healthy, albeit smaller than carrier littermates. This suggests that it took some time for the viral vector to express siRNA and cause an effect.

Although AAV9-siPTEN somewhat rescued the phenotype of these SMNΔ7 mice they were obviously different to carriers. As mentioned they were smaller than carrier littermates, with body weight peaking at 15g for the longest surviving mouse, compared to a peak weight of 29g for a 75 day old carrier. Furthermore the tails of these rescued mice were shorter and thicker than carrier littermates. This defect was not apparent from birth but became more obvious as the animals grew and their tails did not lengthen. As the rescued animals aged their tails began to show signs of necrosis, at around the same time the ear of these animals became red and inflamed and they too began to display necrosis. This phenotype has been reported previously in rescued SMNΔ7 mice (Valori *et al.*, 2010; Dominguez *et al.*, 2011) and also in SMA patients (Araujo *et al.*, 2009; Rudnik-Schoneborn *et al.*, 2010). Distal necrosis is thought to be due to SMN deficiency affecting vasculature however the full reason for this has not yet been resolved. Unfortunately PTEN depletion was not able to rescue these defects, either because the abnormalities occur during early development or because siRNA expression was not high enough in these areas.

Further work needs to be undertaken to fully understand how PTEN knockdown improved survival of these SMNΔ7 mice. The increase in motor neuron numbers seen in the spinal cord suggests that PTEN knockdown improves survival in these cells. Immunofluorescence was used to demonstrate reduction in PTEN levels in motor neurons of the lumbar spinal cord. It may have been possible to quantify the level of PTEN silencing in the lumbar spinal cord by QPCR, however this method may not be sensitive enough to detect a reduction PTEN levels due to the relatively large number of cells in the spinal cord that are not transduced. It would be possible to use laser capture microdissection (LCM) to isolate only motor neurons from spinal cords for QPCR in order to improve sensitivity. However LCM is very time consuming and it may be difficult to isolate enough motor neurons to have sufficient quantities of mRNA for QPCR. The improvement in motor neuron survival seen here corroborates with previously published data showing that PTEN silencing can improve motor neuron survival *in vivo* following intramuscular injection of AAV6 expressing siPTEN (Ning *et al.*, 2010). It would have also been of interest to determine the level of motor neuron survival in the cervical spinal cord as these cells are also affected by SMA, however time constraints meant only the lumbar spinal cord was analysed.

Previous *in vitro* data also shows that axons of cultured motor neurons from SMNΔ7 mice have longer axons, larger growth cones and increased β-actin levels (Ning *et al.*, 2010). This suggests that axon length may also be increased in motor neurons *in vivo* although this is yet to be determined. Defects in axon outgrowth in SMA are thought to be due to impaired trafficking of β-actin and reduced SMN levels in the growth cone. This leads to abnormalities at the synapse and neuromuscular junction. Therefore it can be expected that silencing PTEN *in vivo* will have a similar effect as in cultured motor neurons and improve axon length by increasing β-actin levels in the growth cone.

Our results show that it is possible to improve the phenotype of SMA mice without directly targeting the SMN protein through silencing of PTEN. This builds upon

previously published research showing that silencing PTEN can improve motor neuron survival (Ning *et al.*, 2010).

The increase in life-span seen here was not as impressive as has been reported in studies overexpressing SMN (Bevan *et al.*, 2010; Foust *et al.*, 2010; Valori *et al.*, 2010; Dominguez *et al.*, 2011). However the use of PTEN knockdown to improve motor neuron survival suggests a possible option for increasing survival in a variety of degenerative diseases such as motor neuron disease, Parkinson's disease and Alzheimer's disease. Interestingly, a previous study has demonstrated that PTEN knockdown in dopaminergic neurons can rescue motor deficits in two mouse models of Parkinson's disease (Domanskyi *et al.*, 2011). PTEN silencing could also be used as a combination therapy alongside SMN overexpression.

Chapter 7

DISCUSSION

SMA is a genetic disease caused by recessive mutations in a single SMN gene (Lefebvre *et al.*, 1995). Gene therapy therefore represents an attractive approach for SMN replacement in this devastating disease (Lefebvre *et al.*, 1995; Foust *et al.*, 2010; Passini *et al.*, 2010; Valori *et al.*, 2010; Dominguez *et al.*, 2011; Benkhelifa-Ziyyat *et al.*, 2013). To achieve successful gene therapy for SMA, widespread delivery of therapeutic genes to the CNS is required. There appears to be other disease-modifying genes that also could be targeted for gene therapy-mediated treatment for SMA including hnRNP R and PTEN (Rossoll *et al.*, 2003; Ning *et al.*, 2010). This project had two broad aims: i) to assess different vector systems for gene therapy and ii) to investigate the possibility of rescuing SMA phenotype through SMN-independent targets. Four different vector systems were tested in this project; three serotypes of AAV, namely AAV5, AAV6 and AAV9 as well as a non-viral delivery system, polymersomes. Furthermore we explored novel therapeutic strategies for SMA by modulation of disease modifying genes, hnRNP R and PTEN.

7.1 Project Outcomes

The use of polymersomes as a non-viral delivery method for gene therapy represents a novel technology. We therefore believe that this approach will need extensive optimisation before being ready for *in vivo* applications. DNA encapsulation within polymersomes have previously been reported (Lomas *et al.*, 2007; Lomas *et al.*, 2010), but never tested for therapeutic strategies. Here we show encapsulation occurs in a size-dependent manner with larger vesicles being able to encapsulate more DNA. Furthermore centrifugation was used to sort polymersomes based on size. This enabled the exclusion of polymersomes with low encapsulation thus increasing the amount of encapsulated DNA. Luciferase was used as a reporter plasmid and delivered to HEK293T cells resulting in luciferase expression. A linear relationship was seen between the amount of luminescence detected and the amount of encapsulated DNA in the polymersomes used for transfection. We can therefore conclude from this study that polymersomes encapsulate DNA in a size

dependant manner and transduction is directly related to the amount of encapsulated DNA.

Polymersomes were then used to drive overexpression of SMN through the encapsulation of SMN plasmid DNA and transfection of HEK293T cells and fibroblasts derived from a SMA type I child. Transfection of HEK293T cells resulted in a 2.6-fold increase in SMN protein levels and a 38-fold increase in SMN mRNA levels. Furthermore SMN mRNA levels were increased 367-fold in SMA fibroblasts. SMN restoration in SMN-deficient fibroblasts was confirmed by immunofluorescence. Therefore we can conclude that polymersomes are able to deliver gene therapy for spinal muscular atrophy *in vitro*. However this technology will need further optimisation before use for *in vivo* applications. In particular the main challenge is to target polymersomes to penetrate the BBB and reach target cells such as motor neurons.

The ability of AAV5 to transduce CNS tissue following neonatal IV injection was investigated in a pilot study. Two vector systems were used with different promoters, CAG and CMV. The vector system incorporating the CMV promoter produced almost no transduction in the CNS. A modest amount of transduction was seen in the brain and a small number of transduced cells were detected in the lumbar spinal cord with AAV5-CAG-GFP. Interestingly the highest level of transduction in the brain appeared to be of cells within the ventricles whilst the highest level of transduction in the spinal cord was seen in the dorsal root. Throughout the brain and lumbar spinal cord GFP-positive fibres were detected which appeared to be axons. There also appeared to be some tropism of AAV5 for white matter tissue within the CNS. This pilot study revealed that AAV5 mediates poor gene transfer efficiency in the CNS following IV delivery in neonate mice. Based on this result we decided not to use this AAV5 vector for further *in vivo* studies.

AAV6 was used to express hnRNP R in SMA mice since it was hypothesized that hnRNP R may be a disease modifier of SMA and over expression would improve the phenotype of these mice. A small increase in survival was seen following AAV6-hnRNP R administration compared to controls injected with AAV6-GFP. However, no

difference was seen between the lifespan of treated mice compared to the reported lifespan of this mouse model (Le *et al.*, 2005). A slight improvement in the motor function of these mice was observed by testing their ability to right themselves. Unfortunately there was no difference in the body weight of treated mice compared to controls. Furthermore when the number of motor neurons in the lumbar spinal cord was counted there was no significant difference between motor neuron survival in treated mice and controls. Assessment of the level of transduction in the lumbar spinal cord revealed very low transduction despite robust transduction seen within the gastrocnemius muscle. This low level of motor neuron transduction suggests a possible reason for the modest effect seen on phenotype and motor neuron survival. Therefore hnRNP R remains a candidate as a disease modifier for SMA however more effective gene transfer to the CNS is necessary to achieve robust conclusions over how hnRNP R expression can affect SMA phenotype. This study shows that AAV6 does not transduce motor neurons well following intravenous neonatal injection.

Another possible disease modifier of SMA is PTEN; knockdown of which leads to increased motor neuron survival following intramuscular injection (Ning *et al.*, 2010). We therefore used AAV9 to express siRNA directed towards PTEN by IV injection in neonatal SMA mice. This gene therapy approach resulted in a significant increase in survival in SMNΔ7 mice with the average survival time of siPTEN treated mice being 30.4±7.4 compared to 9.2±1.5 for scrambled-siPTPEN controls. The phenotype of treated mice was also improved as shown by body weight gain and righting-reflex performance. Furthermore animals treated with AAV9-siPTEN had a significantly greater number of lumbar spinal cord motor neurons than controls at disease endstage.

This shows that PTEN is a disease modifier of SMA and silencing PTEN can improve phenotype of SMA mice and increase their survival. The significant increase in motor neuron numbers in the lumbar spinal cord suggests a mechanism by which improved survival was mediated. Moreover immunofluorescence analysis of the lumbar spinal cord revealed that AAV9 mediated robust transduction of motor

neurons with a resulting reduction of PTEN protein levels in transduced cells. This correlates with previous studies that have successfully used AAV9 for gene therapy to the CNS to successfully treat SMA (Foust *et al.*, 2010; Valori *et al.*, 2010; Dominguez *et al.*, 2011).

7.2 Further Considerations

7.2.1 Polymersomes as Gene Therapy Vectors

We have shown that polymersomes can encapsulate DNA in a size dependent manner through sorting polymersomes by size using centrifugation. However size distribution data shows that centrifugation is not wholly effective in separating different sized polymersomes. Therefore it may be possible to further improve the concentration of encapsulated DNA by improving the efficiency of sorting of polymersomes by size. It is possible to separate different sized polymersomes by other methods such as gel permeation chromatography or hollow-fibre filtration (Rameez *et al.*, 2010). It may also be possible to create polymersomes with a greater propensity to form larger particles by changing the block copolymer lengths or adjusting how the polymersomes are made. However larger polymersomes have slower uptake kinetics than small polymersomes which may have consequences for transfection efficiency. Interestingly polymersomes can be formed by using two different block-copolymers to create polymersomes with different surface domains (Massignani *et al.*, 2009). These patches cause large polymersomes to have fast uptake kinetics like small polymersomes.

Transfection of cells by polymersomes was shown to be dependent on the amount of encapsulated DNA therefore improving the amount of encapsulated DNA in a polymersome solution should improve the level of transfection achieved. Polymersomes used for the overexpression study were centrifuged at 10000 rcf in order to collect as many polymersomes that have encapsulated DNA. However size-

sorting data suggests that a higher level of transfection could have been achieved by only using polymersomes centrifuged at a low speed. It therefore may be possible to increase the level of SMN over-expression achieved by selecting only the largest polymersomes and thus delivering a higher amount of DNA.

Another way of improving encapsulation could be to increase the amount of DNA added to the polymer solution. Throughout the characterisation of encapsulation the same amount of DNA was added to the solution, therefore increasing the amount of DNA added to the polymer solution could increase the encapsulation efficiency. There is likely to be an optimum concentration of DNA to be added to polymer solution to be encapsulated, above which no more DNA would be encapsulated. It would therefore be interesting to assess the level of encapsulation following addition of different amounts of DNA. We have shown that polymersomes can be used *in vitro* to restore SMN protein and mRNA levels in SMN-deficient fibroblasts. The next challenge is to design polymersomes that could cross the BBB and widely deliver SMN to the CNS in an *in vivo* model of SMA.

7.2.2 AAV5 Transduction in the CNS

AAV5 was shown to transduce brain and spinal cord tissue with low efficiency using the CAG promoter however almost no transduction was seen with the CMV promoter. The reason for this difference has yet to be elucidated. It would be useful to check transduction levels in other tissues such as the liver which is highly transduced by AAV5 (Zincarelli *et al.*, 2008) in order to check that the AAV5-CMV-GFP vector was working correctly. It would also be interesting to check transduction levels in other tissues to determine whether the variation seen in transduction in the CNS was also present throughout all tissues. The level of variation in transduction between animals meant that it was challenging to compare the effect of the two time-points since only a small number of animals were used in this pilot study and some animals displayed no transduction. Furthermore it may also be necessary to use more time points to analyse the time course of transduction for AAV5. However we have shown here that transduction efficiency within the CNS is low and AAV5 does not appear to pass the BBB therefore there would not be much

benefit in further investigating the use of AAV5 for gene therapy applications in SMA.

The high level of transduction seen in the dorsal root was interesting and it may be worth investigating this further. It would have been very useful to dissect the dorsal root ganglia separately in order to investigate the level of transduction here. However the aim of the project was to investigate gene therapy for SMA therefore the focus was on transduction within the lumbar spinal cord. Unfortunately we did not dissect the DRG to investigate the level of transduction here but fortunately we could see some of the dorsal root attached to the spinal cord sections.

Furthermore it appeared that transduction within the spinal cord may be mediated through the retrograde transport of the vector up the dorsal root, as suggested by the transduction of cells and fibres near the highly transduced dorsal root. It would therefore be interesting to assess the ability of AAV5 to undergo retrograde transport by administering AAV5 by intramuscular injection to the gastrocnemius muscle for example and assessing the level of transduction within the spinal cord, dorsal root and even in sensory nerves. AAV5 has been previously used to drive transgene expression in the spinal cord following intramuscular injection of the gastrocnemius (Petruska *et al.*, 2010). However it is unclear if motor neurons could be transduced efficiently enough for treatment of SMA.

As mentioned this pilot study only used a small number of animals in each group, which coupled with the variation makes it difficult to make confident conclusions. Only a small number of animals were used as this was a pilot study to test whether AAV5 could transduce the CNS, with the aim of following up any positive results in a larger study. We used 3 animals per group so it would still be possible to perform statistics of transduction efficiency results however the variability between animals was unexpected. Transduction was assessed by immunofluorescence using glial and neuronal markers to ascertain the cell types that had been transduced. However there were a number of transduced cells that did not co-localize with either the glial or neuronal markers it would have therefore been useful to use more markers to fully ascertain what cells these were. For

example it is assumed that the small GFP-positive fibres seen throughout the CNS were axons however this has not been confirmed. Furthermore it would be interesting to elucidate exactly what was transduced within the ventricles of the brain, and the transduction within the dorsal root and other white matter areas of the spinal cord.

7.2.3 AAV9-mediated silencing of PTEN

PTEN was shown to be a modifier of SMA, possibly through increasing survival of lumbar spinal cord motor neurons. Unfortunately 4 of the 10 animals injected did not show any improvement in survival. These animals were included in the body weight data and the motor function data, but were not included in the histological analysis and motor neuron survival data. The three animals used for immunofluorescence and motor neuron survival lived for 75, 29 and 25 days. It would be very interesting to use Western blot or QPCR to check the level of gene transfer in the animals that did not display any improvement in phenotype to determine whether the injection and gene transfer was at all successful. Furthermore it would also be interesting to ascertain the level of gene transfer between the other animals as there was some difference in survival times. This could be due to variation in the amount of vector administrated, or could be due to other factors influencing how well the animals thrived such as litter size or ability to feed after weaning.

We have shown that PTEN silencing improves survival of motor neurons but it would be interesting to see whether AAV9-mediated PTEN reduction affects other tissues. This may be important as there is a growing body of evidence showing that SMA is a multi-system disorder affecting many tissues (Hamilton & Gillingwater, 2013). For example patients and mouse models have been shown to display cardiac defects (Rudnik-Schoneborn *et al.*, 2008; Heier *et al.*, 2010; Shababi *et al.*, 2010). Patients and mouse models both also display pancreas defects including hyperglycemia (Bowerman *et al.*, 2012) and liver defects have also been reported in a mouse

model of SMA (Vitte *et al.*, 2004; Hua *et al.*, 2011). Interestingly AAV9 has shown to generate robust gene transfer in the heart, liver, muscle and lung (Zincarelli *et al.*, 2008). It can therefore be expected that AAV9 would mediate PTEN reduction in these tissues as well as in the spinal cord. The widespread transduction profile of AAV9 suggests that this vector would be suitable to deliver gene therapy for SMA since it can transduce many of the tissues effected by the disease. Since PTEN is a known tumour suppressor (Li *et al.*, 1997; Di Cristofano & Pandolfi, 2000), it would be necessary to check for the presence of any cancer markers throughout various tissues especially those known to be highly transduced by AAV9 such as the heart and liver. However the fact that the siRNA used does not generate a full knockdown of PTEN but rather achieves a reduction of around 60% (Ning *et al.*, 2010) may reduce this risk of tumour development.

7.2.4 AAV6-mediated expression of hnRNP R

The study into whether hnRNP R could modify the SMA phenotype *in vivo* was inconclusive due to inefficient gene transfer in the CNS by AAV6. It may have been possible to produce a more reliable conclusion of the study by performing more *in vivo* tests (El-Khodor *et al.*, 2008). Despite a lack of improvement in body weight or survival a positive effect was seen in performance in the righting-reflex test. Therefore if we had applied other tests to assess phenotype improvement in these mice we may have been able to confirm this positive effect (El-Khodor *et al.*, 2008). However it since the effect on phenotype was very mild these test must be sensitive. Two other tests of motor function was carried out on these SMA mice however there was too much variability in the performance of controls in this these two tests that they were not useful in detecting small changes in phenotype. This highlights the difficulties in assessing small changes in phenotype of these mice.

It is clear that AAV6 does not transduce motor neurons sufficiently to be a suitable gene therapy vector to treat SMA. AAV9 however has been previously used successfully to treat SMA (Foust *et al.*, 2010; Valori *et al.*, 2010; Dominguez *et al.*,

2011) and the results from this PTEN study corroborate with previous studies showing that AAV9 is an ideal vector for treatment of SMA. Therefore to better assess the ability of hnRNP R overexpression to modify SMA phenotype the gene should be cloned into an AAV9 vector to achieve better transduction of spinal cord motor neurons. This would also provide a better opportunity to compare the efficacy of hnRNP R overexpression to SMN overexpression and also to PTEN silencing.

It may have been useful to assess transduction efficiency and the effect of AAV6-mediated hnRNP R overexpression in other tissues. For example it is known that AAV6 transduces skeletal muscle with high efficiency (Zincarelli *et al.*, 2008), which was confirmed here by immunofluorescence in the gastrocnemius muscle. It would be interesting to assess SMN levels in the muscle tissue as hnRNP R overexpression has been shown to increase SMN levels. Furthermore increased SMN levels in the muscles may ameliorate the SMA phenotype to some degree. Therefore the slight improvement in phenotype observed could be due to transduction in the muscle. Muscle specific over-expression of IGF-1 has been shown to increase survival in SMA mice suggesting it may be possible to affect the SMA phenotype through targeting muscle tissue (Bosch-Marce *et al.*, 2011). However, expressing SMN in muscle alone has been shown to have no effect on phenotype or survival (Gavrilina *et al.*, 2008).

7.3 Conclusions

We have shown that AAV9-mediated PTEN silencing can improve the phenotype of a mouse model of SMA. AAV6-mediated hnRNP R expression was not able to achieve a similar result possibly due to the inefficiency of AAV6 to transduce spinal cord motor neurons following IV delivery. Furthermore we have shown that AAV5 cannot pass the BBB well following neonatal IV injection and does not efficiently transduce motor neurons therefore is not a suitable candidate for a gene therapy vector system to treat SMA. High transduction of the dorsal root and transduction of axons within the CNS may however be of some interest for targeting of sensory

neurons. Finally we have shown that polymersomes encapsulate plasmid DNA in a size-dependent manner. These polymersomes can be used as a non-viral gene delivery system to increase SMN *in vitro*. However further optimisation may be necessary before they can be successfully used for gene transfer *in vivo*.

7.4 Future Perspectives

As mentioned above there are various points that could be addressed to further this project and advance the outcomes stated here which time constraints have restricted. Furthermore the results outlined here point towards future directions that could be taken to build upon the results of this project. The use of PTEN silencing to ameliorate the phenotype of SMA mice and extend their lifespan demonstrates that PTEN is a disease modifier of SMA. Following on from this work should be undertaken to determine the exact mechanism by which PTEN improves survival in this SMA model. We have shown that siPTEN can improve motor neuron survival in these mice, as has been shown previously (Ning *et al.*, 2010). This study builds on the work of Ning *et al.*, 2010 by demonstrating that PTEN silencing is sufficient to improve the phenotype of a mouse model of SMA and significantly improve survival in these mice. However it is possible that there are other mechanisms that also contribute to the improvement in survival that are yet to be elucidated.

For example PTEN also interacts with β-actin in the actin-remodelling complex to control cell size. β-actin has been shown to be disturbed in SMA and may be a cause of motor neuron dysfunction (Rossoll *et al.*, 2003). Therefore silencing of PTEN may improve cell growth including axon outgrowth to increase survival in SMA. Furthermore PTEN also inhibits cell migration through the ERK/MAPK pathway and migration of motor neurons is also perturbed in SMA, so silencing of PTEN could also affect this. PTEN could also indirectly affect SMN levels, possibly through the mTOR pathway due to the involvement of mTOR in protein synthesis. Interestingly IGF-1 levels are known to be decreased in SMA and IGF-1 can increase levels of phosphorylated Akt (Goto *et al.*, 2009).

Furthermore as mentioned above it would be useful to use AAV9 to assess the effect of overexpressing hnRNP R on SMNΔ7 mice. The data shown here coupled with *in vitro* data from collaborators suggests that hnRNP R can modify the SMA phenotype. Therefore with the level of transduction generated by AAV9 it would be possible to assess how well hnRNP R overexpression can compensate for SMN deficiency *in vivo*.

We have shown that polymersomes are an emerging technology that can be used for *in vitro* delivery of gene therapy. With a small amount of further optimisation this technology could be used to achieve gene transfer *in vitro*. The polymersomes used in this project were made from PMPC-PDPA which was chosen as it is internalised by cells in a short space of time (Lomas *et al.*, 2008). However for delivery to the CNS it may necessary to use a polymer with a longer circulation time that is decorated with a peptide ligand.

Decoration of the outside of polymersomes with a peptide could initiate receptor binding at the BBB causing transcytosis across the endothelium and into the CNS. For example it may be possible to use peptides bound to the polymersome surface to imitate the VR-I and VR-IV amino acids on the surface of AAV9 that are thought to confer the ablity to pass the blood brain barrer to this vector (DiMattia *et al.*, 2012). However this may be difficult to imitate as it appears to be changes to the shape of the protrusions on the capsid that gives AAV9 a different transduction profile than other AAV serotypes. As with all gene therapy methods the limiting factor is transfection efficiency, however a further rate limiting step for transfection using polymersomes is delivery of plasmid DNA to the nucleus. Polymersomes release their encapsulated DNA into the cytoplasm, from where it must get to the nucleus to initiate transfection. Transport of naked DNA through the cytoplasm to the nucleus is slow and inefficient (Lukacs *et al.*, 2000).

Once the DNA reaches the nucleus it must then pass the nuclear membrane to enter the nucleus. During this project it became apparent that dividing cells were more easily transfected than non-dividing cells, possibly because they are more transcriptionally active, or because the plasmid DNA can become trapped within the

nucleus during the reorganisation it undergoes during division (Dean *et al.*, 2005). It may be possible to increase the transduction efficiency of these polymersomes by including a nuclear targeting motif on the plasmid DNA to improve the amount of DNA that is transported to the nucleus.

Finally AAV5 was shown here to not be an appropriate choice of gene therapy vector for SMA due to the low transduction efficiency seen in motor neurons. However a point of interest here was the high level of transduction seen in the dorsal root and the possibility that AAV5 may be able to enter the spinal cord through retrograde transport. It would therefore be interesting to study the efficiency of motor neuron transduction following intramuscular injection of AAV5. However since SMA is a multi-system disorder it would be necessary to transduce more than just motor neurons in order to successfully provide therapy for SMA. Therefore AAV9 appears to be the most appropriate vector to provide gene therapy for SMA as it can achieve high levels of transduction in various tissues including the CNS.

Chapter 8

References

Agut, W., Brulet, A., Schatz, C., Taton, D. & Lecommandoux, S. (2010) pH and temperature responsive polymeric micelles and polymersomes by self-assembly of poly[2-(dimethylamino)ethyl methacrylate]-b-poly(glutamic acid) double hydrophilic block copolymers. *Langmuir : the ACS journal of surfaces and colloids*, **26**, 10546-10554.

Ahmed, F. & Discher, D.E. (2004a) Self-porating polymersomes of PEG-PLA and PEG-PCL: hydrolysis-triggered controlled release vesicles. *Journal of controlled release : official journal of the Controlled Release Society*, **96**, 37-53.

Ahmed, F. & Discher, D.E. (2004b) Self-porating polymersomes of PEG-PLA and PEG-PCL: hydrolysis-triggered controlled release vesicles. *Journal of Controlled Release*, **96**, 37-53.

Ahmed, F., Pakunlu, R.I., Brannan, A., Bates, F., Minko, T. & Discher, D.E. (2006a) Biodegradable polymersomes loaded with both paclitaxel and doxorubicin permeate and shrink tumors, inducing apoptosis in proportion to accumulated drug. *Journal of controlled release : official journal of the Controlled Release Society*, **116**, 150-158.

Ahmed, F., Pakunlu, R.I., Srinivas, G., Brannan, A., Bates, F., Klein, M.L., Minko, T. & Discher, D.E. (2006b) Shrinkage of a rapidly growing tumor by drug-loaded polymersomes: pH-triggered release through copolymer degradation. *Molecular pharmaceutics*, **3**, 340-350.

Akten, B., Kye, M.J., Hao le, T., Wertz, M.H., Singh, S., Nie, D., Huang, J., Merianda, T.T., Twiss, J.L., Beattie, C.E., Steen, J.A. & Sahin, M. (2011) Interaction of survival of motor neuron (SMN) and HuD proteins with mRNA cpg15 rescues motor neuron axonal deficits. *Proceedings of the National Academy of Sciences of the United States of America*, **108**, 10337-10342.

Alcantar, N.A., Aydil, E.S. & Israelachvili, J.N. (2000) Polyethylene glycol-coated biocompatible surfaces. *Journal of biomedical materials research*, **51**, 343-351.

Araujo, A., Araujo, M. & Swoboda, K.J. (2009) Vascular perfusion abnormalities in infants with spinal muscular atrophy. *The Journal of pediatrics*, **155**, 292-294.

Azzouz, M., Le, T., Ralph, G.S., Walmsley, L., Monani, U.R., Lee, D.C., Wilkes, F., Mitrophanous, K.A., Kingsman, S.M., Burghes, A.H. & Mazarakis, N.D. (2004) Lentivector-mediated SMN replacement in a mouse model of spinal muscular atrophy. *The Journal of clinical investigation*, **114**, 1726-1731.

Bach, J.R. & Bianchi, C. (2003) Prevention of pectus excavatum for children with spinal muscular atrophy type 1. *American journal of physical medicine & rehabilitation / Association of Academic Physiatrists*, **82**, 815-819.

Bach, J.R., Niranjan, V. & Weaver, B. (2000) Spinal muscular atrophy type 1: A noninvasive respiratory management approach. *Chest*, **117**, 1100-1105.

Backman, S.A., Stambolic, V., Suzuki, A., Haight, J., Elia, A., Pretorius, J., Tsao, M.S., Shannon, P., Bolon, B., Ivy, G.O. & Mak, T.W. (2001) Deletion of Pten in mouse brain causes seizures, ataxia and defects in soma size resembling Lhermitte-Duclos disease. *Nature genetics*, **29**, 396-403.

Bantel-Schaal, U., Delius, H., Schmidt, R. & zur Hausen, H. (1999) Human adeno-associated virus type 5 is only distantly related to other known primate helper-dependent parvoviruses. *Journal of virology*, **73**, 939-947.

Bantel-Schaal, U., Hub, B. & Kartenbeck, J. (2002) Endocytosis of adeno-associated virus type 5 leads to accumulation of virus particles in the Golgi compartment. *Journal of virology*, **76**, 2340-2349.

Battaglia, G., Princivalle, A., Forti, F., Lizier, C. & Zeviani, M. (1997) Expression of the SMN gene, the spinal muscular atrophy determining gene, in the mammalian central nervous system. *Human molecular genetics*, **6**, 1961-1971.

Battaglia, G. & Ryan, A.J. (2005) Bilayers and interdigitation in block copolymer vesicles. *Journal of the American Chemical Society*, **127**, 8757-8764.

Battaglia, G. & Ryan, A.J. (2006) Neuron-like tubular membranes made of diblock copolymer amphiphiles. *Angew Chem Int Ed Engl*, **45**, 2052-2056.

Baughan, T., Shababi, M., Coady, T.H., Dickson, A.M., Tullis, G.E. & Lorson, C.L. (2006) Stimulating full-length SMN2 expression by delivering bifunctional RNAs via a viral vector. *Molecular therapy : the journal of the American Society of Gene Therapy*, **14**, 54-62.

Baughan, T.D., Dickson, A., Osman, E.Y. & Lorson, C.L. (2009) Delivery of bifunctional RNAs that target an intronic repressor and increase SMN levels in an animal model of spinal muscular atrophy. *Human molecular genetics*, **18**, 1600-1611.

Bell, C.L., Gurda, B.L., Van Vliet, K., Agbandje-McKenna, M. & Wilson, J.M. (2012) Identification of the galactose binding domain of the adeno-associated virus serotype 9 capsid. *Journal of virology*, **86**, 7326-7333.

Benkhelifa-Ziyyat, S., Besse, A., Roda, M., Duque, S., Astord, S., Carcenac, R., Marais, T. & Barkats, M. (2013) Intramuscular scAAV9-SMN injection mediates widespread gene delivery to the spinal cord and decreases disease severity in SMA mice. *Molecular therapy : the journal of the American Society of Gene Therapy*, **21**, 282-290.

Bensadoun, J.C., Deglon, N., Tseng, J.L., Ridet, J.L., Zurn, A.D. & Aebischer, P. (2000) Lentiviral vectors as a gene delivery system in the mouse midbrain: cellular and behavioral improvements in a 6-OHDA model of Parkinson's disease using GDNF. *Experimental neurology*, **164**, 15-24.

Bevan, A.K., Hutchinson, K.R., Foust, K.D., Braun, L., McGovern, V.L., Schmelzer, L., Ward, J.G., Petruska, J.C., Lucchesi, P.A., Burghes, A.H. & Kaspar, B.K. (2010) Early heart failure in the SMNDelta7 model of spinal muscular atrophy and correction by postnatal scAAV9-SMN delivery. *Human molecular genetics*, **19**, 3895-3905.

Blacklow, N.R., Hoggan, M.D. & Rowe, W.P. (1967) Isolation of adenovirus-associated viruses from man. *Proceedings of the National Academy of Sciences of the United States of America*, **58**, 1410-1415.

Blits, B., Derks, S., Twisk, J., Ehlert, E., Prins, J. & Verhaagen, J. (2010) Adeno-associated viral vector (AAV)-mediated gene transfer in the red nucleus of the adult rat brain: comparative analysis of the transduction properties of seven AAV serotypes and lentiviral vectors. *Journal of neuroscience methods*, **185**, 257-263.

Blomer, U., Naldini, L., Kafri, T., Trono, D., Verma, I.M. & Gage, F.H. (1997) Highly efficient and sustained gene transfer in adult neurons with a lentivirus vector. *Journal of virology*, **71**, 6641-6649.

Boon, K.L., Xiao, S., McWhorter, M.L., Donn, T., Wolf-Saxon, E., Bohnsack, M.T., Moens, C.B. & Beattie, C.E. (2009) Zebrafish survival motor neuron mutants exhibit presynaptic neuromuscular junction defects. *Human molecular genetics*, **18**, 3615-3625.

Bosch-Marce, M., Wee, C.D., Martinez, T.L., Lipkes, C.E., Choe, D.W., Kong, L., Van Meerbeke, J.P., Musaro, A. & Sumner, C.J. (2011) Increased IGF-1 in muscle modulates the phenotype of severe SMA mice. *Human molecular genetics*, **20**, 1844-1853.

Bowerman, M., Anderson, C.L., Beauvais, A., Boyl, P.P., Witke, W. & Kothary, R. (2009) SMN, profilin IIa and plastin 3: a link between the deregulation of actin dynamics and SMA pathogenesis. *Molecular and cellular neurosciences*, **42**, 66-74.

Bowerman, M., Swoboda, K.J., Michalski, J.P., Wang, G.S., Reeks, C., Beauvais, A., Murphy, K., Woulfe, J., Screaton, R.A., Scott, F.W. & Kothary, R. (2012) Glucose metabolism and pancreatic defects in spinal muscular atrophy. *Annals of neurology*, **72**, 256-268.

Brahe, C., Vitali, T., Tiziano, F.D., Angelozzi, C., Pinto, A.M., Borgo, F., Moscato, U., Bertini, E., Mercuri, E. & Neri, G. (2005) Phenylbutyrate increases SMN gene expression in spinal muscular atrophy patients. *European journal of human genetics : EJHG*, **13**, 256-259.

Brichta, L., Holker, I., Haug, K., Klockgether, T. & Wirth, B. (2006) In vivo activation of SMN in spinal muscular atrophy carriers and patients treated with valproate. *Annals of neurology*, **59**, 970-975.

Broz, P., Benito, S.M., Saw, C., Burger, P., Heider, H., Pfisterer, M., Marsch, S., Meier, W. & Hunziker, P. (2005) Cell targeting by a generic receptor-targeted polymer nanocontainer platform. *Journal of controlled release : official journal of the Controlled Release Society*, **102**, 475-488.

Burger, C., Gorbatyuk, O.S., Velardo, M.J., Peden, C.S., Williams, P., Zolotukhin, S., Reier, P.J., Mandel, R.J. & Muzyczka, N. (2004) Recombinant AAV viral vectors pseudotyped with viral capsids from serotypes 1, 2, and 5 display differential efficiency and cell tropism after delivery to different regions of the central nervous system. *Molecular therapy : the journal of the American Society of Gene Therapy*, **10**, 302-317.

Candolfi, M., Pluhar, G.E., Kroeger, K., Puntel, M., Curtin, J., Barcia, C., Muhammad, A.K., Xiong, W., Liu, C., Mondkar, S., Kuoy, W., Kang, T., McNeil, E.A., Freese, A.B., Ohlfest, J.R., Moore, P., Palmer, D., Ng, P., Young, J.D., Lowenstein, P.R. & Castro, M.G. (2007) Optimization of adenoviral vector-mediated transgene expression in the canine brain in vivo, and in canine glioma cells in vitro. *Neuro-oncology*, **9**, 245-258.

Canton, I. & Battaglia, G. (2013) Polymersomes-mediated delivery of fluorescent probes for targeted and long-term imaging in live cell microscopy. *Methods Mol Biol*, **991**, 343-351.

Canton, I., Massignani, M., Patikarnmonthon, N., Chierico, L., Robertson, J., Renshaw, S.A., Warren, N.J., Madsen, J.P., Armes, S.P., Lewis, A.L. & Battaglia, G. (2013) Fully synthetic polymer vesicles for intracellular delivery of antibodies in live cells. *FASEB journal : official publication of the Federation of American Societies for Experimental Biology*, **27**, 98-108.

Cartegni, L. & Krainer, A.R. (2002) Disruption of an SF2/ASF-dependent exonic splicing enhancer in SMN2 causes spinal muscular atrophy in the absence of SMN1. *Nature genetics*, **30**, 377-384.

Chan, Y.B., Miguel-Aliaga, I., Franks, C., Thomas, N., Trulzsch, B., Sattelle, D.B., Davies, K.E. & van den Heuvel, M. (2003) Neuromuscular defects in a Drosophila survival motor neuron gene mutant. *Human molecular genetics*, **12**, 1367-1376.

Chen, H.H., Chang, J.G., Lu, R.M., Peng, T.Y. & Tarn, W.Y. (2008) The RNA binding protein hnRNP Q modulates the utilization of exon 7 in the survival motor neuron 2 (SMN2) gene. *Molecular and cellular biology*, **28**, 6929-6938.

Chen, S., Kapturczak, M., Loiler, S.A., Zolotukhin, S., Glushakova, O.Y., Madsen, K.M., Samulski, R.J., Hauswirth, W.W., Campbell-Thompson, M., Berns, K.I., Flotte, T.R., Atkinson, M.A., Tisher, C.C. & Agarwal, A. (2005a) Efficient transduction of vascular endothelial cells with recombinant adeno-associated virus serotype 1 and 5 vectors. *Human gene therapy*, **16**, 235-247.

Chen, S., Zheng, J., Li, L. & Jiang, S. (2005b) Strong resistance of phosphorylcholine self-assembled monolayers to protein adsorption: insights into nonfouling properties of zwitterionic materials. *Journal of the American Chemical Society*, **127**, 14473-14478.

Chen, T.H., Chang, J.G., Yang, Y.H., Mai, H.H., Liang, W.C., Wu, Y.C., Wang, H.Y., Huang, Y.B., Wu, S.M., Chen, Y.C., Yang, S.N. & Jong, Y.J. (2010a) Randomized, double-blind, placebo-controlled trial of hydroxyurea in spinal muscular atrophy. *Neurology*, **75**, 2190-2197.

Chen, W., Meng, F., Cheng, R. & Zhong, Z. (2010b) pH-Sensitive degradable polymersomes for triggered release of anticancer drugs: a comparative study with micelles. *Journal of controlled release : official journal of the Controlled Release Society*, **142**, 40-46.

Chiorini, J.A., Afione, S. & Kotin, R.M. (1999) Adeno-associated virus (AAV) type 5 Rep protein cleaves a unique terminal resolution site compared with other AAV serotypes. *Journal of virology*, **73**, 4293-4298.

Chirmule, N., Propert, K., Magosin, S., Qian, Y., Qian, R. & Wilson, J. (1999) Immune responses to adenovirus and adeno-associated virus in humans. *Gene therapy*, **6**, 1574-1583.

Cifuentes-Diaz, C., Frugier, T., Tiziano, F.D., Lacene, E., Roblot, N., Joshi, V., Moreau, M.H. & Melki, J. (2001) Deletion of murine SMN exon 7 directed to skeletal muscle leads to severe muscular dystrophy. *The Journal of cell biology*, **152**, 1107-1114.

Coady, T.H., Baughan, T.D., Shababi, M., Passini, M.A. & Lorson, C.L. (2008) Development of a single vector system that enhances trans-splicing of SMN2 transcripts. *PloS one*, **3**, e3468.

Coady, T.H., Shababi, M., Tullis, G.E. & Lorson, C.L. (2007) Restoration of SMN function: delivery of a trans-splicing RNA re-directs SMN2 pre-mRNA splicing. *Molecular therapy : the journal of the American Society of Gene Therapy*, **15**, 1471-1478.

Coovert, D.D., Le, T.T., McAndrew, P.E., Strasswimmer, J., Crawford, T.O., Mendell, J.R., Coulson, S.E., Androphy, E.J., Prior, T.W. & Burghes, A.H. (1997) The survival motor neuron protein in spinal muscular atrophy. *Human molecular genetics*, **6**, 1205-1214.

Dale, J.M., Shen, H., Barry, D.M., Garcia, V.B., Rose, F.F., Jr., Lorson, C.L. & Garcia, M.L. (2011) The spinal muscular atrophy mouse model, SMADelta7, displays altered axonal transport without global neurofilament alterations. *Acta neuropathologica*, **122**, 331-341.

Darbar, I.A., Plaggert, P.G., Resende, M.B., Zanoteli, E. & Reed, U.C. (2011) Evaluation of muscle strength and motor abilities in children with type II and III spinal muscle atrophy treated with valproic acid. *BMC neurology*, **11**, 36.

Davidson, B.L., Stein, C.S., Heth, J.A., Martins, I., Kotin, R.M., Derksen, T.A., Zabner, J., Ghodsi, A. & Chiorini, J.A. (2000) Recombinant adeno-associated virus type 2, 4, and 5 vectors: transduction of variant cell types and regions in the mammalian central nervous system. *Proceedings of the National Academy of Sciences of the United States of America*, **97**, 3428-3432.

Dean, D.A., Strong, D.D. & Zimmer, W.E. (2005) Nuclear entry of nonviral vectors. *Gene therapy*, **12**, 881-890.

Deglon, N. & Aebischer, P. (2002) Lentiviruses as vectors for CNS diseases. *Current topics in microbiology and immunology*, **261**, 191-209.

Di Cristofano, A. & Pandolfi, P.P. (2000) The multiple roles of PTEN in tumor suppression. *Cell*, **100**, 387-390.

DiMatteo, D., Callahan, S. & Kmiec, E.B. (2008) Genetic conversion of an SMN2 gene to SMN1: a novel approach to the treatment of spinal muscular atrophy. *Experimental cell research*, **314**, 878-886.

DiMattia, M.A., Nam, H.J., Van Vliet, K., Mitchell, M., Bennett, A., Gurda, B.L., McKenna, R., Olson, N.H., Sinkovits, R.S., Potter, M., Byrne, B.J., Aslanidi, G., Zolotukhin, S., Muzyczka, N., Baker, T.S. & Agbandje-McKenna, M. (2012) Structural insight into the unique properties of adeno-associated virus serotype 9. *Journal of virology*, **86**, 6947-6958.

Discher, B.M., Won, Y.Y., Ege, D.S., Lee, J.C., Bates, F.S., Discher, D.E. & Hammer, D.A. (1999) Polymersomes: tough vesicles made from diblock copolymers. *Science*, **284**, 1143-1146.

Discher, D.E. & Eisenberg, A. (2002) Polymer vesicles. *Science*, **297**, 967-973.

Domanskyi, A., Geissler, C., Vinnikov, I.A., Alter, H., Schober, A., Vogt, M.A., Gass, P., Parlato, R. & Schutz, G. (2011) Pten ablation in adult dopaminergic neurons is neuroprotective in Parkinson's disease models. *FASEB journal : official publication of the Federation of American Societies for Experimental Biology*, **25**, 2898-2910.

Dominguez, E., Marais, T., Chatauret, N., Benkhelifa-Ziyyat, S., Duque, S., Ravassard, P., Carcenac, R., Astord, S., Pereira de Moura, A., Voit, T. & Barkats, M. (2011) Intravenous scAAV9 delivery of a codon-optimized SMN1 sequence rescues SMA mice. *Human molecular genetics*, **20**, 681-693.

Donsante, A., Miller, D.G., Li, Y., Vogler, C., Brunt, E.M., Russell, D.W. & Sands, M.S. (2007) AAV vector integration sites in mouse hepatocellular carcinoma. *Science*, **317**, 477.

Du, J. & Armes, S.P. (2005) pH-responsive vesicles based on a hydrolytically self-cross-linkable copolymer. *Journal of the American Chemical Society*, **127**, 12800-12801.

Du, J., Tang, Y., Lewis, A.L. & Armes, S.P. (2005) pH-sensitive vesicles based on a biocompatible zwitterionic diblock copolymer. *Journal of the American Chemical Society*, **127**, 17982-17983.

Dull, T., Zufferey, R., Kelly, M., Mandel, R.J., Nguyen, M., Trono, D. & Naldini, L. (1998) A third-generation lentivirus vector with a conditional packaging system. *Journal of virology*, **72**, 8463-8471.

Edelstein, M. (2013) Worldwide Gene Therapy Clinical Trials http://www.wiley.com/legacy/wileychi/genmed/clinical/. The Journal of Gene Medicine.

Egli, S., Nussbaumer, M.G., Balasubramanian, V., Chami, M., Bruns, N., Palivan, C. & Meier, W. (2011) Biocompatible functionalization of polymersome surfaces: a new approach to surface immobilization and cell targeting using polymersomes. *Journal of the American Chemical Society*, **133**, 4476-4483.

El-Khodor, B.F., Edgar, N., Chen, A., Winberg, M.L., Joyce, C., Brunner, D., Suarez-Farinas, M. & Heyes, M.P. (2008) Identification of a battery of tests for drug candidate evaluation in the SMNDelta7 neonate model of spinal muscular atrophy. *Experimental neurology*, **212**, 29-43.

Escors, D. & Breckpot, K. (2010) Lentiviral vectors in gene therapy: their current status and future potential. *Archivum immunologiae et therapiae experimentalis*, **58**, 107-119.

Fallini, C., Zhang, H., Su, Y., Silani, V., Singer, R.H., Rossoll, W. & Bassell, G.J. (2011) The survival of motor neuron (SMN) protein interacts with the mRNA-binding protein HuD and regulates localization of poly(A) mRNA in primary motor neuron axons. *The Journal of neuroscience : the official journal of the Society for Neuroscience*, **31**, 3914-3925.

Foust, K.D., Nurre, E., Montgomery, C.L., Hernandez, A., Chan, C.M. & Kaspar, B.K. (2009) Intravascular AAV9 preferentially targets neonatal neurons and adult astrocytes. *Nature biotechnology*, **27**, 59-65.

Foust, K.D., Wang, X., McGovern, V.L., Braun, L., Bevan, A.K., Haidet, A.M., Le, T.T., Morales, P.R., Rich, M.M., Burghes, A.H. & Kaspar, B.K. (2010) Rescue of the spinal muscular atrophy phenotype in a mouse model by early postnatal delivery of SMN. *Nature biotechnology*, **28**, 271-274.

Fraser, M.M., Bayazitov, I.T., Zakharenko, S.S. & Baker, S.J. (2008) Phosphatase and tensin homolog, deleted on chromosome 10 deficiency in brain causes defects in synaptic structure, transmission and plasticity, and myelination abnormalities. *Neuroscience*, **151**, 476-488.

Frugier, T., Tiziano, F.D., Cifuentes-Diaz, C., Miniou, P., Roblot, N., Dierich, A., Le Meur, M. & Melki, J. (2000) Nuclear targeting defect of SMN lacking the C-terminus in a mouse model of spinal muscular atrophy. *Human molecular genetics*, **9**, 849-858.

Gao, G., Vandenberghe, L.H., Alvira, M.R., Lu, Y., Calcedo, R., Zhou, X. & Wilson, J.M. (2004) Clades of Adeno-associated viruses are widely disseminated in human tissues. *Journal of virology*, **78**, 6381-6388.

Gary, D.S. & Mattson, M.P. (2002) PTEN regulates Akt kinase activity in hippocampal neurons and increases their sensitivity to glutamate and apoptosis. *Neuromolecular medicine*, **2**, 261-269.

Gavrilina, T.O., McGovern, V.L., Workman, E., Crawford, T.O., Gogliotti, R.G., DiDonato, C.J., Monani, U.R., Morris, G.E. & Burghes, A.H. (2008) Neuronal SMN expression corrects spinal muscular atrophy in severe SMA mice while muscle-specific SMN expression has no phenotypic effect. *Human molecular genetics*, **17**, 1063-1075.

Germano, I.M., Fable, J., Gultekin, S.H. & Silvers, A. (2003) Adenovirus/herpes simplex-thymidine kinase/ganciclovir complex: preliminary results of a phase I trial in patients with recurrent malignant gliomas. *Journal of neuro-oncology*, **65**, 279-289.

Giacomelli, C., Le Men, L., Borsali, R., Lai-Kee-Him, J., Brisson, A., Armes, S.P. & Lewis, A.L. (2006) Phosphorylcholine-based pH-responsive diblock copolymer micelles as drug delivery vehicles: light scattering, electron microscopy, and fluorescence experiments. *Biomacromolecules*, **7**, 817-828.

Giesemann, T., Rathke-Hartlieb, S., Rothkegel, M., Bartsch, J.W., Buchmeier, S., Jockusch, B.M. & Jockusch, H. (1999) A role for polyproline motifs in the spinal muscular atrophy protein SMN. Profilins bind to and colocalize with smn in nuclear gems. *The Journal of biological chemistry*, **274**, 37908-37914.

Glinka, M., Herrmann, T., Funk, N., Havlicek, S., Rossoll, W., Winkler, C. & Sendtner, M. (2010) The heterogeneous nuclear ribonucleoprotein-R is necessary for axonal beta-actin mRNA translocation in spinal motor neurons. *Human molecular genetics*, **19**, 1951-1966.

Goto, M., Iwase, A., Harata, T., Takigawa, S., Suzuki, K., Manabe, S. & Kikkawa, F. (2009) IGF1-induced AKT phosphorylation and cell proliferation are suppressed with the increase in PTEN during luteinization in human granulosa cells. *Reproduction*, **137**, 835-842.

Gray, S.J., Foti, S.B., Schwartz, J.W., Bachaboina, L., Taylor-Blake, B., Coleman, J., Ehlers, M.D., Zylka, M.J., McCown, T.J. & Samulski, R.J. (2011) Optimizing promoters for recombinant adeno-associated virus-mediated gene expression in the peripheral and central nervous system using self-complementary vectors. *Human gene therapy*, **22**, 1143-1153.

Groszer, M., Erickson, R., Scripture-Adams, D.D., Lesche, R., Trumpp, A., Zack, J.A., Kornblum, H.I., Liu, X. & Wu, H. (2001) Negative regulation of neural stem/progenitor cell proliferation by the Pten tumor suppressor gene in vivo. *Science*, **294**, 2186-2189.

Halbert, C.L., Rutledge, E.A., Allen, J.M., Russell, D.W. & Miller, A.D. (2000) Repeat transduction in the mouse lung by using adeno-associated virus vectors with different serotypes. *Journal of virology*, **74**, 1524-1532.

Hamilton, G. & Gillingwater, T.H. (2013) Spinal muscular atrophy: going beyond the motor neuron. *Trends in molecular medicine*, **19**, 40-50.

Hao, L.T., Duy, P.Q., Jontes, J.D., Wolman, M., Granato, M. & Beattie, C.E. (2013) Temporal requirement for SMN in motoneuron development. *Human molecular genetics*, **22**, 2612-2625.

Hassfeld, W., Chan, E.K., Mathison, D.A., Portman, D., Dreyfuss, G., Steiner, G. & Tan, E.M. (1998) Molecular definition of heterogeneous nuclear ribonucleoprotein R (hnRNP R) using autoimmune antibody: immunological relationship with hnRNP P. *Nucleic acids research*, **26**, 439-445.

Heier, C.R., Satta, R., Lutz, C. & DiDonato, C.J. (2010) Arrhythmia and cardiac defects are a feature of spinal muscular atrophy model mice. *Human molecular genetics*, **19**, 3906-3918.

Hillgenberg, M., Tonnies, H. & Strauss, M. (2001) Chromosomal integration pattern of a helper-dependent minimal adenovirus vector with a selectable marker inserted into a 27.4-kilobase genomic stuffer. *Journal of virology*, **75**, 9896-9908.

Hocine, S., Cui, D., Rager, M.N., Di Cicco, A., Liu, J.M., Wdzieczak-Bakala, J., Brulet, A. & Li, M.H. (2013) Polymersomes with PEG corona: structural changes and controlled release induced by temperature variation. *Langmuir : the ACS journal of surfaces and colloids*, **29**, 1356-1369.

Hsieh-Li, H.M., Chang, J.G., Jong, Y.J., Wu, M.H., Wang, N.M., Tsai, C.H. & Li, H. (2000) A mouse model for spinal muscular atrophy. *Nature genetics*, **24**, 66-70.

Hua, Y., Sahashi, K., Hung, G., Rigo, F., Passini, M.A., Bennett, C.F. & Krainer, A.R. (2010) Antisense correction of SMN2 splicing in the CNS rescues necrosis in a type III SMA mouse model. *Genes & development*, **24**, 1634-1644.

Hua, Y., Sahashi, K., Rigo, F., Hung, G., Horev, G., Bennett, C.F. & Krainer, A.R. (2011) Peripheral SMN restoration is essential for long-term rescue of a severe spinal muscular atrophy mouse model. *Nature*, **478**, 123-126.

Hua, Y., Vickers, T.A., Baker, B.F., Bennett, C.F. & Krainer, A.R. (2007) Enhancement of SMN2 exon 7 inclusion by antisense oligonucleotides targeting the exon. *PLoS biology*, **5**, e73.

Hua, Y., Vickers, T.A., Okunola, H.L., Bennett, C.F. & Krainer, A.R. (2008) Antisense masking of an hnRNP A1/A2 intronic splicing silencer corrects SMN2 splicing in transgenic mice. *American journal of human genetics*, **82**, 834-848.

Hubers, L., Valderrama-Carvajal, H., Laframboise, J., Timbers, J., Sanchez, G. & Cote, J. (2011) HuD interacts with survival motor neuron protein and can rescue spinal muscular atrophy-like neuronal defects. *Human molecular genetics*, **20**, 553-579.

Iannaccone, S.T. (2007) Modern management of spinal muscular atrophy. *Journal of child neurology*, **22**, 974-978.

Imlach, W.L., Beck, E.S., Choi, B.J., Lotti, F., Pellizzoni, L. & McCabe, B.D. (2012) SMN is required for sensory-motor circuit function in Drosophila. *Cell*, **151**, 427-439.

Immonen, A., Vapalahti, M., Tyynela, K., Hurskainen, H., Sandmair, A., Vanninen, R., Langford, G., Murray, N. & Yla-Herttuala, S. (2004) AdvHSV-tk gene therapy with intravenous ganciclovir improves survival in human malignant glioma: a randomised, controlled study. *Molecular therapy : the journal of the American Society of Gene Therapy*, **10**, 967-972.

Jablonka, S., Wiese, S. & Sendtner, M. (2004) Axonal defects in mouse models of motoneuron disease. *Journal of neurobiology*, **58**, 272-286.

Jia, L., Ji, S., Maillet, J.C. & Zhang, X. (2010) PTEN suppression promotes neurite development exclusively in differentiating PC12 cells via PI3-kinase and MAP kinase signaling. *Journal of cellular biochemistry*, **111**, 1390-1400.

Jin, Y., Liu, S., Yu, B., Golan, S., Koh, C.G., Yang, J., Huynh, L., Yang, X., Pang, J., Muthusamy, N., Chan, K.K., Byrd, J.C., Talmon, Y., Lee, L.J., Lee, R.J. & Marcucci, G. (2010) Targeted delivery of antisense oligodeoxynucleotide by transferrin conjugated pH-sensitive lipopolyplex nanoparticles: a novel oligonucleotide-based therapeutic strategy in acute myeloid leukemia. *Molecular pharmaceutics*, **7**, 196-206.

Jones, M.A., McEwen, I.R. & Hansen, L. (2003) Use of power mobility for a young child with spinal muscular atrophy. *Physical therapy*, **83**, 253-262.

Kaludov, N., Brown, K.E., Walters, R.W., Zabner, J. & Chiorini, J.A. (2001) Adeno-associated virus serotype 4 (AAV4) and AAV5 both require sialic acid binding for hemagglutination and efficient transduction but differ in sialic acid linkage specificity. *Journal of virology*, **75**, 6884-6893.

Kamat, N.P., Robbins, G.P., Rawson, J.S., Therien, M.J., Dmochowski, I.J. & Hammer, D.A. (2010) A Generalized System for Photo-Responsive Membrane Rupture in Polymersomes. *Advanced functional materials*, **20**, 2588-2596.

Kaplitt, M.G., Leone, P., Samulski, R.J., Xiao, X., Pfaff, D.W., O'Malley, K.L. & During, M.J. (1994) Long-term gene expression and phenotypic correction using adeno-associated virus vectors in the mammalian brain. *Nature genetics*, **8**, 148-154.

Kato, Z., Okuda, M., Okumura, Y., Arai, T., Teramoto, T., Nishimura, M., Kaneko, H. & Kondo, N. (2009) Oral administration of the thyrotropin-releasing hormone (TRH) analogue, taltireline hydrate, in spinal muscular atrophy. *Journal of child neurology*, **24**, 1010-1012.

Kim, Y., Tewari, M., Pajerowski, J.D., Cai, S., Sen, S., Williams, J.H., Sirsi, S.R., Lutz, G.J. & Discher, D.E. (2009) Polymersome delivery of siRNA and antisense oligonucleotides. *Journal of controlled release : official journal of the Controlled Release Society*, **134**, 132-140.

Kinali, M., Mercuri, E., Main, M., De Biasia, F., Karatza, A., Higgins, R., Banks, L.M., Manzur, A.Y. & Muntoni, F. (2002) Pilot trial of albuterol in spinal muscular atrophy. *Neurology*, **59**, 609-610.

Kissel, J.T., Scott, C.B., Reyna, S.P., Crawford, T.O., Simard, L.R., Krosschell, K.J., Acsadi, G., Elsheik, B., Schroth, M.K., D'Anjou, G., LaSalle, B., Prior, T.W., Sorenson, S., Maczulski, J.A., Bromberg, M.B., Chan, G.M. & Swoboda, K.J. (2011) SMA CARNIVAL TRIAL PART II: a prospective, single-armed trial of L-carnitine and valproic acid in ambulatory children with spinal muscular atrophy. *PloS one*, **6**, e21296.

Kochanek, S., Schiedner, G. & Volpers, C. (2001) High-capacity 'gutless' adenoviral vectors. *Current opinion in molecular therapeutics*, **3**, 454-463.

Koeberl, D.D., Alexander, I.E., Halbert, C.L., Russell, D.W. & Miller, A.D. (1997) Persistent expression of human clotting factor IX from mouse liver after intravenous injection of adeno-associated virus vectors. *Proceedings of the National Academy of Sciences of the United States of America*, **94**, 1426-1431.

Koerber, J.T., Jang, J.H. & Schaffer, D.V. (2008) DNA shuffling of adeno-associated virus yields functionally diverse viral progeny. *Molecular therapy : the journal of the American Society of Gene Therapy*, **16**, 1703-1709.

Kong, L., Wang, X., Choe, D.W., Polley, M., Burnett, B.G., Bosch-Marce, M., Griffin, J.W., Rich, M.M. & Sumner, C.J. (2009) Impaired synaptic vesicle release and immaturity of neuromuscular junctions in spinal muscular atrophy mice. *The Journal of neuroscience : the official journal of the Society for Neuroscience*, **29**, 842-851.

Kordower, J.H., Emborg, M.E., Bloch, J., Ma, S.Y., Chu, Y., Leventhal, L., McBride, J., Chen, E.Y., Palfi, S., Roitberg, B.Z., Brown, W.D., Holden, J.E., Pyzalski, R., Taylor, M.D., Carvey, P., Ling, Z., Trono, D., Hantraye, P., Deglon, N. & Aebischer, P. (2000) Neurodegeneration prevented by lentiviral vector delivery of GDNF in primate models of Parkinson's disease. *Science*, **290**, 767-773.

Kwon, C.H., Luikart, B.W., Powell, C.M., Zhou, J., Matheny, S.A., Zhang, W., Li, Y., Baker, S.J. & Parada, L.F. (2006) Pten regulates neuronal arborization and social interaction in mice. *Neuron*, **50**, 377-388.

Kwon, C.H., Zhu, X., Zhang, J., Knoop, L.L., Tharp, R., Smeyne, R.J., Eberhart, C.G., Burger, P.C. & Baker, S.J. (2001) Pten regulates neuronal soma size: a mouse model of Lhermitte-Duclos disease. *Nature genetics*, **29**, 404-411.

Le, T.T., Pham, L.T., Butchbach, M.E., Zhang, H.L., Monani, U.R., Coovert, D.D., Gavrilina, T.O., Xing, L., Bassell, G.J. & Burghes, A.H. (2005) SMNDelta7, the major product of the centromeric survival motor neuron (SMN2) gene, extends survival in mice with spinal muscular atrophy and associates with full-length SMN. *Human molecular genetics*, **14**, 845-857.

Lee, J.S., Ankone, M., Pieters, E., Schiffelers, R.M., Hennink, W.E. & Feijen, J. (2011a) Circulation kinetics and biodistribution of dual-labeled polymersomes with modulated surface charge in tumor-bearing mice: comparison with stealth liposomes. *Journal of controlled release : official journal of the Controlled Release Society*, **155**, 282-288.

Lee, Y.I., Mikesh, M., Smith, I., Rimer, M. & Thompson, W. (2011b) Muscles in a mouse model of spinal muscular atrophy show profound defects in neuromuscular development even in the absence of failure in neuromuscular transmission or loss of motor neurons. *Developmental biology*, **356**, 432-444.

Lefebvre, S., Burglen, L., Reboullet, S., Clermont, O., Burlet, P., Viollet, L., Benichou, B., Cruaud, C., Millasseau, P., Zeviani, M. & et al. (1995) Identification and characterization of a spinal muscular atrophy-determining gene. *Cell*, **80**, 155-165.

Lewis, A.L. (2000) Phosphorylcholine-based polymers and their use in the prevention of biofouling. *Colloids and surfaces. B, Biointerfaces*, **18**, 261-275.

Lewis, P.F. & Emerman, M. (1994) Passage through mitosis is required for oncoretroviruses but not for the human immunodeficiency virus. *Journal of virology*, **68**, 510-516.

Li, H., Malani, N., Hamilton, S.R., Schlachterman, A., Bussadori, G., Edmonson, S.E., Shah, R., Arruda, V.R., Mingozzi, F., Wright, J.F., Bushman, F.D. & High, K.A. (2011) Assessing the potential for AAV vector genotoxicity in a murine model. *Blood*, **117**, 3311-3319.

Li, J., Yen, C., Liaw, D., Podsypanina, K., Bose, S., Wang, S.I., Puc, J., Miliaresis, C., Rodgers, L., McCombie, R., Bigner, S.H., Giovanella, B.C., Ittmann, M., Tycko, B., Hibshoosh, H., Wigler, M.H. & Parsons, R. (1997) PTEN, a putative protein tyrosine phosphatase gene mutated in human brain, breast, and prostate cancer. *Science*, **275**, 1943-1947.

Li, L., Liu, F., Salmonsen, R.A., Turner, T.K., Litofsky, N.S., Di Cristofano, A., Pandolfi, P.P., Jones, S.N., Recht, L.D. & Ross, A.H. (2002) PTEN in neural precursor cells: regulation of migration, apoptosis, and proliferation. *Molecular and cellular neurosciences*, **20**, 21-29.

Li, P.P. & Peng, H.B. (2012) Regulation of axonal growth and neuromuscular junction formation by neuronal phosphatase and tensin homologue signaling. *Molecular biology of the cell*, **23**, 4109-4117.

Li, S., Byrne, B., Welsh, J. & Palmer, A.F. (2007) Self-assembled poly(butadiene)-b-poly(ethylene oxide) polymersomes as paclitaxel carriers. *Biotechnology progress*, **23**, 278-285.

Lin, D.S., Hsiao, C.D., Liau, I., Lin, S.P., Chiang, M.F., Chuang, C.K., Wang, T.J., Wu, T.Y., Jian, Y.R., Huang, S.F. & Liu, H.L. (2011) CNS-targeted AAV5 gene transfer results in global dispersal of vector and prevention of morphological and function deterioration in CNS of globoid cell leukodystrophy mouse model. *Molecular genetics and metabolism*, **103**, 367-377.

Ling, K.K., Gibbs, R.M., Feng, Z. & Ko, C.P. (2012) Severe neuromuscular denervation of clinically relevant muscles in a mouse model of spinal muscular atrophy. *Human molecular genetics*, **21**, 185-195.

Liu, K., Lu, Y., Lee, J.K., Samara, R., Willenberg, R., Sears-Kraxberger, I., Tedeschi, A., Park, K.K., Jin, D., Cai, B., Xu, B., Connolly, L., Steward, O., Zheng, B. & He, Z. (2010) PTEN deletion enhances the regenerative ability of adult corticospinal neurons. *Nature neuroscience*, **13**, 1075-1081.

Liu, Q. & Dreyfuss, G. (1996) A novel nuclear structure containing the survival of motor neurons protein. *The EMBO journal*, **15**, 3555-3565.

Liu, Q. & Muruve, D.A. (2003) Molecular basis of the inflammatory response to adenovirus vectors. *Gene therapy*, **10**, 935-940.

Lo, S.H. (2004) Tensin. *The international journal of biochemistry & cell biology*, **36**, 31-34.

Lomas, H., Canton, I., MacNeil, S., Du, J., Armes, S.P., Ryan, A.J., Lewis, A.L. & Battaglia, G. (2007) Biomimetic pH sensitive polymersomes for efficient DNA encapsulation and delivery. *Adv Mater*, **19**, 4238-4243.

Lomas, H., Du, J., Canton, I., Madsen, J., Warren, N., Armes, S.P., Lewis, A.L. & Battaglia, G. (2010) Efficient encapsulation of plasmid DNA in pH-sensitive PMPC-PDPA polymersomes: study of the effect of PDPA block length on copolymer-DNA binding affinity. *Macromolecular bioscience*, **10**, 513-530.

Lomas, H., Johnston, A.P., Such, G.K., Zhu, Z., Liang, K., van Koeverden, M.P., Alongkornchotikul, S. & Caruso, F. (2011) Polymersome-loaded capsules for controlled release of DNA. *Small*, **7**, 2109-2119.

Lomas, H., Massignani, M., Abdullah, K.A., Canton, I., Lo Presti, C., MacNeil, S., Du, J., Blanazs, A., Madsen, J., Armes, S.P., Lewis, A.L. & Battaglia, G. (2008) Non-cytotoxic polymer vesicles for

rapid and efficient intracellular delivery. *Faraday discussions*, **139**, 143-159; discussion 213-128, 419-120.

Lorson, C.L., Hahnen, E., Androphy, E.J. & Wirth, B. (1999) A single nucleotide in the SMN gene regulates splicing and is responsible for spinal muscular atrophy. *Proceedings of the National Academy of Sciences of the United States of America*, **96**, 6307-6311.

Luikart, B.W., Schnell, E., Washburn, E.K., Bensen, A.L., Tovar, K.R. & Westbrook, G.L. (2011) Pten knockdown in vivo increases excitatory drive onto dentate granule cells. *The Journal of neuroscience : the official journal of the Society for Neuroscience*, **31**, 4345-4354.

Lukacs, G.L., Haggie, P., Seksek, O., Lechardeur, D., Freedman, N. & Verkman, A.S. (2000) Size-dependent DNA mobility in cytoplasm and nucleus. *The Journal of biological chemistry*, **275**, 1625-1629.

Lunn, M.R. & Wang, C.H. (2008) Spinal muscular atrophy. *Lancet*, **371**, 2120-2133.

Madsen, J., Warren, N.J., Armes, S.P. & Lewis, A.L. (2011) Synthesis of Rhodamine 6G-Based Compounds for the ATRP Synthesis of Fluorescently Labeled Biocompatible Polymers. *Biomacromolecules*, **12**, 2225-2234.

Maehama, T. & Dixon, J.E. (1998) The tumor suppressor, PTEN/MMAC1, dephosphorylates the lipid second messenger, phosphatidylinositol 3,4,5-trisphosphate. *The Journal of biological chemistry*, **273**, 13375-13378.

Markowitz, J.A., Singh, P. & Darras, B.T. (2012) Spinal muscular atrophy: a clinical and research update. *Pediatric neurology*, **46**, 1-12.

Martinez-Hernandez, R., Bernal, S., Also-Rallo, E., Alias, L., Barcelo, M.J., Hereu, M., Esquerda, J.E. & Tizzano, E.F. (2013) Synaptic defects in type I spinal muscular atrophy in human development. *The Journal of pathology*, **229**, 49-61.

Martinez, T.L., Kong, L., Wang, X., Osborne, M.A., Crowder, M.E., Van Meerbeke, J.P., Xu, X., Davis, C., Wooley, J., Goldhamer, D.J., Lutz, C.M., Rich, M.M. & Sumner, C.J. (2012) Survival motor neuron protein in motor neurons determines synaptic integrity in spinal muscular atrophy. *The Journal of neuroscience : the official journal of the Society for Neuroscience*, **32**, 8703-8715.

Mason, M.R., Ehlert, E.M., Eggers, R., Pool, C.W., Hermening, S., Huseinovic, A., Timmermans, E., Blits, B. & Verhaagen, J. (2010) Comparison of AAV serotypes for gene delivery to dorsal root ganglion neurons. *Molecular therapy : the journal of the American Society of Gene Therapy*, **18**, 715-724.

Massignani, M., LoPresti, C., Blanazs, A., Madsen, J., Armes, S.P., Lewis, A.L. & Battaglia, G. (2009) Controlling Cellular Uptake by Surface Chemistry, Size, and Surface Topology at the Nanoscale. *Small*, **5**, 2424-2432.

Mastakov, M.Y., Baer, K., Symes, C.W., Leichtlein, C.B., Kotin, R.M. & During, M.J. (2002) Immunological aspects of recombinant adeno-associated virus delivery to the mammalian brain. *Journal of virology*, **76**, 8446-8454.

Mattar, C.N., Waddington, S.N., Biswas, A., Johana, N., Ng, X.W., Fisk, A.S., Fisk, N.M., Tan, L.G., Rahim, A.A., Buckley, S.M., Tan, M.H., Lu, J., Choolani, M. & Chan, J.K. (2013) Systemic delivery of scAAV9 in fetal macaques facilitates neuronal transduction of the central and peripheral nervous systems. *Gene therapy*, **20**, 69-83.

Mazarakis, N.D., Azzouz, M., Rohll, J.B., Ellard, F.M., Wilkes, F.J., Olsen, A.L., Carter, E.E., Barber, R.D., Baban, D.F., Kingsman, S.M., Kingsman, A.J., O'Malley, K. & Mitrophanous, K.A. (2001) Rabies virus glycoprotein pseudotyping of lentiviral vectors enables retrograde axonal transport and access to the nervous system after peripheral delivery. *Human molecular genetics*, **10**, 2109-2121.

McCarty, D.M. (2008) Self-complementary AAV vectors; advances and applications. *Molecular therapy : the journal of the American Society of Gene Therapy*, **16**, 1648-1656.

McCarty, D.M., Monahan, P.E. & Samulski, R.J. (2001) Self-complementary recombinant adeno-associated virus (scAAV) vectors promote efficient transduction independently of DNA synthesis. *Gene therapy*, **8**, 1248-1254.

McKelvey, T., Tang, A., Bett, A.J., Casimiro, D.R. & Chastain, M. (2004) T-cell response to adenovirus hexon and DNA-binding protein in mice. *Gene therapy*, **11**, 791-796.

McWhorter, M.L., Monani, U.R., Burghes, A.H. & Beattie, C.E. (2003) Knockdown of the survival motor neuron (Smn) protein in zebrafish causes defects in motor axon outgrowth and pathfinding. *The Journal of cell biology*, **162**, 919-931.

Mentis, G.Z., Blivis, D., Liu, W., Drobac, E., Crowder, M.E., Kong, L., Alvarez, F.J., Sumner, C.J. & O'Donovan, M.J. (2011) Early functional impairment of sensory-motor connectivity in a mouse model of spinal muscular atrophy. *Neuron*, **69**, 453-467.

Mercuri, E., Bertini, E., Messina, S., Solari, A., D'Amico, A., Angelozzi, C., Battini, R., Berardinelli, A., Boffi, P., Bruno, C., Cini, C., Colitto, F., Kinali, M., Minetti, C., Mongini, T., Morandi, L., Neri, G., Orcesi, S., Pane, M., Pelliccioni, M., Pini, A., Tiziano, F.D., Villanova, M., Vita, G. & Brahe, C. (2007) Randomized, double-blind, placebo-controlled trial of phenylbutyrate in spinal muscular atrophy. *Neurology*, **68**, 51-55.

Merdan, T., Kopecek, J. & Kissel, T. (2002) Prospects for cationic polymers in gene and oligonucleotide therapy against cancer. *Advanced drug delivery reviews*, **54**, 715-758.

Miller, D.G., Rutledge, E.A. & Russell, D.W. (2002) Chromosomal effects of adeno-associated virus vector integration. *Nature genetics*, **30**, 147-148.

Miyake, N., Miyake, K., Yamamoto, M., Hirai, Y. & Shimada, T. (2011) Global gene transfer into the CNS across the BBB after neonatal systemic delivery of single-stranded AAV vectors. *Brain research*, **1389**, 19-26.

Monani, U.R., Sendtner, M., Coovert, D.D., Parsons, D.W., Andreassi, C., Le, T.T., Jablonka, S., Schrank, B., Rossoll, W., Prior, T.W., Morris, G.E. & Burghes, A.H. (2000) The human centromeric survival motor neuron gene (SMN2) rescues embryonic lethality in Smn(-/-) mice and results in a mouse with spinal muscular atrophy. *Human molecular genetics*, **9**, 333-339.

Myers, M.P., Stolarov, J.P., Eng, C., Li, J., Wang, S.I., Wigler, M.H., Parsons, R. & Tonks, N.K. (1997) P-TEN, the tumor suppressor from human chromosome 10q23, is a dual-specificity phosphatase. *Proceedings of the National Academy of Sciences of the United States of America*, **94**, 9052-9057.

Nakai, H., Montini, E., Fuess, S., Storm, T.A., Grompe, M. & Kay, M.A. (2003) AAV serotype 2 vectors preferentially integrate into active genes in mice. *Nature genetics*, **34**, 297-302.

Naldini, L., Blomer, U., Gage, F.H., Trono, D. & Verma, I.M. (1996) Efficient transfer, integration, and sustained long-term expression of the transgene in adult rat brains injected with a lentiviral vector. *Proceedings of the National Academy of Sciences of the United States of America*, **93**, 11382-11388.

Napoli, A., Valentini, M., Tirelli, N., Muller, M. & Hubbell, J.A. (2004) Oxidation-responsive polymeric vesicles. *Nature materials*, **3**, 183-189.

Narver, H.L., Kong, L., Burnett, B.G., Choe, D.W., Bosch-Marce, M., Taye, A.A., Eckhaus, M.A. & Sumner, C.J. (2008) Sustained improvement of spinal muscular atrophy mice treated with trichostatin A plus nutrition. *Annals of neurology*, **64**, 465-470.

Ning, K., Drepper, C., Valori, C.F., Ahsan, M., Wyles, M., Higginbottom, A., Herrmann, T., Shaw, P., Azzouz, M. & Sendtner, M. (2010) PTEN depletion rescues axonal growth defect and improves survival in SMN-deficient motor neurons. *Human molecular genetics*, **19**, 3159-3168.

Ogino, S., Gao, S., Leonard, D.G., Paessler, M. & Wilson, R.B. (2003) Inverse correlation between SMN1 and SMN2 copy numbers: evidence for gene conversion from SMN2 to SMN1. *European journal of human genetics : EJHG*, **11**, 723.

Ogura, T., Mizukami, H., Mimuro, J., Madoiwa, S., Okada, T., Matsushita, T., Urabe, M., Kume, A., Hamada, H., Yoshikawa, H., Sakata, Y. & Ozawa, K. (2006) Utility of intraperitoneal administration as a route of AAV serotype 5 vector-mediated neonatal gene transfer. *The journal of gene medicine*, **8**, 990-997.

Oskoui, M. & Kaufmann, P. (2008) Spinal muscular atrophy. *Neurotherapeutics : the journal of the American Society for Experimental NeuroTherapeutics*, **5**, 499-506.

Otter, S., Grimmler, M., Neuenkirchen, N., Chari, A., Sickmann, A. & Fischer, U. (2007) A comprehensive interaction map of the human survival of motor neuron (SMN) complex. *The Journal of biological chemistry*, **282**, 5825-5833.

Palladino, A., Passamano, L., Taglia, A., D'Ambrosio, P., Scutifero, M., Cecio, M.R., Picillo, E., Viggiano, E., Torre, V., De Luca, F., Nigro, G. & Politano, L. (2011) Cardiac involvement in patients with spinal muscular atrophies. *Acta myologica : myopathies and cardiomyopathies : official journal of the Mediterranean Society of Myology / edited by the Gaetano Conte Academy for the study of striated muscle diseases*, **30**, 175-178.

Pane, M., Staccioli, S., Messina, S., D'Amico, A., Pelliccioni, M., Mazzone, E.S., Cuttini, M., Alfieri, P., Battini, R., Main, M., Muntoni, F., Bertini, E., Villanova, M. & Mercuri, E. (2008) Daily salbutamol in young patients with SMA type II. *Neuromuscular disorders : NMD*, **18**, 536-540.

Pang, J., Boye, S.E., Lei, B., Boye, S.L., Everhart, D., Ryals, R., Umino, Y., Rohrer, B., Alexander, J., Li, J., Dai, X., Li, Q., Chang, B., Barlow, R. & Hauswirth, W.W. (2010) Self-complementary AAV-mediated gene therapy restores cone function and prevents cone degeneration in two models of Rpe65 deficiency. *Gene therapy*, **17**, 815-826.

Park, K.K., Liu, K., Hu, Y., Smith, P.D., Wang, C., Cai, B., Xu, B., Connolly, L., Kramvis, I., Sahin, M. & He, Z. (2008) Promoting axon regeneration in the adult CNS by modulation of the PTEN/mTOR pathway. *Science*, **322**, 963-966.

Passini, M.A., Bu, J., Roskelley, E.M., Richards, A.M., Sardi, S.P., O'Riordan, C.R., Klinger, K.W., Shihabuddin, L.S. & Cheng, S.H. (2010) CNS-targeted gene therapy improves survival and motor function in a mouse model of spinal muscular atrophy. *The Journal of clinical investigation*, **120**, 1253-1264.

Pearn, J. (1978) Incidence, prevalence, and gene frequency studies of chronic childhood spinal muscular atrophy. *Journal of medical genetics*, **15**, 409-413.

Penaud-Budloo, M., Le Guiner, C., Nowrouzi, A., Toromanoff, A., Cherel, Y., Chenuaud, P., Schmidt, M., von Kalle, C., Rolling, F., Moullier, P. & Snyder, R.O. (2008) Adeno-associated virus vector genomes persist as episomal chromatin in primate muscle. *Journal of virology*, **82**, 7875-7885.

Perdigoto, A.L., Chaudhry, N., Barnes, G.N., Filbin, M.T. & Carter, B.D. (2011) A novel role for PTEN in the inhibition of neurite outgrowth by myelin-associated glycoprotein in cortical neurons. *Molecular and cellular neurosciences*, **46**, 235-244.

Petruska, J.C., Kitay, B., Boyce, V.S., Kaspar, B.K., Pearse, D.D., Gage, F.H. & Mendell, L.M. (2010) Intramuscular AAV delivery of NT-3 alters synaptic transmission to motoneurons in adult rats. *The European journal of neuroscience*, **32**, 997-1005.

Prior, T.W., Snyder, P.J., Rink, B.D., Pearl, D.K., Pyatt, R.E., Mihal, D.C., Conlan, T., Schmalz, B., Montgomery, L., Ziegler, K., Noonan, C., Hashimoto, S. & Garner, S. (2010) Newborn and carrier screening for spinal muscular atrophy. *American journal of medical genetics. Part A*, **152A**, 1608-1616.

Qiu, J., Nayak, R., Tullis, G.E. & Pintel, D.J. (2002) Characterization of the transcription profile of adeno-associated virus type 5 reveals a number of unique features compared to previously characterized adeno-associated viruses. *Journal of virology*, **76**, 12435-12447.

Rajendra, T.K., Gonsalvez, G.B., Walker, M.P., Shpargel, K.B., Salz, H.K. & Matera, A.G. (2007) A Drosophila melanogaster model of spinal muscular atrophy reveals a function for SMN in striated muscle. *The Journal of cell biology*, **176**, 831-841.

Rameez, S., Bamba, I. & Palmer, A.F. (2010) Large scale production of vesicles by hollow fiber extrusion: a novel method for generating polymersome encapsulated hemoglobin dispersions. *Langmuir : the ACS journal of surfaces and colloids*, **26**, 5279-5285.

Rathod, R., Havlicek, S., Frank, N., Blum, R. & Sendtner, M. (2012) Laminin induced local axonal translation of beta-actin mRNA is impaired in SMN-deficient motoneurons. *Histochemistry and cell biology*, **138**, 737-748.

Rodriguez, P.L., Harada, T., Christian, D.A., Pantano, D.A., Tsai, R.K. & Discher, D.E. (2013) Minimal "Self" peptides that inhibit phagocytic clearance and enhance delivery of nanoparticles. *Science*, **339**, 971-975.

Ross, A.H., Lachyankar, M.B. & Recht, L.D. (2001) PTEN: a newly identified regulator of neuronal differentiation. *The Neuroscientist : a review journal bringing neurobiology, neurology and psychiatry*, **7**, 278-281.

Rossoll, W., Jablonka, S., Andreassi, C., Kroning, A.K., Karle, K., Monani, U.R. & Sendtner, M. (2003) Smn, the spinal muscular atrophy-determining gene product, modulates axon growth and localization of beta-actin mRNA in growth cones of motoneurons. *The Journal of cell biology*, **163**, 801-812.

Rossoll, W., Kroning, A.K., Ohndorf, U.M., Steegborn, C., Jablonka, S. & Sendtner, M. (2002) Specific interaction of Smn, the spinal muscular atrophy determining gene product, with hnRNP-R and gry-rbp/hnRNP-Q: a role for Smn in RNA processing in motor axons? *Human molecular genetics*, **11**, 93-105.

Roth, C.M. & Sundaram, S. (2004) Engineering synthetic vectors for improved DNA delivery: insights from intracellular pathways. *Annual review of biomedical engineering*, **6**, 397-426.

Rudnik-Schoneborn, S., Heller, R., Berg, C., Betzler, C., Grimm, T., Eggermann, T., Eggermann, K., Wirth, R., Wirth, B. & Zerres, K. (2008) Congenital heart disease is a feature of severe infantile spinal muscular atrophy. *Journal of medical genetics*, **45**, 635-638.

Rudnik-Schoneborn, S., Vogelgesang, S., Armbrust, S., Graul-Neumann, L., Fusch, C. & Zerres, K. (2010) Digital necroses and vascular thrombosis in severe spinal muscular atrophy. *Muscle & nerve*, **42**, 144-147.

Ruiz, R. & Tabares, L. (2013) Neurotransmitter release in motor nerve terminals of a mouse model of mild spinal muscular atrophy. *Journal of anatomy*.

Russman, B.S., Iannaccone, S.T. & Samaha, F.J. (2003) A phase 1 trial of riluzole in spinal muscular atrophy. *Archives of neurology*, **60**, 1601-1603.

Rutledge, E.A., Halbert, C.L. & Russell, D.W. (1998) Infectious clones and vectors derived from adeno-associated virus (AAV) serotypes other than AAV type 2. *Journal of virology*, **72**, 309-319.

Sakhuja, K., Reddy, P.S., Ganesh, S., Cantaniag, F., Pattison, S., Limbach, P., Kayda, D.B., Kadan, M.J., Kaleko, M. & Connelly, S. (2003) Optimization of the generation and propagation of gutless adenoviral vectors. *Human gene therapy*, **14**, 243-254.

Salegio, E.A., Samaranch, L., Kells, A.P., Mittermeyer, G., San Sebastian, W., Zhou, S., Beyer, J., Forsayeth, J. & Bankiewicz, K.S. (2012) Axonal transport of adeno-associated viral vectors is serotype-dependent. *Gene therapy*.

Sanchez, G., Dury, A.Y., Murray, L.M., Biondi, O., Tadesse, H., El Fatimy, R., Kothary, R., Charbonnier, F., Khandjian, E.W. & Cote, J. (2013) A novel function for the survival motoneuron protein as a translational regulator. *Human molecular genetics*, **22**, 668-684.

Schrank, B., Gotz, R., Gunnersen, J.M., Ure, J.M., Toyka, K.V., Smith, A.G. & Sendtner, M. (1997) Inactivation of the survival motor neuron gene, a candidate gene for human spinal muscular atrophy, leads to massive cell death in early mouse embryos. *Proceedings of the National Academy of Sciences of the United States of America*, **94**, 9920-9925.

Setola, V., Terao, M., Locatelli, D., Bassanini, S., Garattini, E. & Battaglia, G. (2007) Axonal-SMN (a-SMN), a protein isoform of the survival motor neuron gene, is specifically involved in axonogenesis. *Proceedings of the National Academy of Sciences of the United States of America*, **104**, 1959-1964.

Shababi, M., Habibi, J., Yang, H.T., Vale, S.M., Sewell, W.A. & Lorson, C.L. (2010) Cardiac defects contribute to the pathology of spinal muscular atrophy models. *Human molecular genetics*, **19**, 4059-4071.

Shanmugarajan, S., Swoboda, K.J., Iannaccone, S.T., Ries, W.L., Maria, B.L. & Reddy, S.V. (2007) Congenital bone fractures in spinal muscular atrophy: functional role for SMN protein in bone remodeling. *Journal of child neurology*, **22**, 967-973.

Shanmugarajan, S., Tsuruga, E., Swoboda, K.J., Maria, B.L., Ries, W.L. & Reddy, S.V. (2009) Bone loss in survival motor neuron (Smn(-/-) SMN2) genetic mouse model of spinal muscular atrophy. *The Journal of pathology*, **219**, 52-60.

Simic, G. (2008) Pathogenesis of proximal autosomal recessive spinal muscular atrophy. *Acta neuropathologica*, **116**, 223-234.

Simic, G., Mladinov, M., Seso Simic, D., Jovanov Milosevic, N., Islam, A., Pajtak, A., Barisic, N., Sertic, J., Lucassen, P.J., Hof, P.R. & Kruslin, B. (2008) Abnormal motoneuron migration, differentiation, and axon outgrowth in spinal muscular atrophy. *Acta neuropathologica*, **115**, 313-326.

Skordis, L.A., Dunckley, M.G., Yue, B., Eperon, I.C. & Muntoni, F. (2003) Bifunctional antisense oligonucleotides provide a trans-acting splicing enhancer that stimulates SMN2 gene expression in patient fibroblasts. *Proceedings of the National Academy of Sciences of the United States of America*, **100**, 4114-4119.

Smart, T., Lomas, H., Massignani, M., Flores-Merino, M.V., Perez, L.R. & Battaglia, G. (2008) Block copolymer nanostructures. *Nano Today*, **3**, 38-46.

Somers, E., Stencel, Z., Wishart, T.M., Gillingwater, T.H. & Parson, S.H. (2012) Density, calibre and ramification of muscle capillaries are altered in a mouse model of severe spinal muscular atrophy. *Neuromuscular disorders : NMD*, **22**, 435-442.

Song, Y., Ori-McKenney, K.M., Zheng, Y., Han, C., Jan, L.Y. & Jan, Y.N. (2012) Regeneration of Drosophila sensory neuron axons and dendrites is regulated by the Akt pathway involving Pten and microRNA bantam. *Genes & development*, **26**, 1612-1625.

Stambolic, V., Suzuki, A., de la Pompa, J.L., Brothers, G.M., Mirtsos, C., Sasaki, T., Ruland, J., Penninger, J.M., Siderovski, D.P. & Mak, T.W. (1998) Negative regulation of PKB/Akt-dependent cell survival by the tumor suppressor PTEN. *Cell*, **95**, 29-39.

Steck, P.A., Pershouse, M.A., Jasser, S.A., Yung, W.K., Lin, H., Ligon, A.H., Langford, L.A., Baumgard, M.L., Hattier, T., Davis, T., Frye, C., Hu, R., Swedlund, B., Teng, D.H. & Tavtigian, S.V. (1997) Identification of a candidate tumour suppressor gene, MMAC1, at chromosome 10q23.3 that is mutated in multiple advanced cancers. *Nature genetics*, **15**, 356-362.

Swoboda, K.J., Prior, T.W., Scott, C.B., McNaught, T.P., Wride, M.C., Reyna, S.P. & Bromberg, M.B. (2005) Natural history of denervation in SMA: relation to age, SMN2 copy number, and function. *Annals of neurology*, **57**, 704-712.

Swoboda, K.J., Scott, C.B., Crawford, T.O., Simard, L.R., Reyna, S.P., Krosschell, K.J., Acsadi, G., Elsheik, B., Schroth, M.K., D'Anjou, G., LaSalle, B., Prior, T.W., Sorenson, S.L., Maczulski, J.A., Bromberg, M.B., Chan, G.M. & Kissel, J.T. (2010) SMA CARNI-VAL trial part I: double-blind, randomized, placebo-controlled trial of L-carnitine and valproic acid in spinal muscular atrophy. *PloS one*, **5**, e12140.

Swoboda, K.J., Scott, C.B., Reyna, S.P., Prior, T.W., LaSalle, B., Sorenson, S.L., Wood, J., Acsadi, G., Crawford, T.O., Kissel, J.T., Krosschell, K.J., D'Anjou, G., Bromberg, M.B., Schroth, M.K., Chan, G.M., Elsheikh, B. & Simard, L.R. (2009) Phase II open label study of valproic acid in spinal muscular atrophy. *PloS one*, **4**, e5268.

Tanford, C. (1979) Interfacial free energy and the hydrophobic effect. *Proceedings of the National Academy of Sciences of the United States of America*, **76**, 4175-4176.

Thomas, C.E., Birkett, D., Anozie, I., Castro, M.G. & Lowenstein, P.R. (2001) Acute direct adenoviral vector cytotoxicity and chronic, but not acute, inflammatory responses correlate with decreased vector-mediated transgene expression in the brain. *Molecular therapy : the journal of the American Society of Gene Therapy*, **3**, 36-46.

Thomas, C.E., Edwards, P., Wickham, T.J., Castro, M.G. & Lowenstein, P.R. (2002) Adenovirus binding to the coxsackievirus and adenovirus receptor or integrins is not required to elicit brain inflammation but is necessary to transduce specific neural cell types. *Journal of virology*, **76**, 3452-3460.

Tiziano, F.D., Lomastro, R., Pinto, A.M., Messina, S., D'Amico, A., Fiori, S., Angelozzi, C., Pane, M., Mercuri, E., Bertini, E., Neri, G. & Brahe, C. (2010) Salbutamol increases survival motor neuron (SMN) transcript levels in leucocytes of spinal muscular atrophy (SMA) patients: relevance for clinical trial design. *Journal of medical genetics*, **47**, 856-858.

Todd, A.G., Morse, R., Shaw, D.J., McGinley, S., Stebbings, H. & Young, P.J. (2010) SMN, Gemin2 and Gemin3 associate with beta-actin mRNA in the cytoplasm of neuronal cells in vitro. *Journal of molecular biology*, **401**, 681-689.

Torres-Benito, L., Neher, M.F., Cano, R., Ruiz, R. & Tabares, L. (2011) SMN requirement for synaptic vesicle, active zone and microtubule postnatal organization in motor nerve terminals. *PloS one*, **6**, e26164.

Towne, C., Raoul, C., Schneider, B.L. & Aebischer, P. (2008) Systemic AAV6 delivery mediating RNA interference against SOD1: neuromuscular transduction does not alter disease progression in fALS mice. *Molecular therapy : the journal of the American Society of Gene Therapy*, **16**, 1018-1025.

Towne, C., Schneider, B.L., Kieran, D., Redmond, D.E., Jr. & Aebischer, P. (2010) Efficient transduction of non-human primate motor neurons after intramuscular delivery of recombinant AAV serotype 6. *Gene therapy*, **17**, 141-146.

Towne, C., Setola, V., Schneider, B.L. & Aebischer, P. (2011) Neuroprotection by gene therapy targeting mutant SOD1 in individual pools of motor neurons does not translate into therapeutic benefit in fALS mice. *Molecular therapy : the journal of the American Society of Gene Therapy*, **19**, 274-283.

Trulzsch, B., Davies, K. & Wood, M. (2004) Survival of motor neuron gene downregulation by RNAi: towards a cell culture model of spinal muscular atrophy. *Molecular Brain Research*, **120**, 145-150.

Trulzsch, B., Garnett, C., Davies, K. & Wood, M. (2007) Knockdown of SMN by RNA interference induces apoptosis in differentiated P19 neural stem cells. *Brain research*, **1183**, 1-9.

Tsai, L.K., Yang, C.C., Hwu, W.L. & Li, H. (2007) Valproic acid treatment in six patients with spinal muscular atrophy. *European journal of neurology : the official journal of the European Federation of Neurological Societies*, **14**, e8-9.

Tzeng, A.C., Cheng, J., Fryczynski, H., Niranjan, V., Stitik, T., Sial, A., Takeuchi, Y., Foye, P., DePrince, M. & Bach, J.R. (2000) A study of thyrotropin-releasing hormone for the treatment of spinal muscular atrophy: a preliminary report. *American journal of physical medicine & rehabilitation / Association of Academic Physiatrists*, **79**, 435-440.

Valori, C.F., Ning, K., Wyles, M., Mead, R.J., Grierson, A.J., Shaw, P.J. & Azzouz, M. (2010) Systemic delivery of scAAV9 expressing SMN prolongs survival in a model of spinal muscular atrophy. *Science translational medicine*, **2**, 35ra42.

Vitte, J.M., Davoult, B., Roblot, N., Mayer, M., Joshi, V., Courageot, S., Tronche, F., Vadrot, J., Moreau, M.H., Kemeny, F. & Melki, J. (2004) Deletion of murine Smn exon 7 directed to liver leads to severe defect of liver development associated with iron overload. *The American journal of pathology*, **165**, 1731-1741.

Voigt, T., Meyer, K., Baum, O. & Schumperli, D. (2010) Ultrastructural changes in diaphragm neuromuscular junctions in a severe mouse model for Spinal Muscular Atrophy and their prevention by bifunctional U7 snRNA correcting SMN2 splicing. *Neuromuscular disorders : NMD*, **20**, 744-752.

Walters, R.W., Agbandje-McKenna, M., Bowman, V.D., Moninger, T.O., Olson, N.H., Seiler, M., Chiorini, J.A., Baker, T.S. & Zabner, J. (2004) Structure of adeno-associated virus serotype 5. *Journal of virology*, **78**, 3361-3371.

Wang, C.H., Finkel, R.S., Bertini, E.S., Schroth, M., Simonds, A., Wong, B., Aloysius, A., Morrison, L., Main, M., Crawford, T.O. & Trela, A. (2007) Consensus statement for standard of care in spinal muscular atrophy. *Journal of child neurology*, **22**, 1027-1049.

Wang, L., Chierico, L., Little, D., Patikarnmonthon, N., Yang, Z., Azzouz, M., Madsen, J., Armes, S.P. & Battaglia, G. (2012) Encapsulation of biomacromolecules within polymersomes by electroporation. *Angew Chem Int Ed Engl*, **51**, 11122-11125.

Wang, Z., Ma, H.I., Li, J., Sun, L., Zhang, J. & Xiao, X. (2003) Rapid and highly efficient transduction by double-stranded adeno-associated virus vectors in vitro and in vivo. *Gene therapy*, **10**, 2105-2111.

Weihl, C.C., Connolly, A.M. & Pestronk, A. (2006) Valproate may improve strength and function in patients with type III/IV spinal muscle atrophy. *Neurology*, **67**, 500-501.

Weiss, B., Schneider, M., Muys, L., Taetz, S., Neumann, D., Schaefer, U.F. & Lehr, C.M. (2007) Coupling of biotin-(poly(ethylene glycol))amine to poly(D,L-lactide-co-glycolide) nanoparticles for versatile surface modification. *Bioconjugate chemistry*, **18**, 1087-1094.

Williams, J.H., Schray, R.C., Patterson, C.A., Ayitey, S.O., Tallent, M.K. & Lutz, G.J. (2009) Oligonucleotide-mediated survival of motor neuron protein expression in CNS improves phenotype in a mouse model of spinal muscular atrophy. *The Journal of neuroscience : the official journal of the Society for Neuroscience*, **29**, 7633-7638.

Wilson, R.B. & Ogino, S. (2008) Carrier frequency of spinal muscular atrophy. *Lancet*, **372**, 1542; author reply 1542.

Winkler, C., Eggert, C., Gradl, D., Meister, G., Giegerich, M., Wedlich, D., Laggerbauer, B. & Fischer, U. (2005) Reduced U snRNP assembly causes motor axon degeneration in an animal model for spinal muscular atrophy. *Genes & development*, **19**, 2320-2330.

Workman, E., Saieva, L., Carrel, T.L., Crawford, T.O., Liu, D., Lutz, C., Beattie, C.E., Pellizzoni, L. & Burghes, A.H. (2009) A SMN missense mutation complements SMN2 restoring snRNPs and rescuing SMA mice. *Human molecular genetics*, **18**, 2215-2229.

Xiao, W., Chirmule, N., Berta, S.C., McCullough, B., Gao, G. & Wilson, J.M. (1999) Gene therapy vectors based on adeno-associated virus type 1. *Journal of virology*, **73**, 3994-4003.

Xiao, W., Chirmule, N., Schnell, M.A., Tazelaar, J., Hughes, J.V. & Wilson, J.M. (2000) Route of administration determines induction of T-cell-independent humoral responses to adeno-associated virus vectors. *Molecular therapy : the journal of the American Society of Gene Therapy*, **1**, 323-329.

Yonekawa, T., Komaki, H., Saito, Y., Sugai, K. & Sasaki, M. (2013) Peripheral nerve abnormalities in pediatric patients with spinal muscular atrophy. *Brain & development*, **35**, 165-171.

Zabner, J., Seiler, M., Walters, R., Kotin, R.M., Fulgeras, W., Davidson, B.L. & Chiorini, J.A. (2000) Adeno-associated virus type 5 (AAV5) but not AAV2 binds to the apical surfaces of airway epithelia and facilitates gene transfer. *Journal of virology*, **74**, 3852-3858.

Zhang, H., Yang, B., Mu, X., Ahmed, S.S., Su, Q., He, R., Wang, H., Mueller, C., Sena-Esteves, M., Brown, R., Xu, Z. & Gao, G. (2011) Several rAAV vectors efficiently cross the blood-brain barrier and transduce neurons and astrocytes in the neonatal mouse central nervous system. *Molecular therapy : the journal of the American Society of Gene Therapy*, **19**, 1440-1448.

Zhang, Y., Granholm, A.C., Huh, K., Shan, L., Diaz-Ruiz, O., Malik, N., Olson, L., Hoffer, B.J., Lupica, C.R., Hoffman, A.F. & Backman, C.M. (2012) PTEN deletion enhances survival, neurite outgrowth and function of dopamine neuron grafts to MitoPark mice. *Brain : a journal of neurology*, **135**, 2736-2749.

Zincarelli, C., Soltys, S., Rengo, G. & Rabinowitz, J.E. (2008) Analysis of AAV serotypes 1-9 mediated gene expression and tropism in mice after systemic injection. *Molecular therapy : the journal of the American Society of Gene Therapy*, **16**, 1073-1080.

Zufferey, R., Dull, T., Mandel, R.J., Bukovsky, A., Quiroz, D., Naldini, L. & Trono, D. (1998) Self-inactivating lentivirus vector for safe and efficient in vivo gene delivery. *Journal of virology*, **72**, 9873-9880.